

# Evaluation of Green Roof Water Quantity and Quality Performance in an Urban Climate



SCIENCE

**Evaluation of Green Roof Water  
Quantity and Quality  
Performance in an Urban Climate**

By

Patricia Culligan  
Tyler Carson  
Stuart Gaffin  
Rebecca Gibson  
Raha Hakimdavar  
Diana Hsueh  
Nadine Hunter  
Daniel Marasco  
Wade McGillis  
Columbia University  
New York, NY 10027

Thomas P. O'Connor  
Urban Watershed Management Branch  
Water Supply and Water Resources Division  
National Risk Management Research Laboratory  
Edison, NJ 08837

Cooperative Agreement No. AE-83484601-0

OFFICE OF RESEARCH AND DEVELOPMENT  
U.S. ENVIRONMENTAL PROTECTION AGENCY

September 2014

## **Notice**

The U.S. Environmental Protection Agency, through its Office of Research and Development, funded and managed, or partially funded and collaborated in, the research described herein. It has been subjected to the Agency's peer and administrative review and has been approved for publication. Any opinions expressed in this report are those of the authors and do not necessarily reflect the views of the Agency, therefore, no official endorsement should be inferred. Any mention of trade names or commercial products does not constitute endorsement or recommendation for use.

## Abstract

Green roofs are increasingly seen as an established ‘green infrastructure’ technology that confers many environmental benefits. This is especially the case in urban areas where rooftops comprise a large fraction of the landscape, are typically low albedo and add to widespread impervious surfaces. The benefits of green roofs include urban heat island mitigation, reduced or eliminated roof façade heat transfer with associated building energy benefits, stormwater retention and detention, ecosystem service benefits and aesthetic amenity value, to name a few. Stormwater mitigation and subsequent receiving water quality improvement are increasingly perceived as an important function of this technology.

In this report we present an analysis of water benefits from an array of observed green roof and control (non-vegetated) roof project sites throughout New York City, where average annual precipitation in New York’s Central Park is over 1200 mm for the 40-year historic period 1971-2010. The projects are located on a variety of building sites and represent a diverse set of available extensive green roof installation types, including vegetated mat, built up, and modular tray systems, as well as plant types. Moreover the projects have been monitored for a few years and are being observed in an urban climate.

For water retention performance, we monitored runoff from four full-scale green roofs, including one built up system, one modular tray system and two vegetated mat systems. We gathered roof runoff data for over 100 storm events for each green roof over a period of 23-months. Our main findings for water *quantity* performance include: (i) runoff from green roofs has a quadratic relationship to precipitation depth, where the percent retention decreases as storm size increases; (ii) the relationship between precipitation depth and green roof runoff depth (runoff volume divided by rooftop drainage area) can be described by a Characteristic Runoff Equation (CRE) for each roof; (iii) the CRE can be used with historic rainfall data to reduce bias in reported green roof retention performance, which might arise due to a bias in the distribution of storm events during a monitoring period; (iv) the modular tray system captured the lowest percentage of precipitation among all green roof systems for storms 0-20 mm in depth, and the highest for storms above 30 mm; (v) multi-year predictions show that on an annual basis, the built up system will retain more rainfall than the modular tray system, which will retain more rainfall than the vegetated mat systems. Our findings reveal the importance of green roof technical design, as well as substrate capacity, for stormwater retention at different storm sizes. The Natural Resources Conservation Service curve number (CN) method, while providing similar average results to the CRE, could not capture observed relative differences between the retention performance of the built up, modular tray and mat systems in different storm categories.

For *water quality* performance with respect to stormwater runoff, we undertook a 16-month survey of stormwater runoff quality from five full-scale green roofs, including two built up systems, one modular tray system and two vegetated mat systems. For comparison, we also surveyed the chemical composition of runoff from five non-vegetated (control) roofs as well as local precipitation. In total we collected and analyzed over 100 water samples. Our results show that the pH of runoff from green roofs was consistently higher than that from the control roofs and precipitation with observed average pH’s equal to 7.28, 6.27 and 4.82 for the green roofs, control roofs and precipitation, respectively. Thus, the green roofs neutralized the acid rain. In general, we observed lower  $\text{NO}_3^-$  (nitrate) and  $\text{NH}_4^+$  (ammonium) concentrations in green runoff than control roof runoff, with the exception of runoff from the built up system, which had higher  $\text{NO}_3^-$  concentrations than the control roof runoff. Overall, total P (phosphorus) concentrations were higher in green roof runoff than control roof runoff. Finally, with respect to micronutrients and heavy metals: we either detected these constituents at very low concentrations or not at all (concentrations were below the detection limit), with a few exceptions. One exception related to the detection of boron in runoff from one of the vegetated mat systems, and another related to the detection of Ca (calcium) and Na (sodium) in runoff from all five green roofs. Based on our results, we estimated that annual mass loading per unit rooftop area

of  $\text{NO}_3^-$ ,  $\text{NH}_4^+$  and total P discharging from all five green roofs was considerably less than that from their respective control roofs, due to the ability of green roofs to retain precipitation. Thus, green roof implementation could improve urban stormwater and subsequently urban receiving water quality if achieved at large areal scales.

In order to investigate monitoring schemes that could be used on a wider scale of study, a new method for green roof runoff and evapotranspiration estimation was derived. Termed the Soil Water Apportioning Method (SWAM), this is a water balance approach which analytically links precipitation to substrate moisture, and enables inference of green roof runoff and evapotranspiration from information on substrate moisture changes over time. Twelve months of in situ rainfall and soil moisture observations from two green roofs, both vegetated mat systems, were used to test the reliability of the proposed approach using two different low-cost soil moisture probes. SWAM estimates of runoff were compared with observed runoff data for the entire duration of the study period. Preliminary results indicate that SWAM can be an effective low-cost and low-maintenance alternative to the custom made weir and lysimeter systems frequently used to quantify runoff during green roof studies. The method may also provide a simple way of estimating green roof evapotranspiration.

# Table of Contents

Notice.....	ii
Abstract.....	iii
Contents.....	v
List of Figures.....	vi
List of Tables.....	vii
Acronyms and Abbreviations.....	viii
Acknowledgements.....	x
Executive Summary.....	1
Chapter 1 Introduction.....	1-1
Chapter 2 Overall Conclusions and Recommendations.....	2-1
2.1 Conclusions.....	2-1
2.2 Recommendations for Further Study.....	2-2
Chapter 3 Monitoring Sites and Systems.....	3-1
3.1 Green Roofs and Monitoring Equipment.....	3-1
3.2 Green Roof Site Descriptions.....	3-3
Chapter 4 Water Quantity Study.....	4-1
4.1 Introduction.....	4-1
4.2 Methodology.....	4-2
4.3 Results.....	4-4
4.4 Results from BDCA and Regis.....	4-9
4.5 Discussion of Results.....	4-10
4.6 Conclusions.....	4-12
Chapter 5 Water Quality Study.....	5-1
5.1 Introduction.....	5-1
5.2 Methodology.....	5-1
5.3 Results.....	5-3
5.4 Discussion of Results.....	5-3
5.5 Conclusions.....	5-9
Chapter 6 Soil Moisture Water Balance Study.....	6-1
6.1 Introduction.....	6-1
6.2 Methodology.....	6-1
6.3 Results.....	6-4
6.4 Discussion of Results.....	6-8
6.5 Conclusions.....	6-9
Chapter 7 References.....	7-1
Appendix A Site Equipment.....	A 1
Appendix B Water Quality Results.....	B 1
Appendix C Water Quality Analysis.....	C 1

## List of Figures

Figure 3-1: Locations of monitored green roof sites and priority combined sewer sheds in New York City.....	3-2
Figure 3-2: W115 Roof (A) Satellite photograph (B) Weir device (C) Roof photograph.....	3-3
Figure 3-3: W118 Roof (A) Satellite photograph (B) Weir device (C) Roof photograph.....	3-3
Figure 3-4: Fdston Roof (A) Satellite photograph (B) Equipment (C) Roof photograph.....	3-6
Figure 3-5: BDCA Roof (A) Satellite photograph (B) Weir device (C) Roof photograph.....	3-7
Figure 3-6: Regis Roof (A) Satellite photograph (B) Weir device (C) Roof photograph.....	3-8
Figure 4-1: (A) Runoff monitoring weir device (B) Calibration chamber used to simulate rooftop runoff. ....	4-2
Figure 4-2: Monitored total rainfall retention for the W115, W118, USPS, and ConEd green roofs by event size. ....	4-5
Figure 4-3: Rainfall by event size for monitored and historic (NYC) data as percent of (A) events and (B) depth.....	4-6
Figure 4-4: Characteristic runoff equations and events for (A) W115, (B) W118, (C) USPS, and (D) ConEd. ....	4-7
Figure 4-5: Residuals between characteristic runoff equations and curve number and observed depth for (A) W115, (B) W118, (C) USPS, and (D) ConEd. ....	4-8
Figure 4-6: Predicted rainfall retention over historic period using (A) Characteristic runoff equations (B) Curve number.....	4-9
Figure 4-7: Characteristic runoff equations and events for (A) BDCA (B) Regis.....	4-10
Figure 5-1: Distribution of pH, conductivity, turbidity, and apparent color for all roof types and precipitation. ....	5-4
Figure 5-2 Distribution of nutrient and heavy metal concentration (mg/L) from all roof types.....	5-5
Figure 6-1: NSE and PBIAS for the (a) W118, and (b) W115 roofs at different time aggregates. ....	6-5
Figure 6-2 Precipitation, soil moisture, observed and simulated daily runoff and error for green roof W118. ....	6-5
Figure 6-3: Precipitation, soil moisture, observed and simulated daily runoff and error for green roof W115. ....	6-6
Figure 6-4: Comparison between green roof W118 and W115 from March to May 2012 only.....	6-7
Figure 6-5: Comparison of measured versus modeled evapotranspiration (Dome ET to SWAM ET) on W118.....	6-8

## List of Tables

Table 3-1: Summary of Monitored Green Roof Sites.....	3-1
Table 4-1: Summary of Monitoring Duration and Observed Events.....	4-3
Table 5-1: Water Quality Measurement Parameters.....	5-2
Table 5-2 Summary of Mean Water Quality Results with Standard of Deviation.....	5-3
Table 5-3: Average Concentration (AC) and Annual Mass Loading (AML) of $\text{NH}_4^+$ , $\text{NO}_3^-$ , and P. ....	5-8
Table 5-4: Projected Reduction in Nutrient Loading per Year from Retrofitting Available NYC Rooftops.....	5-9
Table 6-1: Time Aggregate Optimization for W118 and W115 Green Roofs.....	6-4

## Acronyms and Abbreviations

AC	= Average Concentration
Al	= Aluminum
AML	= Annual Mass Loading
ANOVA	= Analysis of Variance
As	= arsenic
ASCE	= American Society of Civil Engineers
ASTM	= American Society for Testing and Materials
B	= boron
Ba	= barium
BDCA	= Bronx Design and Construction Academy
BMP	= Best Management Practices
C	= control roof
C3	= C3 photosynthesis
C4	= C4 photosynthesis
Ca	= calcium
CAM	= crassulacean acid metabolism
Cd	= cadmium
CGRC	= Columbia Green Roof Consortium
CN	= curve number
ConEd	= Con Edison Building
Cr	= chromium
CRE	= characteristic runoff equation
CSO	= Combined Sewage Overflow
CSS	= Combined Sewer System
CU	= Columbia University
Cu	= copper
DEC	= Department of Environmental Conservation (of NYS)
DEP	= Department of Environmental Protection (of NYC)
DIA	= digital image analysis
EB	= energy balance
EPA	= U.S. Environmental Protection Agency
ET	= evapotranspiration
Fdston	= Ethical Culture Fieldston School
Fe	= iron
GI	= green infrastructure
GR	= green roof
ISA	= impervious surface area
K	= potassium
L	= losses
LID	= low impact development
Mg	= magnesium
Mn	= manganese
n	= substrate effective porosity
N	= runoff nitrogen content
NA	= not applicable
Na	= sodium
NH <sub>4</sub> <sup>+</sup>	= ammonium

Ni	= nickel
NO <sub>3</sub> <sup>-</sup>	= nitrate
NOAA	= National Oceanic and Atmospheric Administration
NRCS	= Natural Resources Conservation Service
NSE	= Nash-Sutcliffe Efficiency
NYC	= New York City
NYS	= New York State
P	= total phosphorus or precipitation
Pb	= lead
PBIAS	= percent bias
Pobs	= observed precipitation
Q	= green roof runoff
QC	= location of green roof runoff quality measurement
QG	= location of control roof runoff quality measurement
Qobs	= observed runoff
Qpred	= estimated runoff from SWAM
RARE	= Regional Applied Research Effort
SE	= standard error
SM	= substrate moisture
SMnorm	= normalized soil moisture
SWAM	= Soil Water Apportioning Method
SSO	= Sanitary Sewer Overflow
Tukey HSD	= Tukey Honestly Significant Difference
UHI	= urban heat island
UN	= United Nations
US	= United States
USPS	= US Postal Service Morgan Processing and Distribution Center
VG#	= location of green roof runoff quantity measurement
VMC	= volumetric moisture content
W115	= West 115 <sup>th</sup> Street, NY, NY
W118	= West 118 <sup>th</sup> Street, NY, NY
WWF	= Wet Weather Flow
WWTP	= Waste Water Treatment Plant
Zn	= zinc

## Acknowledgements

This project would not have been possible without the U.S. Environmental Protection Agency's (EPA) Regional Applied Research Effort (RARE) grant. In particular, we are grateful for the support provided by Thomas O'Connor of the EPA's Urban Watershed Management Branch, Edison, NJ and Rabi Kieber, Region 2 Green Building/Sustainability Coordinator at EPA, who enabled this research to be undertaken. Support for the research was also provided, in part, by the National Science Foundation (NSF) grants CMMI-0928604 and DGE-0903597. The authors also wish to thank the following for their contributions to the work: Kevin O'Connor from Con Edison; Helen Bielak, Janice Erskine and Emilio Trejo from the Columbia University Facilities Office and the Columbia University Office of Environmental Stewardship; Jamie Cohen, Luis Correa, Bhupendra Patel and David Stoff from the U.S. Postal Service; Howard Waldman and Beselot Birhanu from Ethical Culture Fieldston School; Frank Barona, Philip Judge and Donald Allison from Regis High School; Nathaniel Wight from the Bronx Design and Construction Academy; GreenGrid; Smartroofs; Liveroofs; Prides Corner Farms; Tecta Green; Greensulate; Xero Flor; Clare Buck; and Ellen Lee. The report was reviewed by Dr. Kimberly DiGiovanni of Drexel University and Dr. Olyssa Starry of the Portland State University. We gratefully acknowledge their helpful comments. Any opinions, findings, and conclusions expressed in this report are those of the authors and do not necessarily reflect the views of any other person or entity.

## Executive Summary

This report is the result of an U.S. Environmental Protection Agency (EPA) Regional Applied Research Effort (RARE) project that documents the *quantity* and *quality* of runoff from a suite of urban green roofs located in New York City (NYC). An overall research goal was to assess green roof performance on actual urban rooftops, which have realistic runoff dimensions to drains and are subject to more realistic urban environmental conditions, as opposed to test plots at academic research campuses or laboratories.

Green roofs are known to provide multiple urban ecosystem services, foremost of which include urban heat island mitigation, reduced rooftop winter and summer heat flows, and stormwater management, including runoff retention and detention. A growing number of different green roof designs are commercially available, although most include the following components: waterproof membrane, geotextile layer, drainage layer, substrate (also known as growth medium) and plants. Such layers can be delivered and installed in various ways, but three common types have emerged: (i) vegetated mat systems that utilize a geo-composite structure to hold substrate, which is then installed like a carpet over other desired geosynthetics; (ii) built up systems that are constructed on the rooftop itself starting from the waterproof layer at the bottom and ending with the plant installation at the top, and (iii) modular tray systems comprising relatively small easy-to-move and manage trays that combine all layers in a single unit and are simply placed tile-like within the desired roof area.

The material design and composition of each layer in a green roof can vary widely but two of the most important variables are the growing substrate composition and depth and the plant selection. With regard to growing substrate depths, a generally accepted definition is that shallow systems, called ‘extensive,’ are usually 100 mm or less, while deeper systems, called ‘intensive’ are usually 150 mm or more. The deeper systems, which are commonly constructed as built up, offer a much greater opportunity for variable plant choices, including native plant options. Shallow systems are mostly planted with hardy *Sedums*, which can thrive in depths as shallow as 25 mm or even less. Generally, extensive green roofs are cheaper, require less maintenance, and are lighter than intensive systems. Therefore, they are implemented more frequently and most especially on existing building stock where rooftop weight limitations come into play. Due to their wider applicability in dense urban environments like NYC, extensive green roofs were the focus of this study.

With respect to stormwater water *quantity* performance, we have been monitoring six full-scale green roofs in NYC, including two vegetated mat systems (named W115 and W118), two built up systems (named USPS and Regis), and two modular tray systems (named ConEd and BDCA). This report focuses on the analysis of four of these systems where monitoring equipment has been in place the longest: W115, W118, USPS and ConEd. Continuous rainfall and runoff data were collected from each green roof between June 2011 and April 2013, resulting in 520 rainfall events, ranging from 0.25 to 180 mm in rainfall depth, which were used for analyses. Rainfall retention over the entire study period was found to be 62% for W115, 42% for W118, 56% for USPS, and 59% for ConEd. However, results also demonstrated that the percent of rainfall retained by the green roofs decreased with increasing rainfall depth and, as a result, the distribution of rainfall during a study period plays a significant role in reported water retention values. To extend the analyses of observations made during the study period to longer (decadal) time periods, we explored the utility of two empirical models, both of which predict runoff from a set of precipitation events. One model used the characteristic runoff equation (CRE) proposed by Carson et al. (2013), and the other used the widely adopted curve number (CN) approach developed by the Natural Resources Conservation Service. Both models were applied to 40-years of historic rainfall events generated from hourly precipitation data recorded in Central Park (NOAA 1971-2010). During the 40-year period, the CRE method estimated total rainfall retention to be 51% for W115, 43% for W118, 57% for USPS, and 54% for ConEd; whereas the CN method estimated rainfall retentions of 53% for W115, 48% for W118, 58% for USPS, and 59% for ConEd. Correlation between predicted and observed runoff was high for both methods, with r-squared values of 0.82 or greater. A major difference between the two models, however, is that the CRE method accounted for observed changes in relative retention performance of the different green roof systems with storm size: for example, the ConEd modular tray system captured the lowest percentage of precipitation among all green roof systems for storms 0-20 mm in depth, and the highest for storms above 30 mm. In contrast, the CN method assumes

that a green roof with a lower CN will always outperform a green roof with a higher CN in every storm category, which belies our monitoring results. Overall, the CN method predicts higher annual rainfall retention than the CRE method for each of the green roofs studied.

To determine the impact of urban green roof establishment on stormwater *quality*, we performed a 16-month water quality survey of stormwater runoff from five full-scale green roofs, including the four systems where water quantity performance was being monitored (the W115 and W118 vegetated mat systems, the USPS built up system and the ConEd tray system) and a second built up system (named Fdston). We also concurrently surveyed water quality at five non-vegetated (control) roofs, which were located near each green roof study site. Over the study period, we collected and analyzed more than 100 water samples. We found the measured pH of green roof runoff to be consistently higher than that of the control roof runoff and precipitation, with observed average pH equal to 7.28, 6.27 and 4.82 for the green roofs, control roofs and precipitation, respectively. All micronutrients (with the exception of sodium) and heavy metals (with the exception of boron at W118) in the green roof runoff were either detected at very low concentrations or were below instrument detection limits. Despite variability in the average concentration of nitrate ( $\text{NO}_3^-$ ), ammonium ( $\text{NH}_4^+$ ) and total phosphorous (P) in green roof runoff across the different roof types, we estimated that the annual mass loading of  $\text{NO}_3^-$ ,  $\text{NH}_4^+$  and total P per unit roof top area discharging from the green roof types was less than that from the nearby control roofs due to the ability of green roofs to retain precipitation. Based on estimated annual mass loadings ( $\text{mg/m}^2$ ) and an assumption that about 20% of rooftops in NYC could be retrofit with an extensive green roof, we project that widespread green roof installation in NYC could decrease annual stormwater nutrient discharge of total P by over 600 kg,  $\text{NH}_4^+$  by over 7,000 kg and  $\text{NO}_3^-$  by over 150,000 kg. Although these amounts are not large in comparison to the annual nutrient discharges from waste water treatment plants (WWTP), this still provides evidence that green roof implementation may improve urban stormwater and subsequent receiving water quality.

Green roof stormwater attenuation performance has often been studied using either lysimeters or custom-made weirs, as were used in this study. While these systems have yielded very good results, issues of cost and labor regarding their application in larger monitoring studies are a concern. To address these issues, a new cost-effective method for green roof hydrologic monitoring that could be implemented on a broad scale was explored. A water balance method – called SWAM – was derived which relies solely on the monitoring of precipitation and green roof substrate moisture content. Eleven months of measurements from the W118 and W115 vegetated mat systems were used to validate the results of this approach. Various statistical tools were used to assess SWAM's performance, with particular focus on maximizing Nash-Sutcliffe Efficiency (NSE) coefficients, which indicate how well the simulated data fit observed values on a 1:1 line. Volumetric substrate moisture was collected with two low-cost soil moisture probes: a CS615 water content reflectometer and an ECH2O EC-5 soil moisture probe. The results from SWAM were compared with observed runoff data from the two green roofs. The method was able to successfully predict daily runoff from the two study sites and appears to have potential for estimating green roof evapotranspiration.

## Chapter 1 Introduction

According to the U.S. Environmental Protection Agency (EPA), non-point source pollution is the currently the Nation's largest water quality problem, leading to the impairment of tens of thousands of rivers, lakes and estuaries across the nation (Berghage et al. 2009). A recent report by the National Oceanic and Atmospheric Administration (NOAA) (Bricker et al. 2007) also cites non-point source pollution as the single, largest threat to US coastal water quality, Non-point source pollution is degrading the functionality of the wetlands, marshes and riparian areas that make up many coastlines, causing eutrophication that is resulting in fish kills, algal blooms and limited growth of sea-grass, threatening commercial shell-fish beds, and causing major human-health concerns related to the presence of water-borne pathogens.

In urban areas, the leading cause of non-point source pollution is urban storm water discharges caused by wet-weather flow (WWF). Problem constituents in WWF include visible matter, pathogenic microorganisms, oxygen-demanding materials, suspended solids, nutrients, and toxicants (EPA 2004). The three most common sources of urban WWF are stormwater runoff, combined sewer overflow (CSO) and sanitary sewer overflow (SSO). A 2008 report by the New York State Department of Environmental Conservation (NYS DEC), which highlights poor water quality in much of the Lower Hudson Watershed, cites urban stormwater runoff and combined sewer overflows as major concerns within this watershed, which incorporates the dense urban area of New York City (NYC) (NYS DEC 2008).

Because of the magnitude of water quality impairment arising from urban WWF, abatement of WWF pollution is a major focus of many US government agencies and municipalities. Abatement options for WWF pollution include control at the source by land management, both in-line and off-line storage, or end of pipe treatment (i.e., in the treatment plant or with satellite treatment facilities at outfall points). According to Field and Sullivan (2001) traditional engineering solutions for WWF abatement, such as off-line storage or end of pipe solutions, are difficult for municipalities and other stakeholders to implement because of design and cost challenges that arise due to the need for low footprint solutions at the ground or in the sub-terrain. This is particularly true in dense urban environments, like NYC, where land costs are high, land availability is scarce and subsurface construction can be prohibitively expensive. As a result, alternatives to traditional solutions to WWF abatement have been aggressively pursued in recent years both by the academic (Montalto et al. 2007) and professional communities (GeoSyntec Consultants Inc. 2012).

One potential low cost and effective strategy for WWF abatement that is rapidly gaining acceptance in the US is Low Impact Development (LID). The intent of LID is to mimic predevelopment hydrology (Coffman 2000) which is based on a combined strategy of conservation to reduce hydrologic impacts and the incorporation of distributed micro-scale Best Management Practices (BMP's) throughout a subcatchment area. These BMPs are intended to ensure that stormwater generated in the subcatchment has the chance to infiltrate or evapotranspire, rather than being transported without reduction to a centralized system. Although LID techniques might not completely eliminate the need for centralized stormwater management systems, they can greatly reduce the dependence of WWF abatement on costly, and often aging, centralized systems (Williams 2003; Williams and Wise 2006).

A large number of US cities, including Portland, Seattle, New York and San Francisco (Erlichman and Peck 2013) as well as cities around the world such as Melbourne, Australia, Shanghai, China and Copenhagen, Denmark (GreenRoofs.com 2014) are investing in urban green infrastructure as part of larger BMP programs to mitigate the detrimental impacts of WWF. Urban green infrastructure, such as green roofs, green streets, advanced street tree pits, rain gardens and bio-swales, introduce vegetation, depression storage, and perviousness back into city landscapes, thereby enabling local capture and management of stormwater and stormwater pollution. In cities with combined sewer systems (CSS) the re-introduction of these landscape features reduces both the volume and peak-rate of flow of stormwater into the CSS, thereby also reducing the occurrence and severity of CSO events.

It has to be recognized, however, that the physical and time scales of green infrastructure implementation needed to help mitigate the impacts of urban WWF are substantial. For example, NYC's 2010 plan to manage WWF generated by an inch of rain falling on 10% of the city's impervious area by incorporating green infrastructure into 52% of urban land served by CSSs at a projected cost of \$2.4 billion over the next 18 years (NYC DEP 2010). Opportunities to better

understand and advance the performance of current, conventional green infrastructure are thus important, and such advances could have significant, positive impact on urban WWF abatement programs for years to come.

In urban areas where land availability for surface area stormwater controls, such as rain gardens and bioswales, is scarce, green roof technology is an important component of many green infrastructure programs. Rooftops can make up to 40 to 50% of impervious urban land area (Mayor's Office of Long-Term Planning and Sustainability 2008), providing a meaningful opportunity for implementation of local stormwater controls.

Green roofs, also known as vegetated roofs, eco-roofs, or living roofs, are typically constructed by placing a drainage course, growing substrate, and vegetation on top of a roof's waterproof membrane. Green roofs have been used for stormwater management for over thirty years in Germany (Köhler and Keeley 2004) and, according to February 2013 information available in the Green Roof and Wall Projects Database (GreenRoofs.com 2014), the number of green roof projects in the US today now exceeds 1,000, with many projects concentrated in metropolitan areas. At present, the US has only recently begun to develop national green roof standards and, as a result, the materials, configuration, and installation methods for green roofs can vary widely from site to site. For example, in some installations, green roofs may also have additional geosynthetic layers for preventing plant root penetration damage of the roof membrane, limiting sediment intrusion into the drainage course, and/or improving water storage.

It is common for green roofs to be classified as either extensive or intensive based on the thickness of the growing substrate layer. Extensive roof substrates are typically 100 mm thick or less and feature short rooting, drought resistant plants, whereas intensive roof substrates are greater than 150 mm thick and may be sowed with deeper rooting plants including shrubs and trees. Generally, extensive green roofs are cheaper, require less maintenance, and are lighter than intensive systems. Thus, they are implemented more frequently, most especially on existing building stock where rooftop weight limitations come into play. Due to their wider applicability in dense urban areas like NYC, extensive green roofs were the focus of this study.

Within the extensive green roof classification, three major construction types have emerged: vegetated mat, built up, and modular tray systems (Oberndorfer et al. 2007). Typically, both the vegetated mat and built up systems require a specialized drainage course to prevent ponding and surface flow that would otherwise cause substrate erosion. The two systems differ, however, in how the substrate is installed. In mat construction the growing substrate is bound within a geo-composite used for off-site pre-planting, whereas the growing substrate for a built up system is placed within bordered rooftop regions and landscaped on site. In contrast, the walls of the modular trays already restrict surface runoff, in turn limiting erosion, and therefore may be placed directly on a roof's waterproof membrane. Each construction type imposes a unique set of boundary conditions on the growing substrate layer that affects the roof's drainage behavior and runoff characteristics. For example, the mat and built up systems promote lateral runoff movement to varying degrees, whereas the unconnected modular trays generally facilitate vertical percolation. The type of construction might also determine the non-vegetated area required for maintenance activities and the feasibility of different vegetation types. As a result, the installation method might be a significant factor in overall green roof performance.

Recently, a number of studies have helped to better understand the role green roofs might play in mitigating CSO pollution and minimizing problems associated with urban runoff in general (Berndtsson 2010). These studies report a wide range of hydrologic behavior due to differences in, among other parameters, green roof construction type, growing substrate depth, vegetation type, and areal coverage. Even similar systems may have significant performance variation since the water retention ability of green roofs is heavily influenced by local climate; where the distribution, size, and intensity of rainfall events (Stovin 2010), as well as seasonal evapotranspiration (ET) rates (Bengtsson et al. 2005), are thought to play a key role.

The goal of this project was to collect data on the hydrological performance of a suite of full-scale extensive green roofs located in an urban area within EPA Region 2, specifically NYC, in order to provide better understanding of the potential role of green roofs in urban WWF abatement. An important research objective was to assess green roof hydrological performance on actual urban rooftops with realistic runoff dimensions to drains, as opposed to test plots at academic

research campuses or laboratories. The seven green roofs that were studied are located on a variety of building sites and represent all common extensive green roof installation types, including the vegetated mat, built up, and modular tray systems. Monitored drainage areas ranged from 38 m<sup>2</sup> to about 1275 m<sup>2</sup>. Water quantity performance was measured and analyzed over a 22-month period for six green roofs, while water quality performance was measured and analyzed over a 16-month period for five green roofs. In what follows, overall conclusions and recommendations from the study are summarized in Chapter 2. Next, Chapter 3 describes the monitoring sites and systems used in the work, while Chapters 4 and 5 provide results from the water quantity and water quality performance monitoring, respectively. Chapter 6 then presents an investigation into a new cost-effective method for green roof hydrologic monitoring, based on substrate moisture (SM) measurements, which has potential for wide scale implementation. SM measurements collected from two green roofs over an 11-month period were used to test the method. Finally, a list of references cited in the text is provided in Chapter 7. Additional tables and figures are contained in the appendices of this report. Appendix A contains a list of equipment at each green roof monitoring site, Appendix B contains a summary of the water quality measurements, while Appendix C contains water quality statistical analysis results.

## Chapter 2 Overall Conclusions and Recommendations

### 2.1 Conclusions

The following conclusions are based on evaluations over two consecutive growing seasons that were obtained from measurements made on seven extensive green roofs in NYC, which shares the cold dominant climate of the continent but has hot summers ( $> 22\text{ }^{\circ}\text{C}$ ) and no discernible dry season (Köppen-Geiger climate classification) (Peel et al. 2007). The roofs that were part of this study are: W115 (a vegetated mat system with a monitored drainage area of  $99\text{ m}^2$  and a substrate depth of 32 mm), W118 (a vegetated mat system with a monitored drainage area of  $310\text{ m}^2$  and a substrate depth of 32 mm), USPS (a built up system with a monitored drainage area of  $390\text{ m}^2$  and a substrate depth of 100 mm), Fdston (a built up system with an estimated monitored drainage area of  $1275\text{ m}^2$  and a substrate depth of 100 mm), BDCA (a tray system with a monitored drainage area of  $112\text{ m}^2$  and a substrate depth of 115 mm) and Regis (a built up systems with two monitored drainage areas of  $38\text{ m}^2$  and a substrate depth of 100 mm).

#### *Water Quantity Study*

Our data indicate that total green roof runoff is strongly correlated to total event precipitation, where the coefficients of determination ( $r$ -squared values) are 0.83 or higher depending on the roof and modeling approach. Our data also show that the percent of green roof rainfall captured decreases with increasing event size. The CRE (Characteristic Runoff Equation) and CN (Curve Number) methods described in Chapter 4 may be used to empirically model long-term green roof water retention performance based only on historic rainfall records, or even projected events from climate change modeling.

During our study period, continuous rainfall and runoff data were collected from six of the seven green roofs between June 2011 and March 2013 (all but Fdston). An in-depth analysis was conducted for four of these roofs: W115, W118, USPS and ConEd. Reliable runoff data from these roofs were obtained from 520 rainfall events ranging from 0.25 to 180 mm in rainfall depth. From our analysis of these events, we determined 62% overall rainfall retention during the 23-month period for W115, 42% for W118, 56% for USPS, and 59% for ConEd. Using the CRE methodology in conjunction with 40-years of historic rainfall records for New York City's Central Park, we estimated the range of annual rainfall capture of the four green roofs to lie between 43-60% for W115, 37-51% for W118, 49-66% for USPS, and 47-61% for ConEd during the modeling period. The CN method predicted higher retentions than the CRE method. Differences between the observed retentions during the study period and those predicted using 40-years of historic rainfall data are attributed to different frequencies in storm sizes between the monitoring period and the historic data. For example, during the study period the average rainfall retention on W115 was higher than that modeled due to a lower frequency of large storms than average on this roof during the study period. The curve number (CN) method, which is a widely used method developed by the Natural Resources Conservation Service (NRCS), could not predict observed variation in comparative green roof performance between storm sizes, whereas the CRE method did. Factors driving differences in performance between the four green roofs are thought to be substrate depth, water holding capacity, and the size and location of non-vegetated areas, i.e. effects of impervious area or other hydrological factors, on each rooftop area.

#### *Water Quality Study*

We performed a 16-month water quality survey of precipitation, and stormwater runoff from five of the seven green roofs (W115, W118, USPS, ConEd and Fdston) and nearby nonvegetated (control) roofs to determine the impact of increased green roof establishment on stormwater runoff quality in an urban environment. The water quality indicators measured included: pH, conductivity, turbidity, apparent and true color, ammonium, nitrate, calcium, potassium, magnesium, phosphorus, aluminum, arsenic, boron, barium, cadmium, chromium, copper, iron, manganese, sodium, nickel, lead and zinc.

The key findings of this portion of the study are i) green roofs neutralize acidic precipitation, ii) nitrate concentration in runoff from the green roofs was lower than that from the control roofs, iii) concentrations of macronutrients, such as

calcium, potassium and magnesium, were higher in green roof runoff than control roof runoff, iv) concentrations of micronutrients observed in green roof and control roof runoff were very low, with the exception of sodium and iv) no significant concentrations of heavy metals were detected in green roof or control roof runoff with the exception of boron at the W118 green roof, which is attributed to pesticide use at the site. While there appears to be more chemical constituents present in green roof runoff than control roof runoff, there is an overall reduction in the volume of runoff from green roofs. Thus, the total mass of nutrient runoff from green roofs is less than that from non-vegetated roofs. As a result, the water quality benefits of green roofs are favorable in urban environments.

### ***Soil Moisture Water Balance Study***

The results from the investigation into a new cost-effective method for green roof hydrologic monitoring indicate that a soil water balance approach using monitored precipitation and SM content, such as the proposed method introduced in Chapter 6, can provide a low-cost and low-maintenance alternative to typical systems used for quantifying green roof runoff. This approach also has potential for estimating green roof ET. The preliminary case study conducted on the W115 and W118 green roofs, which was evaluated using the Nash-Sutcliffe statistical method, yielded Nash-Sutcliffe Efficiency coefficients for estimated runoff ranging between 0.72 and 0.88 at daily time aggregates. While any time aggregate can be used with SWAM, time spans of 24 hours yielded the best results. It was observed that there might be biases in the soil moisture probe readings – affecting the runoff and ET estimates – caused by instrument temperature sensitivities as well as instrument location. While these biases were observed, they have not yet been systematically investigated nor corrected.

## **2.2 Recommendations for Further Study**

The work presented in this report confirms that deploying green roofs on existing buildings can reduce the negative impacts of urban WWF, including water quality and water quality impacts. Nonetheless, meaningful urban WWF abatement in many municipalities will require implementation of green infrastructure options beyond extensive green roofs because aggregate street level impervious area significantly exceeds aggregate rooftop area. Study of the hydrological performance of green streets, expanded tree pits, bioswales and other green infrastructure interventions, which are rapidly being adopted in many US cities, is therefore critical to fully understanding the role of green infrastructure in addressing urban stormwater issues. Expansion of the work presented here to wider green infrastructure systems is therefore recommended, including exploration of the SWAM, or an alternative method, for wide spread monitoring of urban green infrastructure performance. In addition, continued monitoring of the urban green roofs that were part of this project would provide the data needed to understand the evolving performance of urban green roofs with age, as well as the role of seasonality in green roof hydrology. Other recommendations include undertaking relative cost-benefit analysis of green roofs versus other stormwater management technologies, more research experiments considering driving factors for water control such as substrate depth and water holding capacity, and continued studies that will optimize design with respect to maintenance and performance.

## Chapter 3 Monitoring Sites and Systems

### 3.1 Green Roofs and Monitoring Equipment

The following table provides a summary of the green roof installations that were monitored as part of this study. The installations span a variety of commercially available green roofs. The green roof components in each case were all provided and installed by various and independent green roofing companies (Table 3-1). Figure 3-1 illustrates the locations of the green roof sites, which are distributed throughout NYC with a majority of the sites falling within priority combined sewer sheds.

Table 3-1: Summary of Monitored Green Roof Sites

Site	W115	W118	USPS	ConEd	Fdston	BDCA	Regis
Construction Type	Vegetated mat	Vegetated mat	Built up roof	Modular tray	Built up roof	Modular tray	Built up roof
Manufacturer	Xero Flor America	Xero Flor America	Tecta Green	GreenGrid Roofs	American Hydrotech	Liveroofs	Greensulate
Year Built	2007	2007	2009	2008	2007	2010	2010
Substrate Depth (mm)	32	32	100 (200 berms)	100	100	115	100
Vegetation Type	<i>Sedum</i> mix	<i>Sedum</i> mix	<i>Sedum</i> mix and natives	<i>Sedum</i> mix	<i>Sedum</i> mix and natives	<i>Sedum</i> mix	Natives
Monitored Watershed Area (m <sup>2</sup> )	99	310	390	940	1275 (assumed)	112	38
Watershed Vegetated (%)	58	53	67	52	50	65	65
Monitoring Conducted	Runoff Quantity and Quality	Runoff Quantity and Quality	Runoff Quantity and Quality	Runoff Quantity and Quality	Runoff Quality	Runoff Quantity	Runoff Quantity

The investigation into the hydrological performance of the urban green roofs involved three monitoring components: monitoring of (i) *environmental conditions*, (ii) the *quantity of roof runoff* and (iii) the *water quality of roof runoff*.

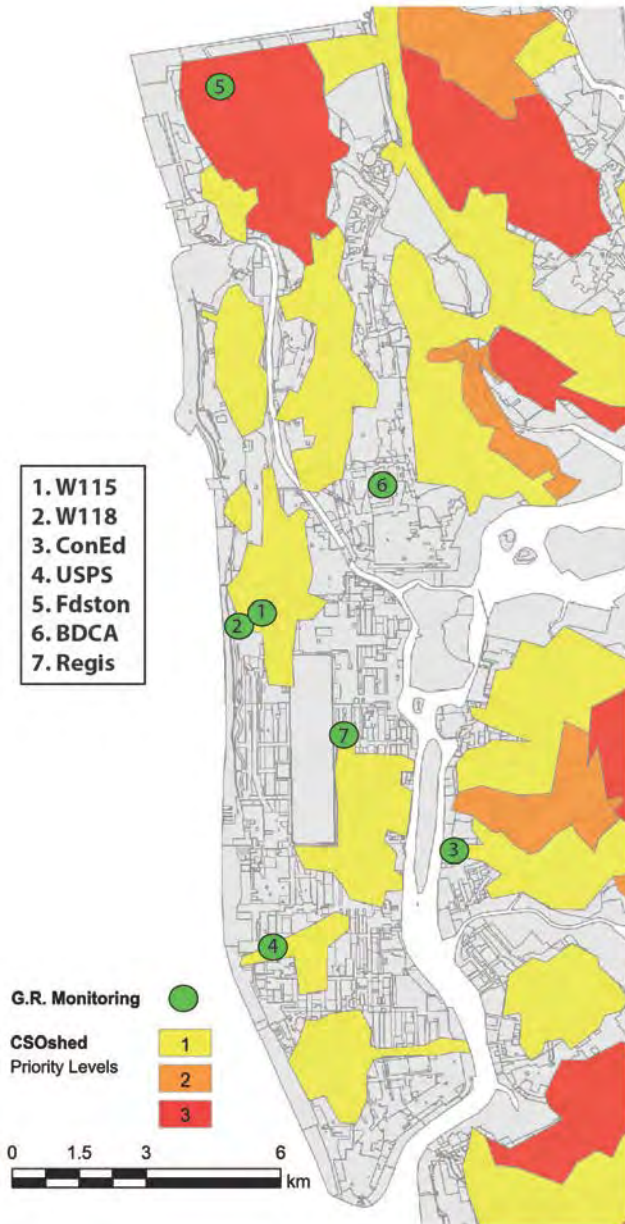


Figure 3-1: Locations of monitored green roof sites and priority combined sewer sheds in New York City

The monitoring of environmental conditions was conducted using weather stations installed on each roof. Measurements of precipitation, runoff, temperature, radiation, humidity, and wind speed and direction were undertaken at the studied green roofs. Monitoring equipment budgets varied for each roof and thus sensor selection was not identical everywhere. Tables in Appendix A provide a description of monitoring equipment installed at each green roof site. Data from the equipment was stored by on-site data loggers at 5-minute intervals. For equipment connected to Wi-Fi or GSM Cellular HOB0 U30 data loggers, sample readings were taken every second and five minute averages were recorded and wirelessly uploaded to the Onset Hobolink data service every hour. Data were then accessible on-line via the Hobolink service. For the equipment connected to the Campbell Scientific data loggers, the data were stored on site and needed to be downloaded from the data logger at periodic intervals. The quantity of roof runoff was measured through use of custom drainage pipe weir devices created for each roof. The quality of roof runoff was measured through lab analysis of manually collected water samples. The methodologies for runoff quantity and quality measurements are further discussed in Chapters 4 and 5, respectively.

### 3.2 Green Roof Site Descriptions

The following paragraphs provide images and descriptions of the study's monitored rooftops. Figure 3-2 through Figure 3-9 consist of: (A) satellite images of each roof (Courtesy Google Maps), with locations of green roof water quantity measurements (VG#), as well as, green roof and control roof water quality measurements (QG and QC, respectively) and drainage areas monitored for green roof water quantity are denoted by the dotted lines; (B) photographs of the weir devices used to measure green roof water quantity (if present); (C) photographs of the roof taken on-site.

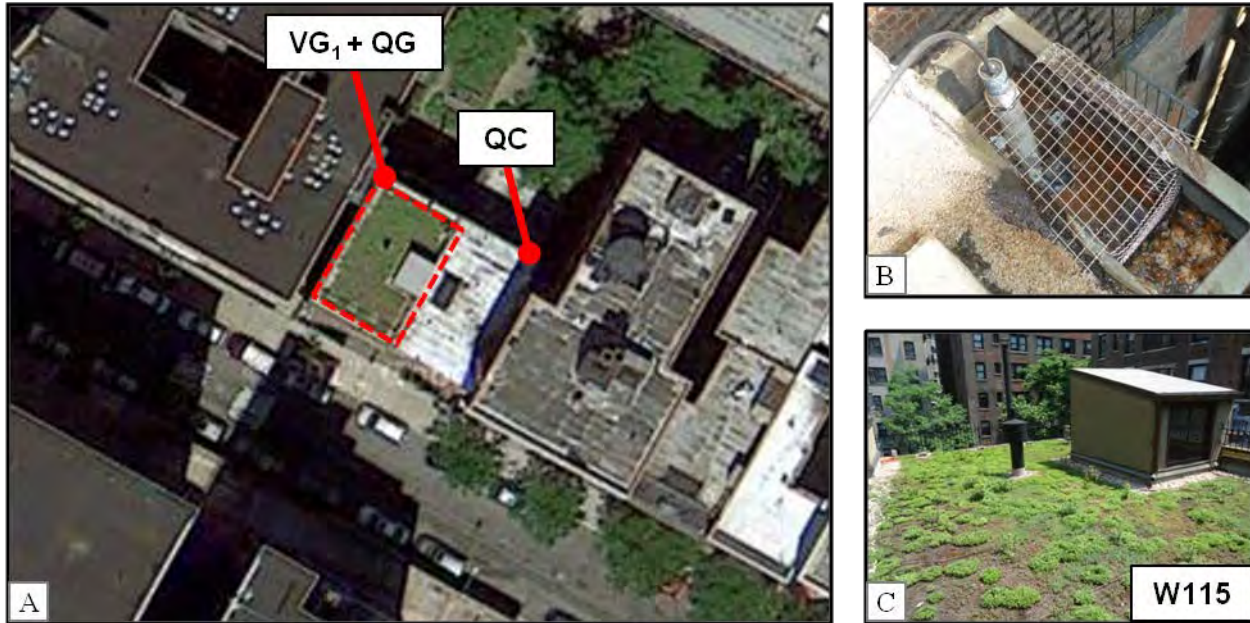


Figure 3-2: W115 Roof (A) Satellite photograph (B) Weir device (C) Roof photograph

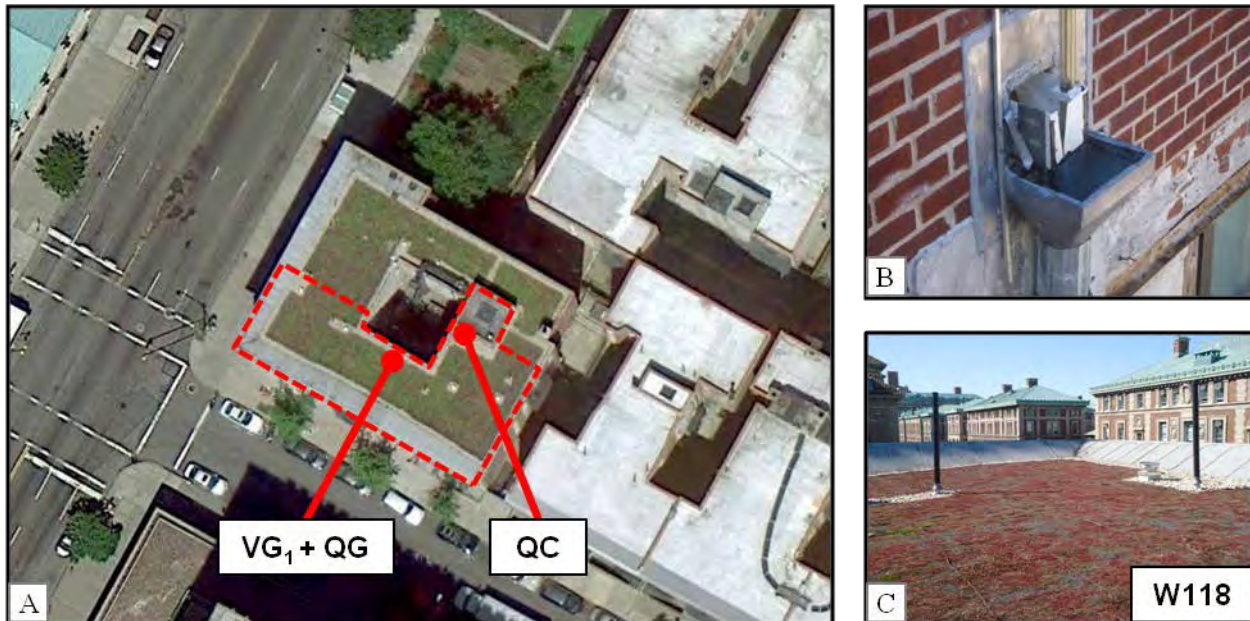


Figure 3-3: W118 Roof (A) Satellite photograph (B) Weir device (C) Roof photograph

**W115 and W118:** The 635 West 115<sup>th</sup> Street building (W115 - Figure 3-2) houses the Columbia University Office of Environmental Stewardship, while the 423 West 118<sup>th</sup> Street building (W118 - Figure 3-3) is a Columbia University graduate student residence. In 2007, a pre-vegetated mat, Xero Flor America's XF301+2FL green roof system, was retrofitted on both buildings. This system consists of a 32 mm thick pre-vegetated mat, supported by two 6 mm thick

water retention fleeces created from recycled synthetic fibers, a 19 mm non-woven polymer drainage mat, and an 0.5 mm polyethylene root barrier. A variety of *Sedum* species, such as *Saxifraga granulata*, *Sedum acre*, *Sedum album*, *Sedum ellacombianum*, *Sedum hybridum* 'Czars Gold', *Sedum oregonum*, *Sedum pulchellum*, *Sedum reflexum*, *Sedum sexangulare*, *Sedum spurium* var. *coccineum*, *Sedum stenopetalum*, are present on these roofs. The growing substrate on these roofs has a water-saturated density of 1.37 g/cm<sup>3</sup>, water storage capacity of 37.1%, and a saturated hydraulic conductivity of 0.021 cm/s, as reported by Hummel and Co., Inc in April 2007. The W115 green roof has a single 99 m<sup>2</sup>, 58% vegetated watershed connected to an exterior parapet downspout. The 600 m<sup>2</sup> W118 total roof area consists of two watersheds connected to exterior parapet downspouts, of which the 310 m<sup>2</sup>, 53% vegetated drainage area of the Southeast watershed was monitored for rainfall and runoff. Gravel walkways, parapets, and the raised rooftop above the elevator shaft comprise the non-vegetated areas of both rooftops.

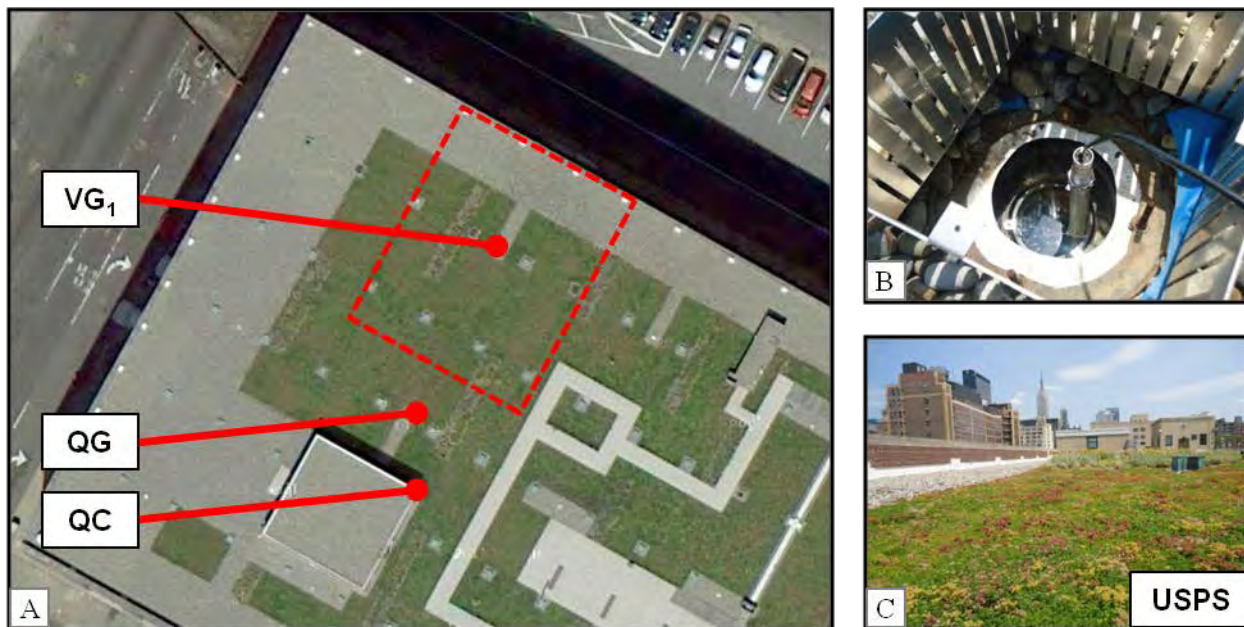


Figure 3-4: USPS Roof (A) Satellite photograph (B) Weir device (C) Roof photograph

**USPS:** Figure 3-4 shows the 10,000 m<sup>2</sup> US Postal Service Morgan Processing and Distribution Center (USPS) green roof in mid-Manhattan, which was installed in 2009 by TectaGreen of Tecta America. The roof was built in-place. Roof edges were established with 100 mm tall metal brackets, and an expanded shale based substrate of varying depth was placed in the bounded area. A majority of the green roof is comprised of 100 mm of substrate depth and was planted with *Sedum* species, including: *Sedum acre*, *Sedum album* 'Coral Carpet', *Sedum album murale*, *Sedum reflexum*, *Sedum sexangulare*, *Sedum reflexum* 'Blue Spruce', *Sedum grisebachii*, *Sedum kamtschaticum*, *Sedum* 'Matrona', *Sedum pluricaule* 'Rosenteppich', *Sedum spurium* 'Roseum', *Sedum telephium* 'Autumn Joy'. Additionally, the 200 mm deep berms throughout the roof, usually about 2 m wide, have the following larger plant species: *Achillea filipendula* 'Moonshine', *Alium schoenoprasum*, *Coreopsis vert* 'Moonbeam', *Silene caroliniana* ssp. *wherryi*, *Talinum calycinum*, *Tradescantia ohiensis*. The growing substrate has a water-saturated density between 1.15-1.35 g/cm<sup>3</sup>, water storage capacity between 35-65%, and a saturated hydraulic conductivity between 0.001-0.120 cm/s, as reported by Skyland USA LLC in March 2011. Monitoring equipment was installed in a 390 m<sup>2</sup> watershed in the Northwest corner of the roof. The watershed has one 6 m long berm and a single internal downspout. The watershed is 67% vegetated with the remaining area consisting of gravel ballast.

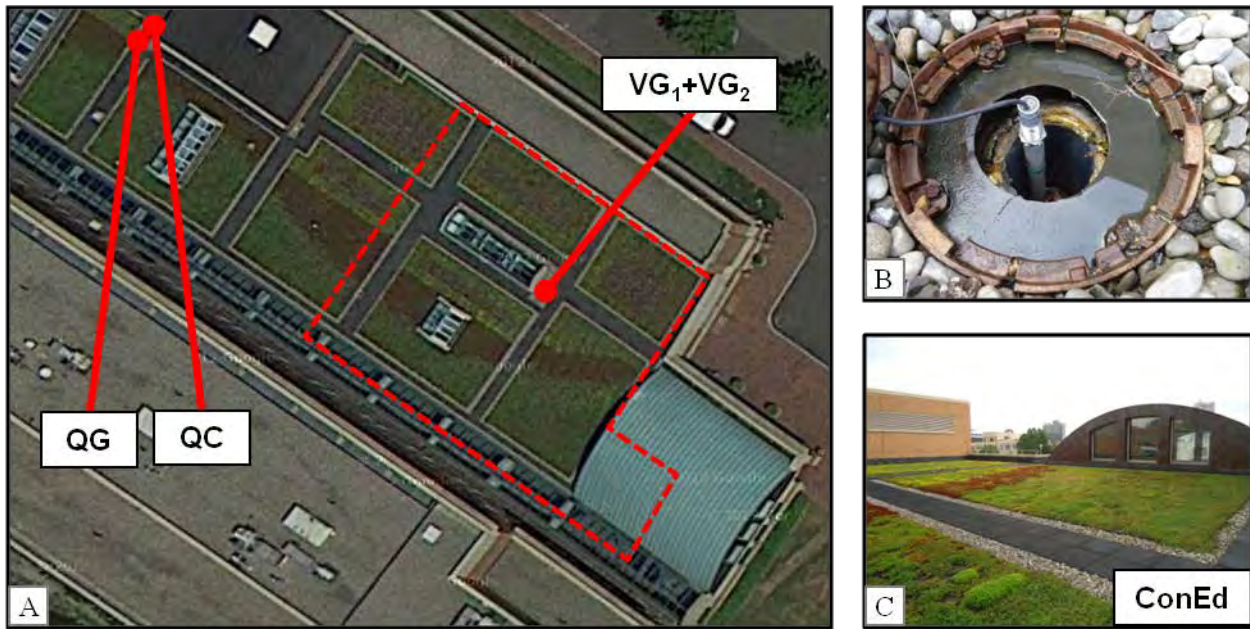


Figure 3-5: ConEd Roof (A) Satellite photograph (B) Weir device (C) Roof photograph

**ConEd:** ConEdison Learning Center (ConEd) green roof in Queens (Figure 3-5), which was installed in 2008, consists of GreenGrid-G2 modular trays with dimensions 61 cm x 122 cm x 10 cm. The trays were packed with a proprietary expanded shale substrate and then placed in adjacent rows on the 2,700 m<sup>2</sup> roof area. The growing substrate has a water-saturated density of 1.18 g/cm<sup>3</sup>, water storage capacity of 31.8%, and a saturated hydraulic conductivity of 0.326 cm/s, as reported by Penn State University's Agricultural Analytical Services Laboratory in July 2008. Plugs and cuttings used to plant were comprised of the following 15 *Sedum* varieties: *Sedum oreganum*, *Sedum kamtschaticum* 'Weihenstephaner Gold', *Sedum kamtschaticum*, *Sedum ternatum*, *Sedum* 'John Creech', *Sedum spurium* 'Album Superbum', *Sedum spurium* 'Fulda Glow', *Sedum spurium* 'Dragons Blood', *Sedum spurium* 'Bronze Carpet', *Sedum angelina*, *Sedum sexangulare*, *Sedum* 'Ruby Glow', *Sedum* 'pachclados', *Sedum* 'Bertram Anderson', *Sedum* 'Vera Jameson'. Monitoring equipment for this study was installed in the 52% vegetated, 940 m<sup>2</sup> Eastern watershed. Both of the watershed's internal downspouts were monitored for runoff. The non-vegetated sections of this roof are comprised of rubber mat walkways, gravel ballast transitions and raised glass skylights.

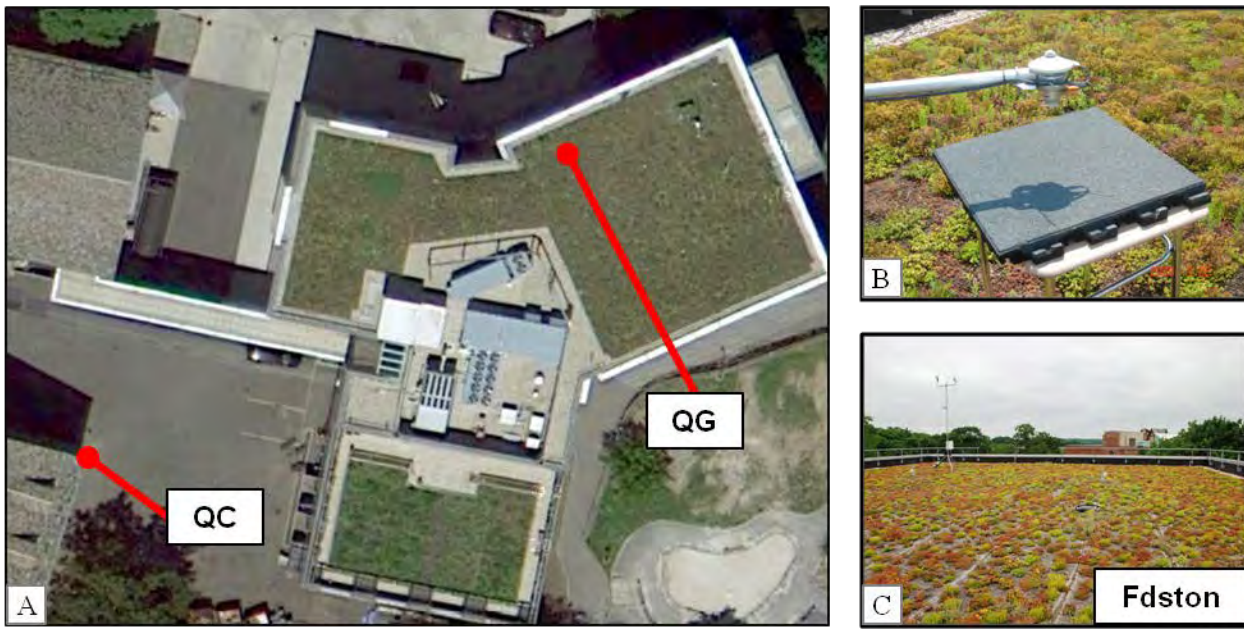


Figure 3-4: Fdston Roof (A) Satellite photograph (B) Equipment (C) Roof photograph

**Fdston:** The Ethical Culture Fieldston School (Fdston), which teaches K-12, has been operating in the Bronx location since 1929. In early 2007 the school began construction of a new middle school building and this provided the opportunity to install two different built up green roofs (Figure 3-4(A)). The green roof installer was the Town and Garden landscaping firm. The larger green roof, which is 5100 m<sup>2</sup> in area with 100 mm of substrate depth, was monitored for water quality only. This roof has four drains, and it is assumed (but not confirmed) that the monitored watershed is 1275 m<sup>2</sup>, i.e. one quarter of the 5100 m<sup>2</sup>. Plants on the roof were installed as plugs in August 2007. The six planted species are: *Sedum album*, *Sedum sexangulare*, *Sedum reflexum*, *Sedum floriferum*, *Sedum hybridum* and *Sedum spurium*. The growing substrate has a water-saturated density of 1.34 g/cm<sup>3</sup>, water storage capacity of 42%, and a saturated hydraulic conductivity of 0.119 cm/s, as reported by Penn State University’s Agricultural Analytical Services Laboratory in May 2007. Growing substrate particle sizes ranged from 0.02 mm to 9.5 mm with the maximum percentage (30%) ranging from 3.2 to 6.3 mm and had an organic mass content of 4.2%. The Fieldston roof is about 50% vegetated, with non-vegetated areas consisting of paved walkways and mechanical equipment.



Figure 3-5: BDCA Roof (A) Satellite photograph (B) Weir device (C) Roof photograph

**BDCA:** The Bronx Design and Construction Academy (BDCA) is a public career and technical education high school located in the Bronx, NY. The 215 m<sup>2</sup> hybrid modular tray green roof in the building's courtyard was constructed in the fall of 2010 by SmartRoofs, LLC, a division of Sustainable South Bronx (Figure 3-5). The roof structural capacity and waterproof membrane condition were evaluated prior to installation. Liveroofs' standard system, consisting of an engineered substrate placed within 25 x 50 x 8 cm trays, was used for the tray system. The trays were overfilled with substrate to 100 mm, with the help of temporary side walls. The plant species, grown from plugs and cuttings by Prides Corner Farms, consist of: *Euphorbia myrsinites*, *Sedum acre* 'Aureum', *Sedum album* ('Coral Carpet', 'Green Ice', and 'Chloroticum'), *Sedum sexangulare*, *Sedum spectabile* ('Brilliant', 'Stardust', and 'Neon'), *Sedum spurium* ('John Creech', 'Summer Glory' and 'Royal Pink'), *Allium senescens ssp. montanum*, *Sedum vera jameson*, *Sempervivum* 'Ruby Heart', *Sedum immergrunchen*, *Sedum* 'Angelina. Once filled and planted, the trays were transported to the roof location, and placed directly on top of the roof's gravel ballast. After all trays were placed, the temporary side walls were removed to create a seamless roof and a barrier was installed at the green roof borders to keep the substrate intact. The growing substrate has a water-saturated density of 1.44 g/cm<sup>3</sup>, water storage capacity of 48.3%, saturated hydraulic conductivity of 0.018 cm/s, organic matter content of 4.5%, and a small (<0.05 mm) particulate concentration of 6.1%, as reported by Penn State University's Agricultural Analytical Services Laboratory in March 2008. The runoff quantity was monitored from the southern 112 m<sup>2</sup> drainage area, which is 65% vegetated. The non-vegetated roof areas consist of gravel ballast.

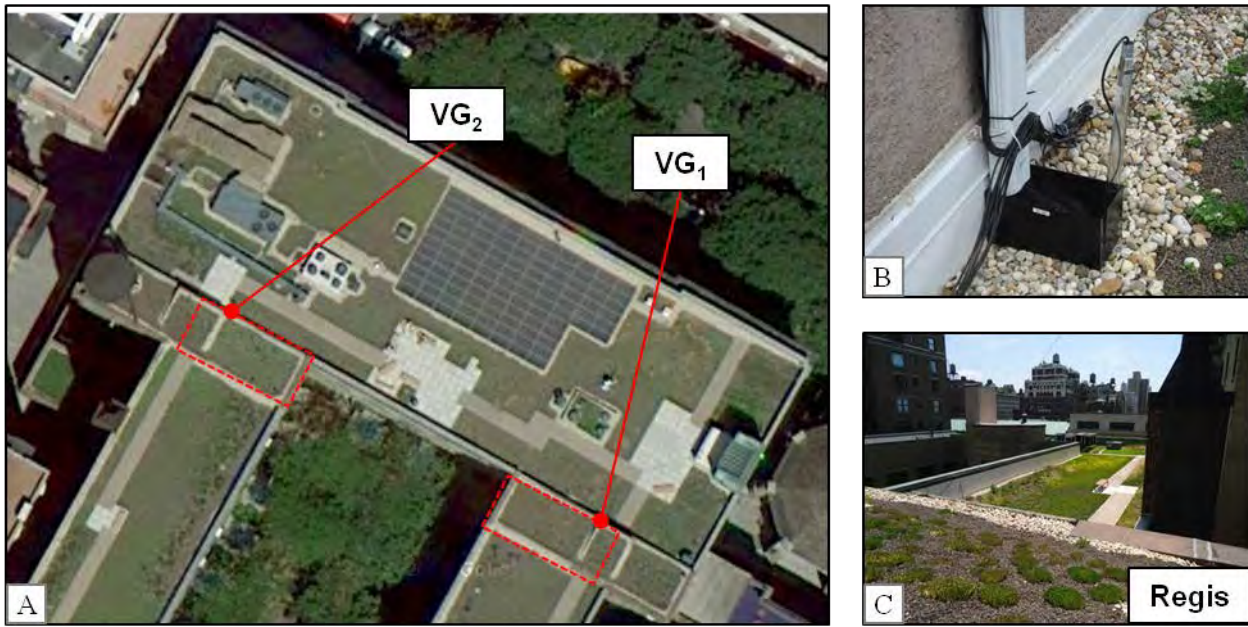


Figure 3-6: Regis Roof (A) Satellite photograph (B) Weir device (C) Roof photograph

**Regis:** Regis High School (Regis) is a private school established in 1914 and located on the Upper West Side of Manhattan, NY. The school's 2000 m<sup>2</sup> hybrid green roof was installed in August 2010 (Figure 3-6). The roof was constructed onsite by Greensulate, who established roof layers before adding an extensive green roof substrate designed and manufactured by Long Island Compost Corp. The monitored water quantity runoff sites consist of two 38 m<sup>2</sup> elevated roof sections with a 100 mm substrate depth. These areas are 65% vegetated, where nonvegetated areas consist of gravel ballast. Dr. Matthew Palmer of Columbia University chose the native plant species, by considering two native shallow substrate environments. The species consist of: *Asclepias tuberosa*, *Baptisia tinctoria*, *Eupatorium hyssopifolium*, *Panicum virgatum*, *Schizachyrium scoparium*, *Solidago nemoralis*, *Sorghastrum nutans*, *Symphytotrichum leave*, *Danthonia spicata*, *Dechampsia flexuosa*, *Dichanthelium clandestinum*, *Eupatorium sesslifolium*, *Lespedeza hirta*, *Pycnanthemum tenuifolium*, *Rudbeckia hirta*, and *Solidago odora*.

## Chapter 4 Water Quantity Study

### 4.1 Introduction

To date, the most cited aspect of green roof behavior is the ability of green roofs to capture rainfall and limit the generation of stormwater runoff. Typically this behavior is quantified using a mass balance approach, where rainfall and runoff are continuously measured and the performance of a system is reported as the total percent of rainfall retention over a given monitoring period. Using this strategy, researchers have reported rainfall retentions of extensive green roofs between 12% and 86% (Hutchinson et al. 2003; De Cuyper et al. 2004; Liu and Minor 2005; Moran et al. 2005; VanWoert et al. 2005; Connelly et al. 2006; Toronto and Region Conservation Authority 2006; Getter et al. 2007; Teemusk and Mander 2007; Hathaway et al. 2008; Kurtz 2008; Spolek 2008; Berghage et al. 2009; Bliss et al. 2009; DiGiovanni et al. 2010; Berghage et al. 2010; Voyde et al. 2010; Gregoire and Clausen 2011; Nardini et al. 2011; Palla et al. 2011; Schroll et al. 2011; Stovin et al. 2012; Carson et al. 2013; Fassman-Beck et al. 2013; Morgan et al. 2013). The large range of reported performance highlights the wide variety of green roof configurations and the multitude of parameters that impact green roof water retention capacity. Considering this, there is a need to quantify the relationships between green roof parameters, storm characteristics and rainfall retention in order to (1) develop industry standards that optimize green roof systems, (2) create more accurate methods for evaluating stormwater management benefits prior to green roof installation and (3) understand the overall potential contribution of widespread adoption of green roofs to urban WWF abatement.

Studies have shown that rainfall capture is influenced by a green roof's substrate depth (De Cuyper et al. 2004; VanWoert et al. 2005), rooftop slope (VanWoert et al. 2005; Getter et al. 2007), areal plant coverage (Berghage et al. 2009; Morgan et al. 2013), plant type (Nardini et al. 2011; Starry 2013), drainage configuration (Berghage and Gu 2009), orientation (Mentens et al. 2003), and location of non-vegetated spaces (Carson et al. 2013). These parameters are generally well reported in green roof literature. However, in addition to characteristics of the green roof itself, climate based factors, such as rainfall event intensity (Villarreal 2007), event size (Berghage et al. 2009), and temperature (Schroll et al. 2011), were found to effect retention. Rainfall event size in particular has been shown to significantly impact reported performance since rainfall retention may vary widely on a per event basis (Stovin et al. 2012). For instance, a study undertaken during a period of mostly small events (<10mm), where retention can be between 80-100%, will report a much better performance than a study with mostly large events (50mm+), where retention might only range from 20-40% (Carson et al. 2013). As a result, it is difficult to make comparisons between studies, even those in similar climates, without a methodology that eliminates the impacts of event variability between studies.

At present, there are two main empirically-based methods for describing the variation of green roof rainfall retention by event size; namely, the curve number (CN) method developed by the NRCS and the characteristic runoff equation (CRE) method recently proposed in Carson et al. 2013. Both methods relate rainfall to green roof runoff and, therefore, may be coupled with historic rainfall data to simulate green roof performance for any number of years. In addition, these methods could also be coupled with climate change forecasts to predict future green roof performance under changing weather patterns. Theoretically, if the CN or CRE were known for multiple green roofs, the impact of widespread green roof adoption on urban WWF mitigation could be explored.

In what follows, hydrologic observations related to *water quantity* are presented for four of the full-scale, extensive green roofs described in Chapter 3, namely W115 (vegetated mat), W118 (vegetated mat), USPS (built up roof), and ConEd (modular tray). The dataset includes information collected from 520 storm events occurring between June 2011 and April 2013, which were used to determine a CRE and CN for each green roof. To estimate the multi-year performance of the green roofs, 40 years of NYC historic precipitation data were used as input to the CRE and CN methods, and predictions from the methods were compared to the measured results as well as to each other. Additionally, preliminary observations from monitoring of BDCA (modular tray) and Regis (built up roof), which do not have sufficient data to perform a historic analysis, are presented. The Chapter ends with a discussion of results and summary conclusions.

## 4.2 Methodology

The W115, W118, USPS, and ConEd green roofs were instrumented to collect a variety of environmental data as described in Chapter 3 and Appendix A. Stormwater attenuation behavior was evaluated using a mass balance approach where rainfall and runoff were measured using a tipping bucket rain gauge and a custom-built weir device, respectively.

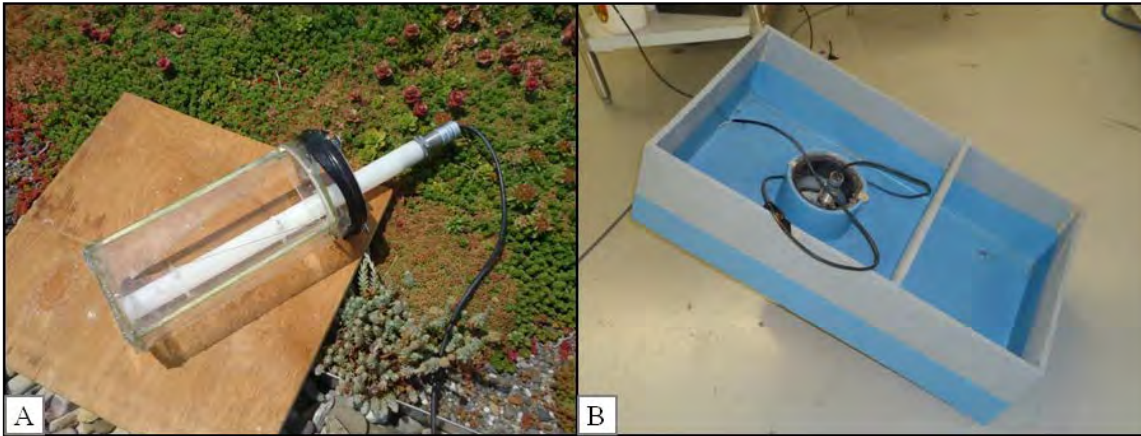


Figure 4-1: (A) Runoff monitoring weir device (B) Calibration chamber used to simulate rooftop runoff.

The weir devices for runoff measurement consist of a runoff chamber with an outlet weir and a Senix TSPC-30S1 ultrasonic sensor, Figure 3-2(A). The ultrasonic depth sensor measures the depth of water behind the weir face as water discharges with a resolution of 0.086 mm, which translates to about 3 ml/min. As flow increases, the water level behind the weir's face rises. The ultrasonic sensor detects the rise in water height and adjusts its output voltage accordingly. The weir devices were sized to fit into existing rooftop downspouts (or parapet drain in the case of W118, Figure 3-3(B)) and accommodate roughly 50 mm/hr of rainfall in saturated substrate conditions based on the drainage area. Above this flow rate, water overflows the weir into the roof drain to prevent backup and ponding of water on the roofs. Each weir was constructed by cutting acrylic parts and joining them with Scotch-Weld DP-810NS acrylic epoxy. The weir face was cut from a flat piece of acrylic and attached to a vertical cutout on the side of the weir cylinder. A baffle was installed at the top of the device and rubber based sealant was applied on all edges to minimize turbulence and eliminate leaks without restricting water flow. The weir devices function between 0° to 70°C. To calibrate each weir, a box was built that effectively simulates water flow conditions into roof drains, Figure 3-2(B). Weirs were sealed into the simulation box, as they would be under field conditions, and calibrated up to their designated maximum capacity. Water was pumped into the simulation box, flowed under the baffle, then rose up to enter the weir from all directions. Repeat measurements were taken at incrementally increasing flow rates using an Armfield F1-10 hydraulic bench, which was supplemented with a 6 L/s pump at high flow rates. The corresponding voltage output was recorded from the Senix ultrasonic sensor. The resulting data points were used to derive a calibration curve that related sensor output voltage and flow rate. This calibration method significantly reduces errors compared to other techniques that rely on, for example, a combination of measurements at low flow rates and reported weir equations. Once calibrated, weirs were sealed into the rooftop drains to prevent water loss prior to measurement. Finally, the voltage output of the Senix ultrasonic sensor was connected to the rooftop data logger for recording.

For the W115, W118, USPS and ConEd roofs, the rainfall and runoff measurement devices were connected to an Onset Hobo U30 data logger. Sample readings were taken every second and five minute averages were recorded and wirelessly uploaded to the the Onset Hobolink data service every hour. The unique calibration equation for each weir device was then applied to the voltage readings and normalized by the monitored drainage area to determine average runoff depth at each five-minute interval. Continuous data were collected between June 2011 and April 2013, with the exception of several intermittent offline periods due to hurricane safety measures, power loss, or equipment failure.

Individual storm events were determined from resultant data considering a 6-hour “no rainfall” period between storm events. This definition was selected based on Strecker et al. (2002) and has been used by VanWoert (2005), Getter et

al. (2007), Berghage et al. (2009), Voyde et al. (2010) and Stovin et al. (2012), amongst others for green roof studies. For the purpose of this study, an event begins when rainfall is first recorded and ends when no precipitation or runoff has been recorded for six hours. Once individual storms were separated in this manner, storm events considered unsuitable for analyses were discarded based on the following four exclusion criteria: (1) peak runoff rate exceeded 90% of the weir device’s voltage output range, since turbulence at the upper limit of the recordable flow rates distort depth recordings (36 Events); (2) precipitation included snowfall, since the time scale of snowmelt runoff prevents reliable application of the NOAA event definition (19 Events); (3) total event runoff exceeded rainfall, which occurred when leaves and other debris clogged the lower portions of the weir causing elevated runoff readings (29 Events); and (4) sensor recording error, due to the loss of power or equipment failure (24 Events). Following removal of data based on the above criteria, 520 so-called “reliable” storm events were identified from the original 628 recorded events across all four monitored roofs over the approximately 2 year study period. From this point forward, all discussion of observed storm events from the monitoring period is limited to this subset of recorded events deemed reliable for analysis. Event details are provided in Table 4-1.

Table 4-1: Summary of Monitoring Duration and Observed Events.

<b>Abbreviated Name</b>	W115	W118	USPS	ConEd
<b>Data Start</b>	7/11	6/11	6/11	7/11
<b>Data End</b>	10/12	4/13	4/13	4/13
<b># Total Events</b>	127	161	199	141
<b># Reliable Events</b>	105	134	179	102
<b># Events (0-10 mm)</b>	77	84	119	67
<b># Events (10-20 mm)</b>	20	20	30	19
<b># Events (20-30 mm)</b>	4	17	13	10
<b># Events (30-40 mm)</b>	2	3	7	1
<b># Events (40-50 mm)</b>	1	3	1	4
<b># Events (50+ mm)</b>	1	7	9	1

Characteristic Runoff Equations (CREs) for each of the four green roofs were derived according to the methodology presented in Carson et al. 2013. Specifically, for each green roof the recorded rainfall and runoff depth were related to each other using a quadratic regression analysis of all events with non-zero roof runoff. Removal of the zero-runoff storms in creation of the CREs limits the lower-bound overestimation of runoff caused by fitting a large number of small events that generate zero runoff. Each of the CREs is considered applicable for event sizes ranging between the equation’s lowest rainfall value associated with roof runoff and 100 mm of rainfall. The 100 mm cap was selected because of the limited number of events exceeding 100 mm that were recorded during the monitoring period. Thus, green roof retention behavior above this threshold is outside the bounds of this analysis. For the purpose of the evaluation that follows, when rooftop rainfall exceeds 100 mm it is assumed that rooftop storage capacity is reached and a fixed attenuation depth (mm) applies, which is equal to the value of the CRE at 100 mm of rainfall. When rainfall is less than the lowest rainfall value associated with roof runoff, runoff is set to zero.

The CN method uses a series of three equations (eq. 4-1 through 4-3) to estimate runoff depth for any rainfall event, assuming that the CN of a particular watershed is known. In practice, the CN is typically selected from a list of recommended CN, provided in the NRCS technical manual, which range from 30-100 depending on hydrologic soil group, cover type, treatment, hydrologic condition, and antecedent runoff conditions of the watershed (NRCS 1986).

$$Q = \frac{(P - I_a)^2}{P - I_a + S} \quad [4 - 1]$$

$$S = \frac{1000}{CN} - 10 \quad [4 - 2]$$

$$I_a = 0.2(S) \quad [4 - 3]$$

where:

- Q = runoff (in)
- P = rainfall (in)
- S = potential maximum retention after runoff begins (in) and
- I<sub>a</sub> = initial abstraction (in)

In this analysis, a best-fit CN was selected for each of the four green roofs. To do this, a program was written which iterates for all possible CNs and calculates runoff using observed rainfall events as inputs in equation 4-1. When input precipitation was less than the initial abstraction, runoff was set to zero. For each CN, an r-squared value relating the predicted performance and observed runoff was calculated. The CN with the highest r-squared value (i.e. the best fit) for each green roof was then selected for use. It is important to note that only events with non-zero runoff were used for generating the CNs presented in this report in order to maintain consistent methodology between the generation of CREs and CNs for each of the roofs.

As the focus of this study was quantification of behavior of full-scale green roofs, and the CREs and CNs reflect full-scale green roof behavior. The calculated CRE and CN represent composites of the vegetated and non-vegetated areas as full-scale green roof systems always include non-vegetated areas.

Hourly precipitation data, recorded by the Belvedere Castle weather station in Central Park, NYC, were downloaded from the NOAA National Climatic Data Center website ([ncdc.noaa.gov](http://ncdc.noaa.gov)) for the years 1971-2010. These records were used to identify storm events based on the NOAA standard of 6-hour dry weather period between individual events. The historic data were continuous with the exception of November 1983 and December 1983, when hourly data were not available. This analysis of hourly precipitation records resulted in the identification of 4,291 historic precipitation events over the 40-year period.

The historic rainfall events were used for two primary purposes. First, the distribution of events over the 40-year period was compared to the distribution of observed events at each of the W115, W118, USPS and ConEd green roof sites. This comparison helped identify whether the frequency of certain event sizes during the monitoring period were atypical compared to “average” conditions in NYC. Since event size influences the percent of rainfall retained by a green roof, atypical events during green roof monitoring periods need to be called out in reported results. Second, the historic events were used as rainfall inputs to the CRE and CN empirical methods to estimate the total rainfall retention that would be anticipated for each of the green roofs over a 40-year period that reflected rainfall patterns similar to those in Central Park from 1971-2010. Because an identical set of rainfall events was used as input to each of the CRE and CN methods, comparisons between the two methods were possible.

### 4.3 Results

The 520 reliable storm events (Table 4-1) were used for analysis. Rainfall depth of the monitored events lay between 0.25 and 180 mm, while green roof runoff depth (runoff volume divided by monitored drainage area) ranged from 0 to 159 mm. The W115, W118, USPS, and ConEd green roofs retained 62%, 42%, 56%, and 59% of the total rainfall in the monitoring period, respectively. Percent of rainfall retention for individual events ranged widely from 28-100% for W115, 3-100% for W118, 10-100% for USPS, and 13-100% for ConEd. The total number of storm events that generated zero runoff was 33, 49, 83, and 20 for the W115, W118, USPS, and ConEd roofs, respectively; while the largest event

with 100% retention was 3.56 mm, 7.62 mm, 16.51 mm, and 2.03 mm, respectively.

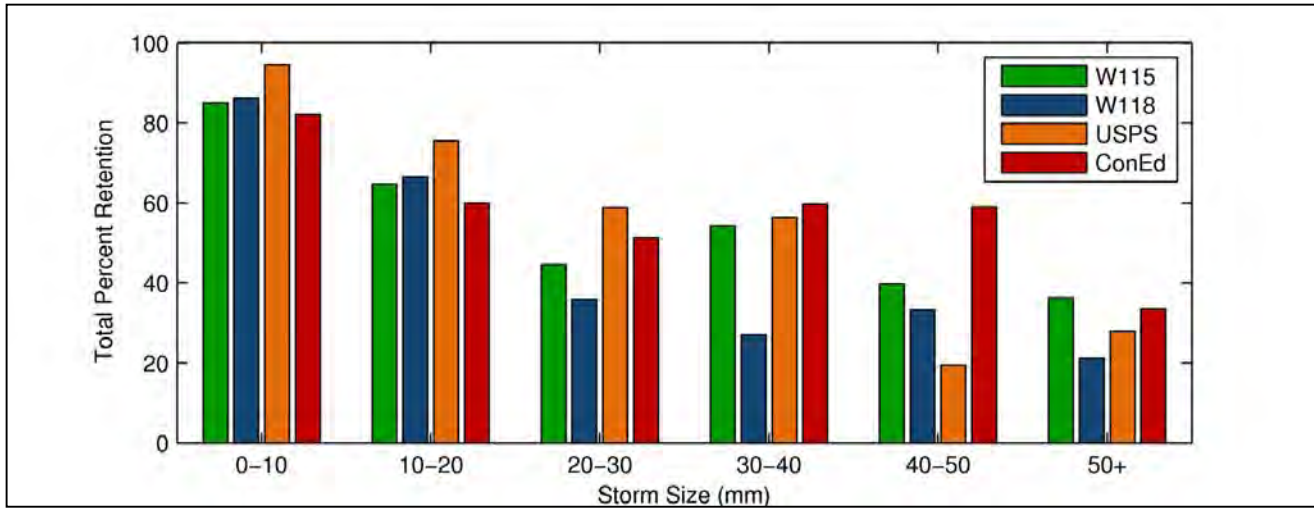


Figure 4-2: Monitored total rainfall retention for the W115, W118, USPS, and ConEd green roofs by event size.

Figure 4-2, shows the total rainfall retention (calculated as the total retention for all events within each size or seasonal category) of each roof for the different storm categories. The figure illustrates that, generally, as rainfall depth increases, the green roof's percent retention is reduced. These results agree with the reported findings of others (Stovin 2010; Berghage et al. 2009; Getter et al. 2007). Total percent retention of storms up to 10 mm was 85%, 86%, 95%, and 82% for the W115, W118, USPS, and ConEd green roofs, respectively. The ConEd modular tray system attenuated less rainfall than the other roofs in the 0-10 and 10-20 mm category, but had better comparative retention performance during larger events (30 mm+). For instance, during storms with 50 mm or more rainfall, the average retention for W115, W118, USPS, and ConEd was 36%, 21%, 28%, and 34% respectively. W115, although the smallest roof, had better overall performance than W118, even though both systems were vegetated mats. This could be due to the higher percent vegetation of W115 (58%) compared to W118 (53%), the differences between the locations of non-vegetated portions of each roof, or the fact that there were fewer larger events recorded on W115; possibly because the taller buildings surrounding W115 create a rain shadow on the W115 roof. The limited numbers of recorded events on W115 above 20 mm (8 Events) undermine the reliability of the W115 retention data for the larger storms. For storms below 20 mm, the W115 and W118 retention performance is similar, although W115 still outperforms W118.

As noted above, the distribution of observed events must be comparable to that of historic precipitation for reported retention to be representative of a green roof's multi-year performance, not accounting for other factors such as substrate consolidation and depletion, changes in plant population and health, etc. Figure 4-3 compares the distribution of rainfall by event size between the 40-year historic data period (Central Park, NYC 1971-2010) and observations during the monitoring period. W115's inflated performance in the 50+ mm category is most likely due to limited recorded events (1%) in that range during the monitoring period, while the green roof's overall performance is influenced by a high number of storms in the 0-10 mm range (73%) (Figure 4-3(A)). Additionally, there is an increased percentage of total volume of events with 50+ mm of rainfall for W118 (48%) and USPS (56%) compared to the historic data (26%). Consequently, the reported overall rainfall retention performance of W118 and USPS during the monitoring period is likely reduced compared to expected multi-year performance.

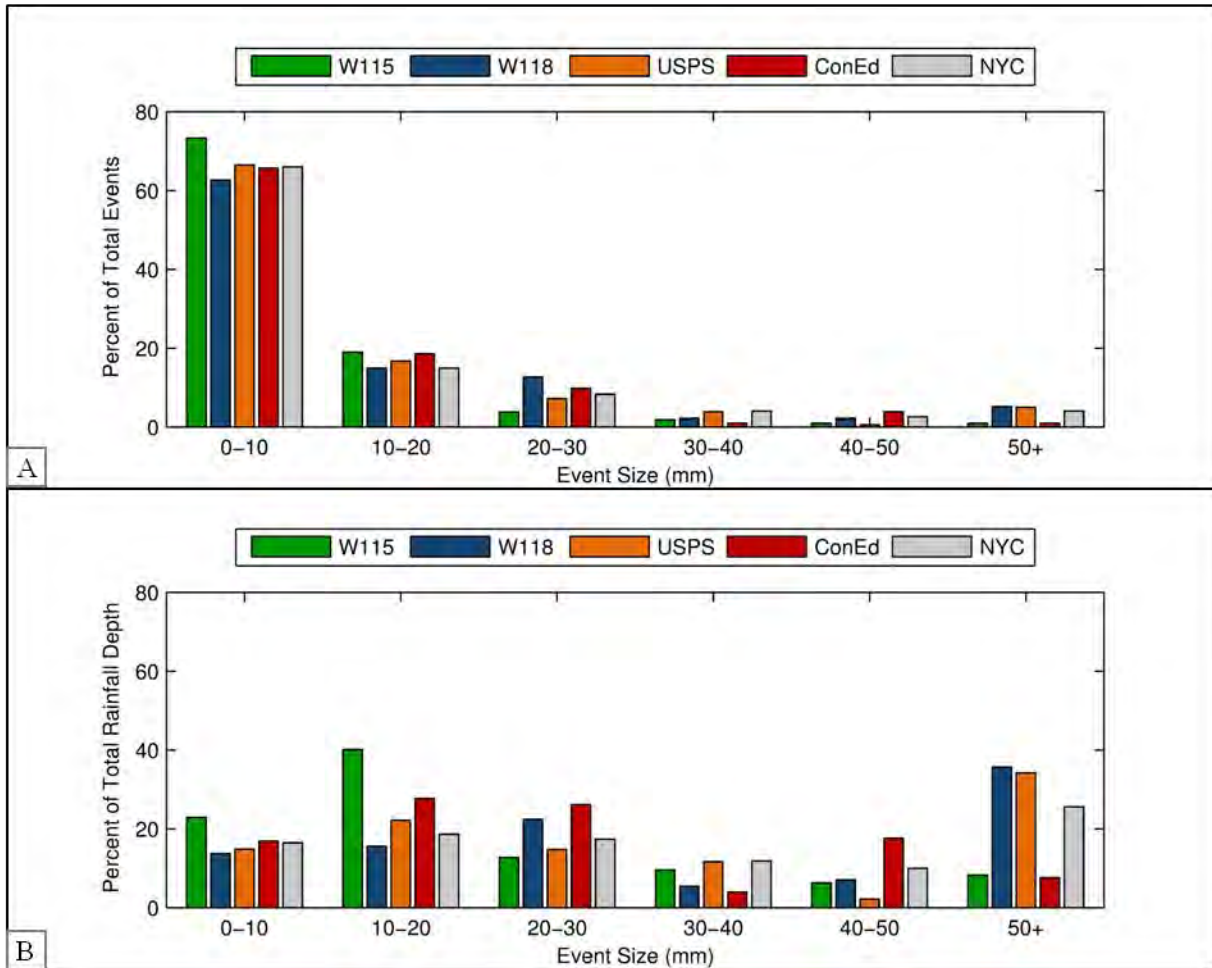


Figure 4-3: Rainfall by event size for monitored and historic (NYC) data as percent of (A) events and (B) depth.

The CREs derived from the monitored storm events (Figure 4-4), were created from regression analyses of events with non-zero runoff. The zero attenuation line in Figure 4-4 represents a hypothetical roof where all precipitation becomes runoff. The CREs have coefficients of determination (r-squared values) of 0.95, 0.97, 0.97, and 0.90 for W115, W118, USPS, and ConEd, respectively. Residuals are randomly distributed where error is likely due to the fact that the CREs do not account for environmental conditions such as temperature, relative humidity and antecedent **SM** conditions that also might impact green roof water balance (Figure 4-5).

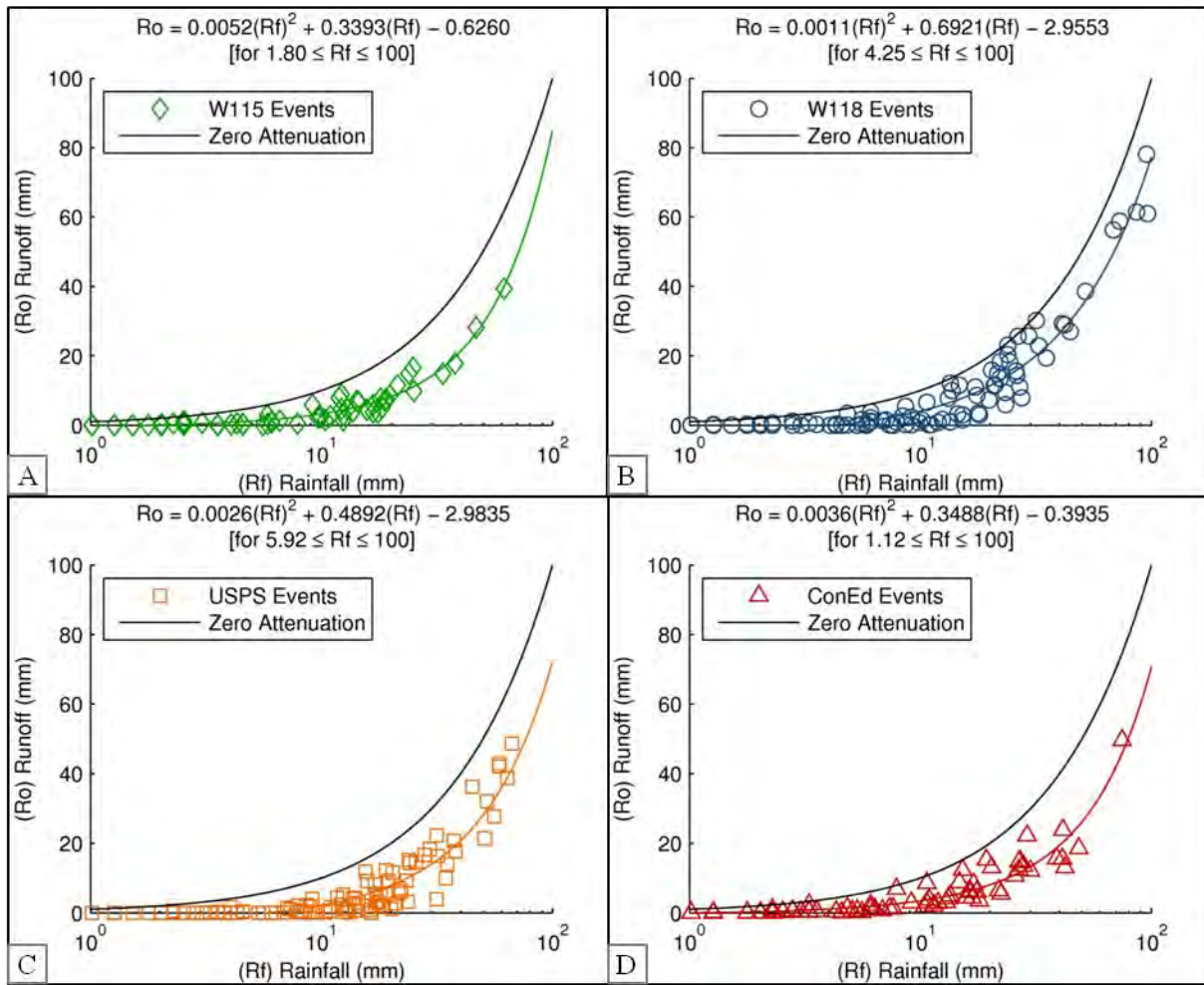


Figure 4-4: Characteristic runoff equations and events for (A) W115, (B) W118, (C) USPS, and (D) ConEd.

The fixed maximum retention depth for storm events in excess of 100 mm for W115, W118, USPS, and ConEd were calculated to be 14.94 mm, 22.64 mm, 27.83 mm, and 29.25 mm, respectively. The x-intercepts of each characteristic runoff curve represent the small event performance for each roof. Based on the CREs, W115, W118, USPS, and ConEd do not generate runoff until 1.80 mm, 4.25 mm, 5.92 mm, and 1.12 mm of rainfall, respectively. According to the derived CREs, USPS will outperform W115 and W118 for all storm sizes, while ConEd will outperform W115, W118, and USPS, in storms greater than 15.39 mm, 7.92 mm, and 21.85 mm, respectively.

The calculated CN, also based on exclusion of non-zero runoff events, were 93.2 for W115, 94.5 for W118, 92 for USPS, and 91.7 for ConEd. In general,  $r^2$  values for the CN method were less than those for the CRE method. The  $r$ -squared values for the CN method were 0.92, 0.96, 0.97, and 0.82 for W115, W118, USPS, and ConEd, respectively. For W118 and USPS, which had similar  $r$ -squared values between methods, errors were randomly distributed, while for W115 and ConEd, The CN method generally under predicted runoff during smaller storms and over predicted runoff during larger events (Figure 4-5).

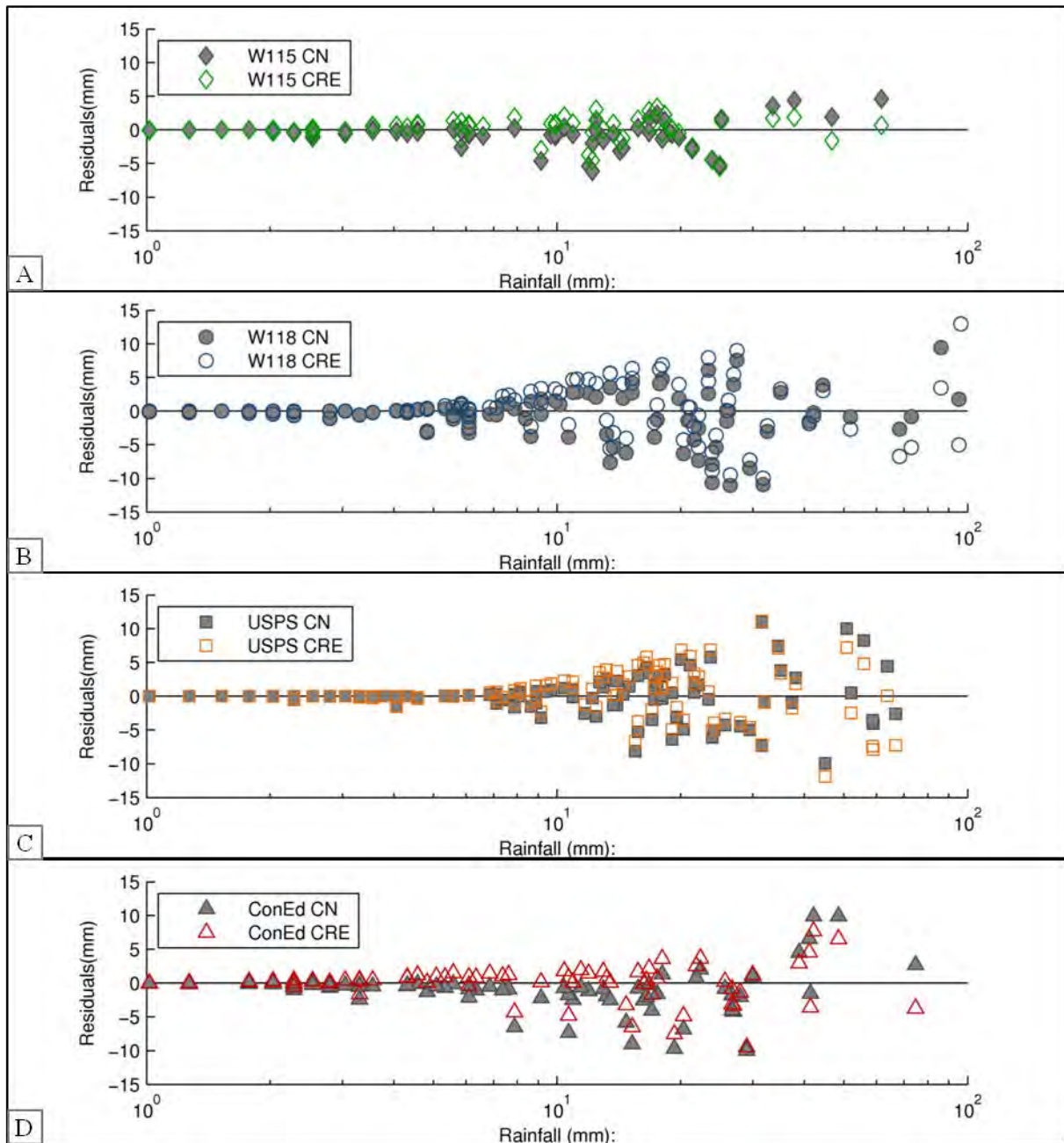


Figure 4-5: Residuals between characteristic runoff equations and curve number and observed depth for (A) W115, (B) W118, (C) USPS, and (D) ConEd.

The CREs were applied to the 40 years of historic data from Central Park, NYC. The predicted rainfall retention during the entire period for W115, W118, USPS, and ConEd was 51.3%, 43.6%, 57.0%, and 54.4%, respectively. As hypothesized, annual performance changed each year due to variation in yearly storm size distribution, with annual rainfall retention of 43-60% for W115, 37-51% for W118, 49-66% for USPS, and 47-61% for ConEd. Figure 4-6 (A) is analogous to Figure 4-2, but now shows the predicted rainfall retention performance for the 40 years. As seen, the ConEd green roof is predicted to retain the least runoff for storms 0-10 mm and the most for storm 20 mm or more. However, USPS had the highest overall retention due to its better comparative retention in the 0-10 and 10-20 mm category (94% and 68%, respectively) and the increased frequency of these storms in the historic data (66%). Nonetheless, the performance difference between USPS and ConEd only varied slightly between 0-5% each year, based on storm size distribution. W115, while no longer showing the best retention among all roofs, still outperforms W118

in storms greater than 10 mm. Application of the CN method showed 0.9-4.5% higher overall retention than the CRE, with predicted retentions of 53.4%, 47.8%, 57.9%, and 58.9% for W115, W118, USPS, and ConEd, respectively (Figure 4-6(B)). For reference, based on the total rainfall depth over the 40-year simulation period, a one percent change in rainfall retention is the equivalent of a 500 mm (~20 inch) change in cumulative retention depth. Because the CN method assumes that a green roof with a lower CN always outperforms a green roof with a higher CN, the CN method did not capture observed changes in comparative performance between the four green roofs with storm size (see Figure 4-2). Instead, the CN method predicted ConEd to have the highest retention of all roofs for all storm size categories.

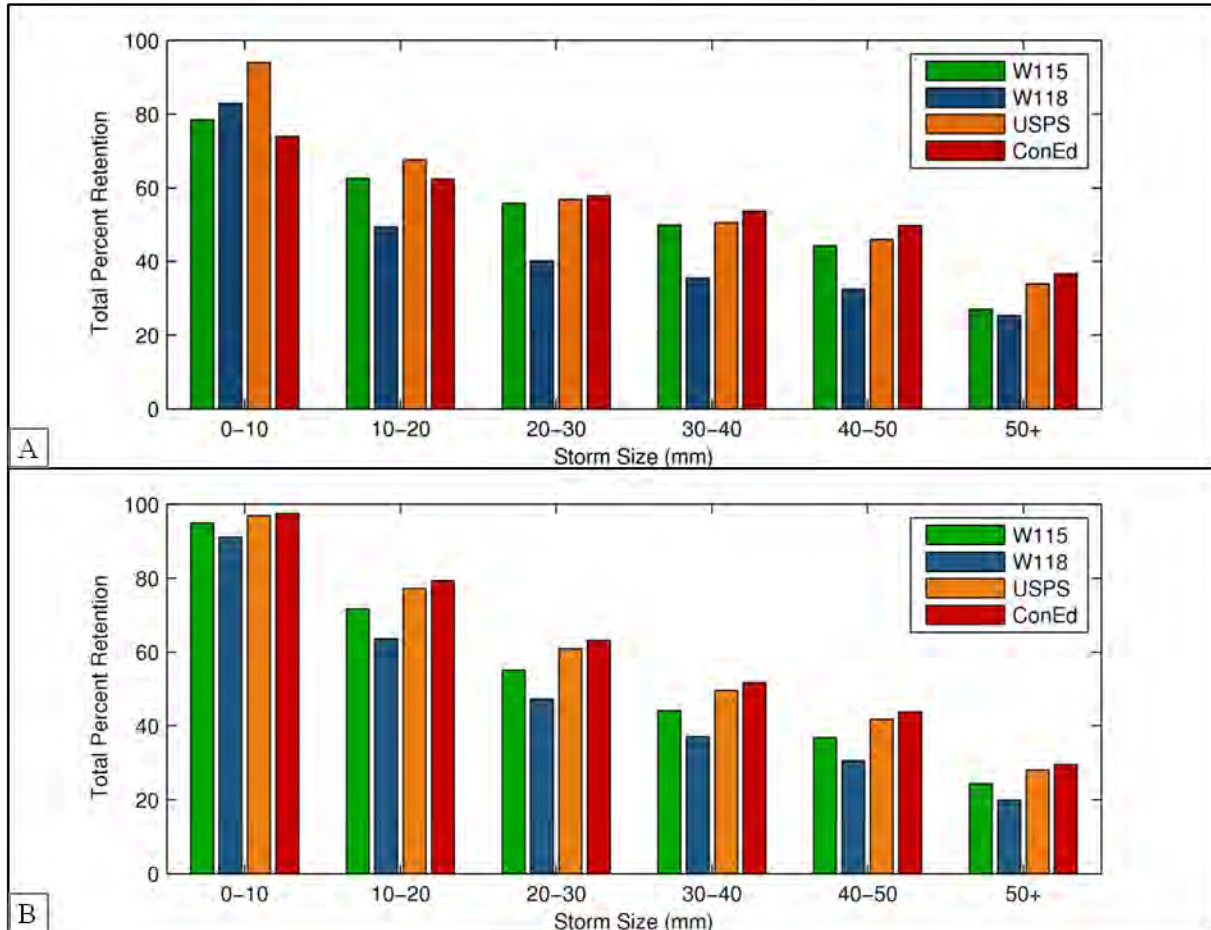


Figure 4-6: Predicted rainfall retention over historic period using (A) Characteristic runoff equations (B) Curve number.

#### 4.4 Results from BDCA and Regis

An analysis was also performed for the BDCA and one of the Regis rooftops (labeled in Figure 3-6(A) as VG<sub>1</sub>). Reliable storms were determined in the same manner as described for the other roofs, resulting in 32 and 23 reliable events for BDCA and Regis, respectively. Results show that BDCA retained 55.6% and Regis retained 54.1% of rainfall during their monitoring periods. Preliminary CREs were generated, but were not applied to the historic data for these roofs due to the absence of large events. With regards to small event performance, the CREs show the BDCA and Regis roofs do not generate runoff until 2.3 mm and 6.6 mm of rain, respectively (Figure 4-7). The fixed nature of the CN method constrains large storm performance and allows a preliminary application of the CN method for these two roofs. The CNs were found to be 97.4 and 95.5 for the BDCA and Regis roofs, respectively which, when applied to the 40-year historic rainfall data, results in 30.5% and 42.8% retention over the simulation period, respectively.

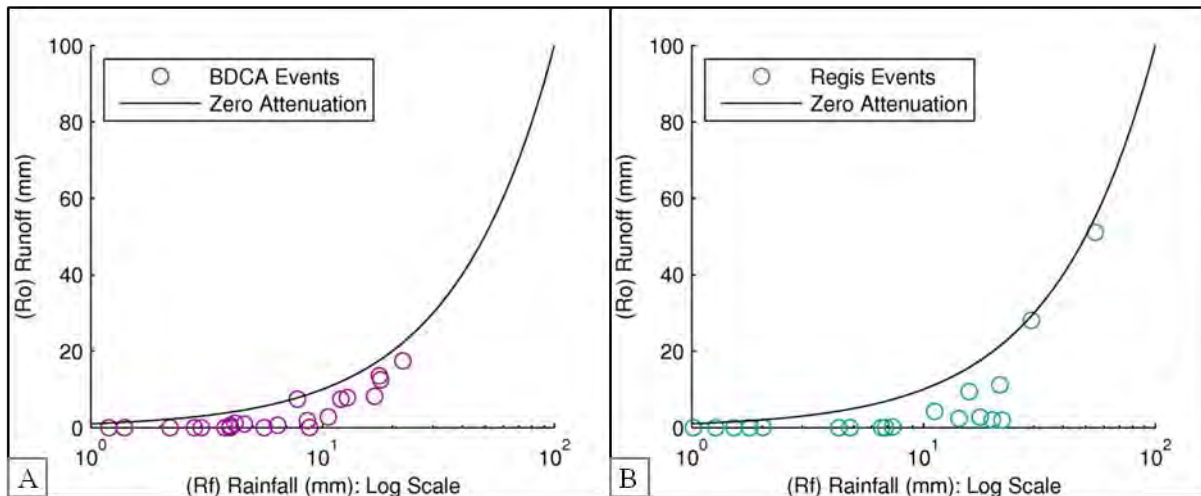


Figure 4-7: Characteristic runoff equations and events for (A) BDCA (B) Regis.

#### 4.5 Discussion of Results

In what follows, discussion of results related to the green roof *water quantity* investigation is presented under three separate headings: observations, predictive methods and findings from the multi-year predictions using historic rainfall data.

##### ***Observations of Green Roof Retention Performance***

The rainfall retention percentages observed for the four green roofs that were analyzed in this study (W115, W118, USPS and ConEd) fall within the range of performance documented by others. In addition, the observed data also agree with the general expectation that the percent of rainfall retained by a green roof will decrease as cumulative event precipitation increases. However, perhaps the most significant finding from the data is that while the ConEd green roof retained less rainfall than USPS in the 0-20 mm categories, it retained more rainfall for all larger event categories. As green roof retention performance is thought to be controlled by substrate depth, it was expected that the comparative performance between ConEd and USPS would be similar no matter the rainfall depth. It is hypothesized that this counter-intuitive observation is due to differences in event-based runoff behavior caused by two main factors: (1) the configuration of non-vegetated regions on the different green roofs; and (2) flow paths through the roof substrate and drainage layers, which differ by construction method.

During small events, runoff from the green roofs is dominated by precipitation on non-vegetated surfaces since the green roof substrate typically remains unsaturated. Compared to W115, W118 and USPS, a significant portion of the non-vegetated area on ConEd is located adjacent to the roof's downspout; as a result, runoff from these sections flows directly to the instrumented roof drain without intercepting greened portions of the roof. In contrast, the distance of non-vegetated areas on W115, W118 and USPS promotes depression storage of runoff before it reaches a roof drain, resulting in higher retention rates for small storms compared to ConEd.

As rainfall increases, the green roof systems reach maximum saturation, such that substrate storage capacity and the conductivity of preferential flow paths begin to play a greater role in determining runoff volume. In all systems, preferential flow paths likely develop within discontinuities of the substrate, through areas where vegetation is absent, and/or along geo-composite planes. For W115, W118 and USPS the hydraulic conductivity along these flow paths are thought to be high, whereas on ConEd the hydraulic conductivity along flow paths is restricted by small outlets at the base of the modular tray system. During large rainfall events, the restriction likely causes the trays to fill, resulting in a higher degree of substrate saturation. This observation is supported by modeling efforts of green roofs by She and Pang (2010) that indicated that rain infiltrates through the substrate prior to saturation. Considering ConEd also has large comparative storage capacity to begin with, this may explain the observed improved water retention performance of this roof during the larger events.

Rooftop configuration (e.g. size, slope, location of vegetated and non-vegetated areas, shading) also appears to impact overall retention performance between rooftops of the same construction type. Specifically, W115 consistently outperformed W118, even though both roofs were constructed at the same time using the same vegetated mat system. W115, although a smaller roof, has higher percent vegetation (58%) than W118 (53%). Additionally, the largest section of non-vegetated area, the elevated housing for the stairwell, drains into the green roof itself, allowing this runoff to be intercepted, thus improving overall rainfall retention ability. However, as the number of events in the 20+ mm category was limited for W115, further monitoring data might change relative runoff performance between these roofs.

The findings above support a recently proposed idea that green roofs may have shape and/or installation factors associated with their runoff attenuation behavior (Miller 2012). It also highlights the importance of considering the non-vegetated regions, common for many full-scale installations, during the interpretation of results from full-scale green roof studies and the development of generalized models for green roof behavior.

### ***Predictions of Green Roof Retention Performance***

The runoff quantity data collected during this study show that green roof runoff depth (defined as runoff volume divided by drainage area) can be reasonably predicted using a quadratic relationship with rainfall, which is described by a CRE for each rooftop. The hydraulic behavior of a green roof during different storm events defines the curvature of the CRE. Relationships between rainfall depth and green roof runoff depth can also be described using the well-known CN method. However, the CN method is limited in its ability to capture relative changes in rainfall retention performance between the green roofs that occur with storm size (see Figure 4-1). This is because the method assumes that a green roof with a lower CN will always outperform a green roof with a higher CN in every single storm category. The residuals of monitored and modeled performance for ConEd (Figure 4-5(D)) show that the CN method generally under predicts runoff in smaller events (in the 0–30 mm categories), while the residuals from the CRE have a more random distribution among event sizes. As, expected, the reduction in  $R^2$  from the CRE to the CN method is the most dramatic for ConEd (0.90 to 0.83). Nonetheless, while the CREs provide a better predictive method based on green roof runoff data, the CN method might be useful in predicting performance of roofs where monitored runoff data are limited.

Unexplained variance in monitored performance compared to the CRE predictions for each roofs is believed to be the result of environmental conditions on the rooftop, such as, temperature, antecedent moisture conditions, vegetation health, rainfall intensity, etc. A better understanding of the influence of these environmental conditions on the quantity of green roof runoff would require expanded hydrological performance data, gathered over multiple years. Although this project has observations from over 100 storm events for each of the green roofs studied, there are still insufficient data to define well the role of seasonality, for example. However, based on the strength of correlation between rainfall depth and runoff depth for each of the green roofs (0.95, 0.97, 0.97, and 0.90 for W115, W118, USPS, and ConEd, respectively), it is uncertain that analyses involving other variables would significantly improve the overall predictive accuracy of the CRE method.

### ***Multi-year Predictions Using Historic Rainfall Data***

Application of the derived green roof CREs to 40 years of historic rainfall data obtained from the Central Park NOAA station revealed performance biases caused by the distribution of storm sizes during the monitoring period. For example, W115's rainfall retention performance from reliable events during the monitoring period was better than that predicted using the 40 years of historic precipitation because of differences in the fraction of small (0-10 mm) storms between the monitored (74%) and predicted (66%) periods. In the same vain, only 1% of events from W115 and ConEd were large storms (50+ mm), compared to 4% recorded from the historic period, and both roofs saw lower predicted retention performance for the 40-year period versus the monitoring period. W118 and USPS, however, received a higher percent of storm volume in the 50+ mm, 48% and 56%, respectively, during the monitoring period in comparison to the historic period (26%). As a result, the retention performance of these green roofs was higher for the multi-decadal predictions generated with the roofs' CREs than was actually observed. Nonetheless, it does need to be recognized that surrounding landscape features in an urban environment can influence rainfall patterns on rooftops. Thus, it remains unknown whether the Central Park NOAA weather data reflect, on average, the rainfall on the individual roofs over a 40-year period.

## 4.6 Conclusions

Governing entities, owners, and other stakeholders will ultimately decide what, if any, green roof system is preferred for managing urban WWF. The results presented here show that for NYC's climate a variety of factors, most importantly, growing substrate depth, installation method, and configuration of non-vegetated areas, impact green roof rainfall retention. Among the three construction types, the modular tray system had the highest total rainfall retention during the monitoring period (61%) and therefore was most effective at reducing runoff volume. However, the NYC Mayor's Office estimates that 62% of CSO events in NYC are caused by storms under 12 mm (Mayor's Office of Long-Term Planning and Sustainability 2008). Therefore, if limiting the number of small storm CSO events, rather than reducing stormwater volume, were the goal, the built up roof system on USPS might be preferred since it had the highest attenuation of 0-10mm storm events and fully captured 46% of all storms. Finally, it is important to note that while USPS and ConEd had better predicted rainfall attenuation performance than W118 and W115 in the historic period, due to thicker growing substrate depths, the vegetated mat system is often the least costly per area of the three extensive roof types to install, and might also be the most constructible on a wider range of existing NYC building stock due to its significantly lower weight.

Continued collection of data and study of urban green roof conditions will help improve understanding of the factors influencing green roof runoff behavior, including seasonal factors such as ET, plant performance and freeze thaw (substrate temp), and allow a more robust analysis of green roof hydrological performance. Nonetheless, the CREs or CNs presented in this Chapter here can provide a good first-order method of estimating the water retention performance of the three common extensive green roof construction types in NYC's urban environment.

## Chapter 5 Water Quality Study

### 5.1 Introduction

Green roofs can have important benefits for diminishing the environmental consequences of stormwater runoff. These benefits are highly pronounced in urban environments, particularly where CSOs are present. While many research studies have focused on the role of green roofs in reducing stormwater runoff quantity (refer to Chapter 4), fewer studies have focused on the impact of green roofs on stormwater runoff quality. The quality of green roof runoff is an equally important factor when determining the role of green roofs in mitigating the harmful pollution impacts of WWF.

In current literature, a debate exists over the role of green roof systems as a source or a sink for stormwater pollutants. While many studies have shown that green roofs have the capacity to sequester pollutants, thereby reducing pollutant concentrations in stormwater (Berghage et al. 2009; Berndtsson et al. 2009; Carpenter and Kaluvakolanu 2011; Gregoire and Clausen 2011), several other studies have shown that the green roof growing media serves as a pollutant source (Moran et al. 2005; Berndtsson et al. 2006; Hathaway et al. 2008; Aitkenhead-Peterson et al. 2010; Dvorak and Volder 2010). However, within all of these studies, there is variability based on pollutant type.

The project work reported in this chapter aimed to provide additional information on the contribution of green roofs to stormwater runoff quality, with a focus on urban green roof behavior. Previous studies have employed a wide variety of methodologies when testing the impact of established green roofs on stormwater quality. Several studies have used test plots/modules (Monterusso et al. 2005; VanWoert et al. 2005; Berghage et al. 2009; Aitkenhead-Peterson et al. 2010; Vijayaraghavan et al. 2012; Morgan et al. 2013) and small pots (Alsup et al. 2010) as proxies for established green roof systems. Others have simulated storm events with artificial precipitation (e.g. distilled water) (Alsup et al. 2010; Vijayaraghavan et al. 2012). Of the research that actually involved monitoring established extensive green roof systems, many studies only incorporated one or two green roofs to represent the variety of extensive green roof types in existence (Moran et al. 2005; Teemusk and Mander 2007; Hathaway et al. 2008; Berndtsson et al. 2009; Bliss et al. 2009; Gregoire and Clausen 2011; Carpenter and Kaluvakolanu 2011). Therefore, a comprehensive examination of green roof runoff quality from a full range of established green roofs, covering the extensive roof typologies commonly implemented in an urban environment, fills an important gap.

During the study, the quality of runoff was quantified for five of the full-scale, extensive green roofs described in Chapter 3, namely W115 (vegetated mat), W118 (vegetated mat), USPS (built up), Fldstn (built up) and ConEd (modular tray), as well as five neighboring control (i.e., non-vegetated) roof areas. Chemical analyses of rain and rooftop runoff were conducted for multiple parameters including conductivity, turbidity, color, and heavy metals. However, a particular emphasis was placed on understanding the impacts of pH and nutrient concentrations (specifically nitrate  $\text{NO}_3^-$ , ammonium  $\text{NH}_4^+$ , total phosphorus P) in runoff. The information gathered on nutrient concentrations in roof runoff was used to estimate the potential water quality impacts associated with installing extensive green roofs on 20% of roof areas in NYC.

### 5.2 Methodology

Stormwater runoff samples were collected over a 16-month period (March 10, 2011 - August 2, 2012) at the five green roof sites: W115, W118, USPS, Fldstn and ConEd. Three different types of samples were collected: i) green roof (GR) runoff, ii) control roof (C) runoff, and iii) precipitation (Rain). Runoff was hand sampled usually during mid-rain events and collected from a previously specified gutter using a disposable 50 mL centrifuge tube. Specified sampling locations were kept constant throughout the 16-month sampling period and are illustrated in Figures 3-2 to 3-6. During sampling, the 50 mL centrifuge tube was placed below the gutter lip and filled six times. The first 50 mL was used to rinse out the previously-used collection bottle to ensure the integrity of the current sample. The subsequent five fills topped off a reusable 250 mL polyethylene collection bottle. The 250 mL collection bottle was then brought back to a Columbia University laboratory for water quality analysis. Control roof (i.e., non-vegetated roof) samples were collected from either a neighboring building, or drains coming down from elevated, non-vegetated parts of the green roof. Control roof sampling points are also shown on Figures 3-2 to 3-6. Precipitation samples were taken from a reusable collection bucket kept on the roof of a Columbia University building that is not part of the green roof monitoring system. The bucket was rinsed and cleaned with de-ionized (DI) water just prior to a rain event to ensure that the sample was not

contaminated by debris in the bucket. It is assumed that rainfall collected at this location is representative of rainwater quality throughout NYC. The constituents in precipitation are mainly governed by regional patterns of air pollutants, which are largely consistent between our study sites (National Atmospheric Deposition Program 2012). Over 100 samples were collected and analyzed over the study period. Appendix B provides a summary of the sampling results.

All samples were analyzed for pH, conductivity, turbidity, apparent color and true color in Columbia University’s Heffner Laboratory, located in the S.W. Mudd Building, NY 10027. If the samples could not be analyzed immediately after they were brought to the laboratory following collection, samples were refrigerated; although a sample was never refrigerated for more than 24 hours prior to analysis. A Fisher Scientific accumet Excel XL50 was used to measure sample pH and conductivity, a La Motte 2020we Turbidimeter was used to measure turbidity, and a Hach DR890 Colorimeter was used to measure both the sample apparent and true color. In addition, samples were sent to the Auburn University Soil Testing Laboratory in Auburn, Alabama for nutrient and heavy metal analyses. To prepare these samples, 40 mL of each parent sample was extracted from the 250 ml collection bottles and then filtered using a syringe and a 0.22 µm filter. The filtered aliquot was then frozen and shipped to the Auburn Laboratory. Table 5-1 summarizes the measurement parameters used for assessing precipitation, green roof and control roof runoff quality during the study.

Table 5-1: Water Quality Measurement Parameters

Standard Parameters	Nutrients (mg/L)		Heavy Metals (mg/L)
	Macronutrients	Micronutrients	
pH	Nitrate (NO <sub>3</sub> <sup>-</sup> )	Copper (Cu)	Barium (Ba)
Conductivity (µS/cm)	Ammonium (NH <sub>4</sub> <sup>+</sup> )	Iron (Fe)	Cadmium (Cd)
Turbidity (NTU)	Calcium (Ca)	Manganese (Mn)	Chromium (Cr)
Apparent Color (PtCo)	Potassium (K)	Zinc (Zn)	Nickel (Ni)
True Color (PtCo)	Magnesium (Mg)	Sodium (Na)	Lead (Pb)
	Phosphorus (P)		Aluminum (Al)
			Arsenic (As)
			Boron (B)

### 5.3 Results

The full assay and statistical results of the study are provided in Appendix B and C, respectively. Analyses with significant findings are displayed as box-plots in Figures 5-1 and 5-2. Letters on Figures 5-1 and 5-2 indicate significantly different groups. A one-way ANOVA and Tukey HSD (honestly significant difference) were used to test for significance ( $p$  value  $< 0.05$ ) between the Rain, GR and C sites for all of the water quality parameters. Statistical tests were run using the R statistical package (<http://www.r-project.org>). Results of these tests are provided in Appendix C. A comparative summary of the mean measurements for GR, C and Rain is provided in Table 5-2.

Table 5-2 Summary of Mean Water Quality Results with Standard of Deviation

Water Quality Measurement	Green Roof		Control Roof		Precipitation	
	Mean	Standard of deviation	Mean	Standard of deviation	Mean	Standard of deviation
pH	7.28	± 0.51	6.27	± 0.69	4.82	± 0.39
Conductivity (uS/cm)	127.67	± 48.89	57.11	± 57.63	32	± 20.71
Turbidity (NTU)	2.47	± 2.74	1.47	± 1.48	0.62	± 0.39
Color (PtCo)	162.53	± 90.24	28.45	± 32.42	5.32	± 9.79
Nitrate (mg/L)	0.27	± 0.59	0.87	± 1.31	0.6	± 0.53
Ammonium (mg/L)	0.86	± 1.86	1.47	± 2.55	1.19	± 1.85
Total phosphorous (mg/L)	0.47	± 0.47	0.25	± 0.38	0.21	± 0.41
Calcium (mg/L)	13.59	± 6.8	3.93	± 5.23	0.74	± 0.50
Potassium (mg/L)	2.22	± 2.86	0.78	± 1.98	0.1	± 0.2
Sodium (mg/L)	3.58	± 3.47	1.8	± 3.01	0.98	± 0.88
Magnesium (mg/L)	2.92	± 1.03	1.31	± 2.30	0.2	± 0.24
Boron (mg/L)	0.58	± 1.19	0.03	± 0.1	0.0	± 0.0

### 5.4 Discussion of Results

In what follows, the discussion of results from the water quality study is presented under separate headings for the three categories of testing: standard parameters, nutrients, and heavy metals (see Table 5-1). In addition, an estimation of the change in the annual mass nutrient loading in stormwater runoff that might be anticipated if green roofs were widely adopted in NYC is provided.

#### *Standard Parameters*

An increase in pH from Rain to C runoff to GR runoff is an often reported benefit of green roof establishment (Teemusk and Mander 2007; Clark et al. 2008; Berghage et al. 2009; Berndtsson et al. 2009; Bliss et al. 2009). This study provided additional support for this reported benefit. At each of the five individual green roof sites monitored for runoff quality, the pH of GR runoff was consistently higher than both the pH of C runoff and Rain, with measured average pH values of 7.28, 6.27 and 4.82, for the GR, C and Rain during the study period, respectively (Appendix B). EPA designates 6.5-8.5 as the standard pH range for safe drinking water (EPA, 2009). The spread of the pH of runoff samples taken from all five green roofs consistently remained within the EPA standard range, while the spread for pH of control roof runoff and precipitation samples fell out of the standard range (Figure 5-1). In the northeast region of the U.S where acid rain is a problem, green roofs therefore might serve as a tool for protecting aquatic ecosystems in nearby water bodies from the consequences of increased acidity. Note, average pH values were calculated by first transforming the pH measurements into hydrogen ion concentrations:  $[H^+] = 10^{-pH}$ . Once averaged, the  $[H^+]$  value was converted back to a pH value:  $pH = -\log [H^+]$ .

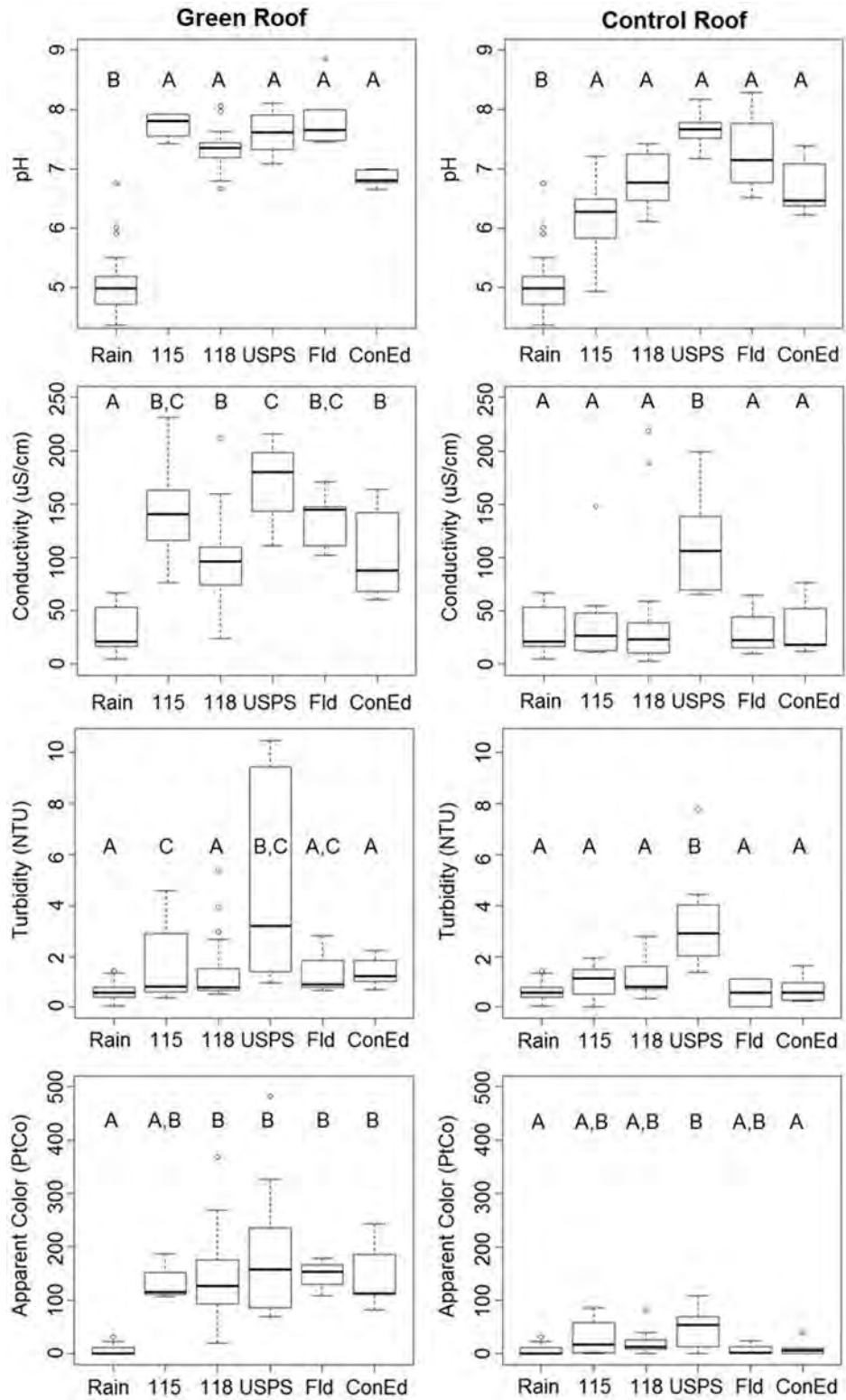


Figure 5-1: Distribution of pH, conductivity, turbidity, and apparent color for all roof types and precipitation.

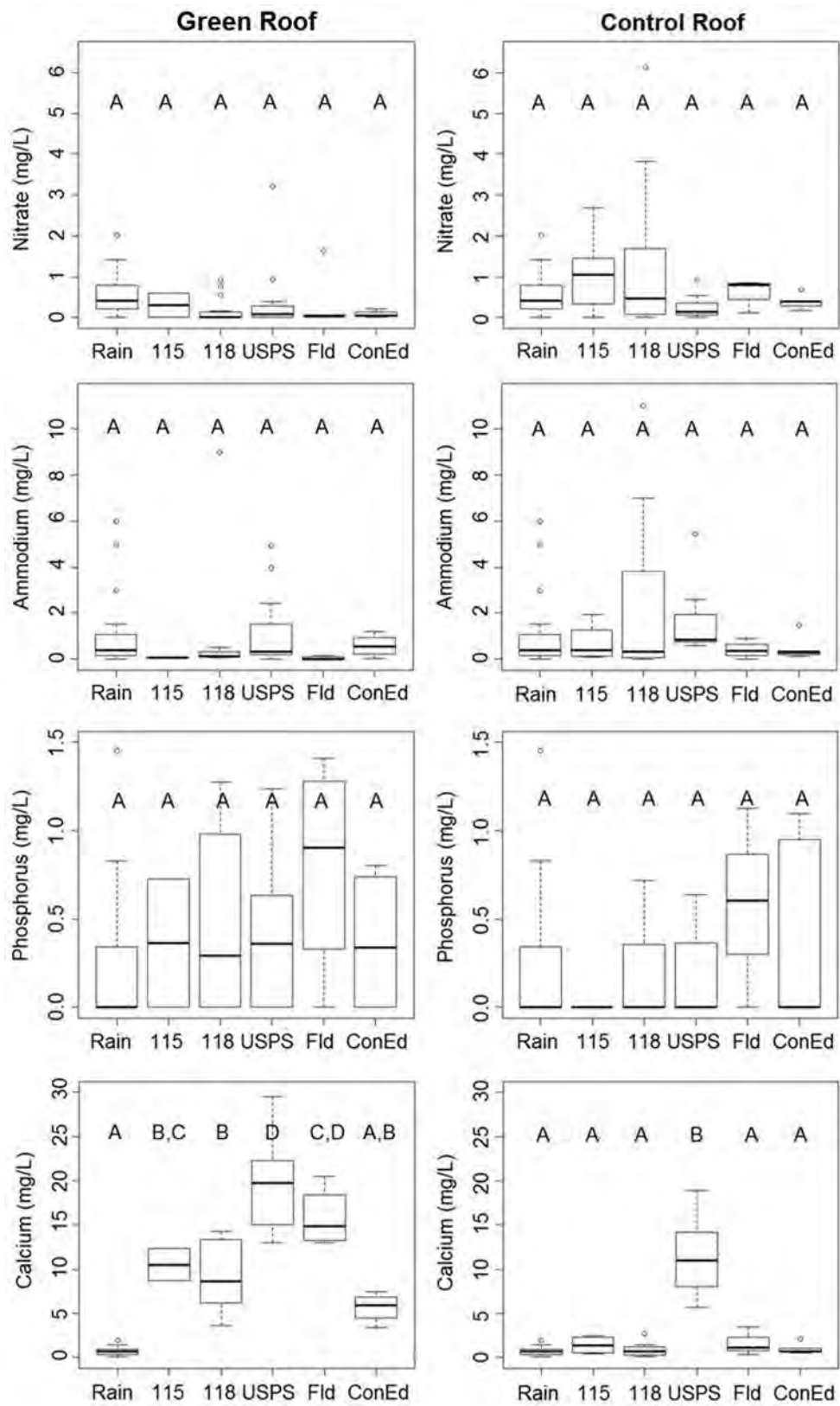


Figure 5-2 Distribution of nutrient and heavy metal concentration (mg/L) from all roof types

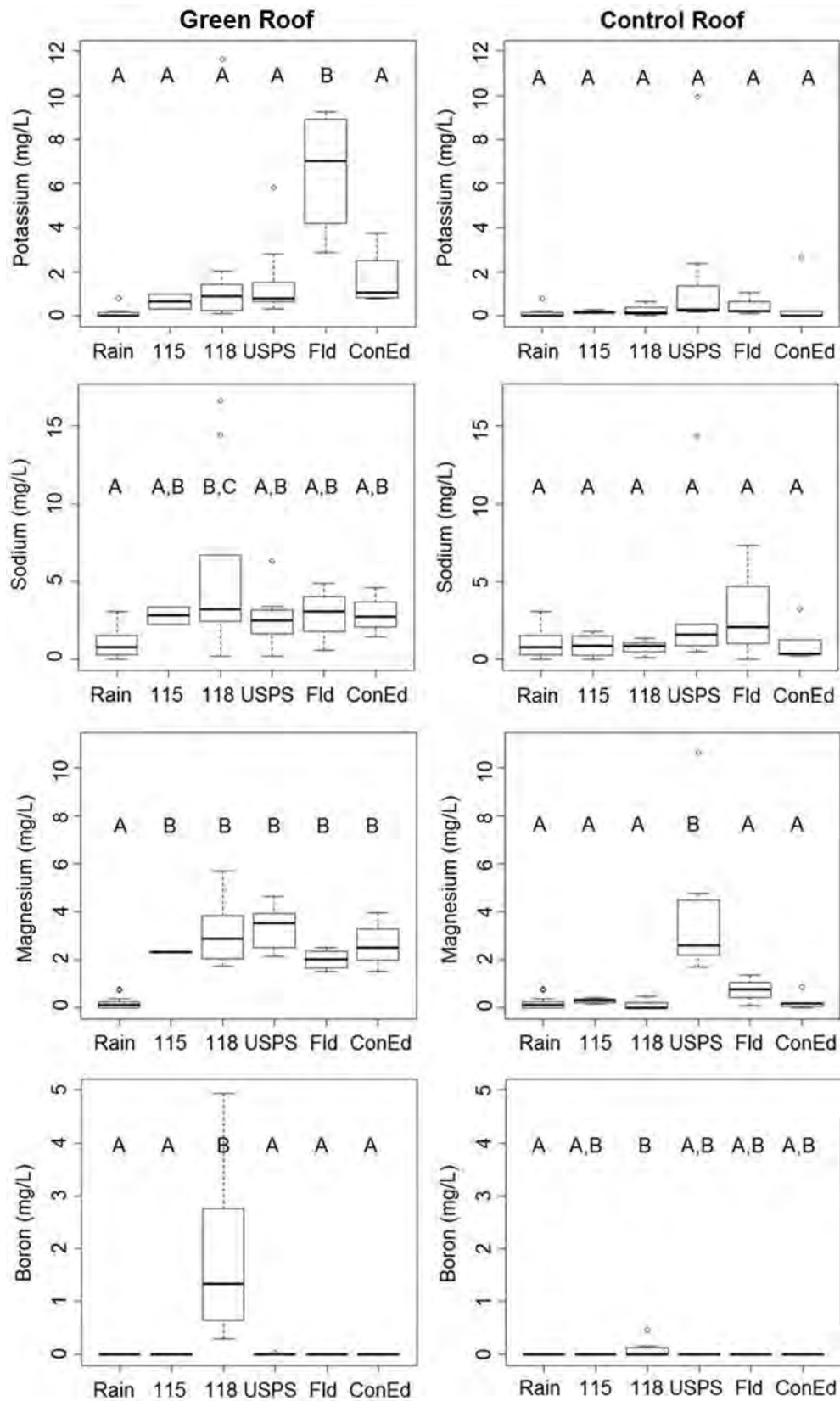


Figure 2 (continued): Distribution of nutrient and heavy metal concentration (mg/L) from all roof types

Few studies report on the overall electrical conductivity levels of green roof runoff, however, the general consensus is that there are higher ion concentrations in green roof runoff than in precipitation or control roof runoff (Teemusk and Mander 2007; Berghage et al. 2009). This trend is consistent with this study, which revealed a statistically significant difference in electrical conductivity between GR runoff samples and both C runoff and Rain samples, with the average GR conductivity being higher than the average C conductivity, which in turn was higher than the average Rain conductivity (Table 5-2).

Only a small number of studies have assessed turbidity in green roof runoff, and results from these studies have been inconclusive. For this study it was found that, on average, green roof runoff had higher turbidity than control roof runoff or precipitation. However, the only statistically significant difference in results lay between Rain and GR. (Appendix C). The GR turbidity values measured during this study are similar to those reported by Berghage et al. (2009) (range: 0.8-5.6 NTU) from their evaluation of runoff from various vegetated test plots. In contrast, Bliss et al. (2009) report their control roof runoff to be more turbid than both green roof runoff and precipitation. These authors hypothesize that this can be explained by accrument of particulates on the control roof during the dry period prior to a rain event.

Color in green roof runoff is a function of the organic materials incorporated in the green roof growing media to enhance plant growth and establishment (Berghage et al. 2009). Prior to making measurements, color was the only visible difference observed between green roof samples (yellow tint), and control roof/precipitation samples (no visible tint). The results of the color measurements showed a significant difference between GR-Rain and GR-C for apparent color, with GR color being higher (Appendix C). This finding is consistent with that of Berghage et al. (2009).

### ***Nutrients***

Conflicting results regarding  $\text{NO}_3^-$  in GR runoff have pervaded the literature. Some studies report no significant difference between  $\text{NO}_3^-$  concentrations in GR and C runoff (Clark et al. 2008; Carpenter and Kaluvakolanu 2011) while others report GR to be a  $\text{NO}_3^-$  sink (Berndtsson et al. 2009; Berghage et al. 2009) or a source (Teemusk and Mander 2007; Carpenter and Kaluvakolanu 2011). Intriguingly, the concentrations of  $\text{NO}_3^-$  in GR runoff from Monterusso et al. (2005) and Morgan et al. (2013) are much greater than those from other studies, including this one. Variation in the literature with regards to runoff of nitrogen and phosphorus green roofs may be due to variations in the amount of organic matter in green roof substrates. Studies have shown that nutrient runoff increases with increasing compost content of substrates (Hathaway et al. 2008) with stronger evidence for the link between compost enrichment of substrates and an increase in phosphorus runoff (Monterusso et al. 2005; Moran et al. 2005; Berndtsson et al. 2006; Teemusk and Mander 2007; Bliss et al. 2009). Of the nutrients examined during this study that are typically associated with eutrophication ( $\text{NO}_3^-$ ,  $\text{NH}_4^+$ , P), there was only a significant difference between GR and C  $\text{NO}_3^-$  levels, with GR  $\text{NO}_3^-$  concentrations being lower (Appendix C).

Consensus regarding P and  $\text{NH}_4^+$  concentrations in GR runoff is also lacking in the literature. In some cases, GR runoff is reported as a statistically significant source of P (Clark et al. 2008; Berghage et al. 2009; Bliss et al. 2009; Fassman-Beck et al. 2013), while in other cases, GR are reported to be sinks of P (Teemusk and Mander 2007; Gregoire and Clausen 2011). In one study, an extensive green roof in Sweden was cited as a source of P while an intensive green roof in Japan was not (Berndtsson et al. 2009). Both green roofs discussed in the Berndtsson et al. (2009) study, however, were reported to be sinks for  $\text{NH}_4^+$ . The data gathered during this study demonstrated that, on average, there was less  $\text{NH}_4^+$  in GR runoff than C runoff. The decrease in  $\text{NH}_4^+$  did not correlate with an increase in  $\text{NO}_3^-$ , which would have indicated nitrification, the two-step process of converting  $\text{NH}_4^+$  to  $\text{NO}_3^-$  (Berndtsson et al. 2009). Overall, this study found no significant difference between the Rain, GR and C for both  $\text{NH}_4^+$  and P (Appendix C).

For other macronutrients such as Ca, K and Mg, there was a significant difference between GR-Rain and between GR-C, with GR concentration values being higher (Appendix C). The observed Ca, K and Mg concentration ranges are similar to those observed in the studies conducted by Berghage et al. (2009) and Berndtsson et al. (2009). Overall, the Ca, K and Mg measurements made during this study demonstrate that GR's role in leaching macronutrients into rooftop runoff.

The micronutrients Cu, Fe and Zn and Mn were either detected in very low amounts or below the detection limit (< 0.1 mg/L) for all runoff and precipitation samples, so these data are not provided in this report. For the micronutrients Na there was a significant difference between GR-Rain, with Na GR concentrations being higher, possibly indicating Na leaching from the green roof substrate. Measured Na GR concentration levels were similar to those reported by Berghage et al. (2009); while the measured Na concentration of C samples were, on average, slightly higher than those reported by these authors. For the other micronutrients, even though the data for this study cannot be directly compared to other studies due to this study's higher detection limit, the measurements of Cu (Berndtsson et al. 2009; Gregoire and Clausen 2011; Fassman-Beck et al. 2013), Fe (Berghage et al. 2009; Berndtsson et al. 2009), Mn (Berghage et al. 2009; Berndtsson et al. 2009) and Zn (Berghage et al. 2009; Berndtsson et al. 2009; Gregoire and Clausen 2011; Fassman-Beck et al. 2013) reported by other researchers also indicate that low quantities of micronutrients would be leached out of a green roof.

**Heavy Metals**

All heavy metal concentrations were either very low or below detection limits (< 0.1 mg/L) for all runoff and precipitation samples, so these data are not provided in this report. The only exception to this was Boron (B) which was detected in the runoff of the W118 GR (Figure 5-2). The W118 GR is a housing building for Columbia University graduate students and various types of insecticide is applied to the building on a routine basis (Trejo 2013). One of the products, Niban-FG, contains Boric Acid. It is thus hypothesized that the Boron measured in the water quality here is a result of this insecticide.

Although the reported detection limits for other studies where heavy metals were measured in green roof runoff (Clark et al. 2008; Berndtsson et al. 2009; Bliss et al. 2009) are much lower than this study, the other studies also conclude that heavy metals are rarely present in green roof runoff. The only exception is Gregoire and Clausen (2011) who observed slightly elevated chromium and lead concentrations in green roof runoff, which the authors attributed to nearby construction and excavation.

**Mass Nutrient Loading**

Interpretation of the nutrient data obtained from this study specifically focused on understanding the potential impacts of widespread green roof implementation on the eutrophication of NYC waterways. As a result, analyses were focused on estimating how green roofs might change the annual mass loading of NO<sub>3</sub><sup>-</sup>, NH<sub>4</sub><sup>+</sup>, and total P in NYC's stormwater runoff.

The mass loading per unit area of NO<sub>3</sub><sup>-</sup>, NH<sub>4</sub><sup>+</sup>, and P leaving the GR and C per rain event was calculated for three of the monitored green roofs (and associated control roofs), namely: W118 (vegetated mat), Con Ed (modular tray), and USPS (built up). These green roofs represent the three commonly installed extensive green roof types and the CREs for these roofs were based on the most runoff quantity data (see Table 4-1). The average annual runoff volume from each green roof (L) was estimated based on historic rainfall data, the CRE for each roof (see Figure 4-4), and the area (m<sup>2</sup>) of the roof. In the case of the control roofs, a blanket 10% retention of all storms was assumed. The annual runoff volume (L) for each green roof or control roof was then multiplied by the average nutrient concentration (mg/L) in the roof runoff and divided by the roof area (m<sup>2</sup>) in order to estimate the annual mass loading (mg/m<sup>2</sup>) of each nutrient from each roof per unit rooftop area. Results are reported in Table 5-3, where bolding and shading indicate which values are higher.

Although Table 5-3 reports that concentrations of nutrients in green roof runoff were sometimes higher or the same as nutrient concentrations in control roof runoff, the total mass (mg) of nutrients leaving each GR per unit area during a storm event was less than that leaving each C per unit area because of GR capacity to hold and store precipitation (refer to Chapter 4). As a result, the annual mass loading (AML) of nutrients from GR is lower than from that of the nearby C.

Table 5-3: Average Concentration (AC) and Annual Mass Loading (AML) of NH<sub>4</sub><sup>+</sup>, NO<sub>3</sub><sup>-</sup>, and P.

Nutrient	W118		USPS		ConEd	
	C	GR	C	GR	C	GR

AC (mg/L)	NH <sub>4</sub> <sup>+</sup>	0.12	0.03	0.27	0.34	0.38	0.08
	NO <sub>3</sub> <sup>-</sup>	2.74	1.08	1.76	1.16	0.50	0.59
	Total P	<0.26	<0.49	<0.25	<0.47	<0.47	<0.42
AML (mg/m <sup>2</sup> )	NH <sub>4</sub> <sup>+</sup>	127.80	19.09	290.02	158.49	416.23	31.66
	NO <sub>3</sub> <sup>-</sup>	2992.77	612.33	1921.72	541.26	548.97	245.57
	Total P	<285.73	<276.44	<276.15	<217.62	<513.43	<175.89

About 8% of NYC land area is estimated to qualify for an extensive green roof retrofit (Culligan 2011), which amounts to a total area of approximately  $6.4 \times 10^7$  m<sup>2</sup>. To evaluate how the difference in AML between C and GR might impact annual nutrient loading in NYC stormwater if all suitable rooftops were retrofit with an extensive vegetated mat green roof, the lightest of the three systems, the AML (mg/m<sup>2</sup>) of W118 GR and W118 C was multiplied by this area. The difference between the two mass loadings (kg) was then assumed to be the decrease in annual nutrient loading (kg) that would be realized by a widespread green roof retro-fitting program in NYC (Table 5-4). According to this analysis, approximately 600, 7,000 and 150,000 kg of P, NH<sub>4</sub><sup>+</sup> and NO<sub>3</sub><sup>-</sup> per year, respectively, would be removed from NYC stormwater runoff if green roofs were widely adopted throughout the city.

Table 5-4: Projected Reduction in Nutrient Loading per Year from Retrofitting Available NYC Rooftops

Nutrient	Project Loading Discharge (kg)		
	Existing rooftop	Green roof retrofit	Reduction
NH <sub>4</sub> <sup>+</sup>	8,182	1,222	6,960
NO <sub>3</sub> <sup>-</sup>	191,610	39,204	152,406
Total P	18,294	17,699	595

Overall, the reductions in annual mass loadings reported in Table 5-4 appear minimal when compared to estimates of annual nitrogen and phosphorus loads to the saline Hudson estuary. For example, Howarth et al. (2011) estimate that  $24 \times 10^3$  metric tons N per year and  $3.7 \times 10^3$  metric tons P per year were input annually into the Hudson River estuary. Based on this fact, retrofitting all available rooftop in NYC with an extensive vegetated matt system would provide less than a 1% decrease in annual nutrient loadings to local waterways. Nonetheless, although minimal, this study still provides evidence that green roof establishment does have an overall benefit on stormwater quality by not exacerbating nutrient loading in stormwater, and thereby provides support for the expansion of green LID in urban areas negatively impacted by WWF.

## 5.5 Conclusions

The results of the water quality study on the five NYC green roofs show that the average pH of GR runoff was 7.28, while the average pH of C runoff and Rain was 6.27 and 4.82, respectively. Statistical analyses show that the difference between the GR runoff and Rain are significant. Thus, the study results confirm, as reported by others, that green roofs neutralize acid rain. On average, lower NO<sub>3</sub><sup>-</sup> and NH<sub>4</sub><sup>+</sup> concentrations were observed in GR runoff than both C runoff and Rain, although the only statistically significant difference lay between the NO<sub>3</sub><sup>-</sup> concentrations in GR and C runoff. In general, total P concentrations were higher in GR runoff than either C runoff or Rain, but none of the differences in concentrations between these three categories of water samples were significant. Finally, all micronutrients and heavy

metals were either detected at very low concentrations or not at all (concentrations were below the detection limit). The two exceptions relate to Boron concentrations on the W118 green roof as well as Na and Ca across all five green roofs.

Although the concentration of nutrients in green roof runoff was sometimes observed to be higher than that in control roof runoff, it was estimated that the annual mass (mg) of nutrients leaving a green roof is less than that leaving a control roof because green roofs discharge less water volume per annum. Based on the work presented in Chapter 4 and the work presented in this chapter, it is projected that universal installation of green roofs in NYC on all suitable rooftops could save about 600 kg of Total P, 7,000 kg of  $\text{NH}_4^+$  and 150,000 kg of  $\text{NO}_3^-$  from discharging into the sewer system and/or local water bodies. Although these amounts are not large in comparison to the annual nutrient discharges from waste water treatment plants, they still provide evidence that green roof establishment does have an overall benefit on urban stormwater quality. However, improved management through lower fertilization of green roofs may also contribute to reduced nutrient discharges (Oberndorfer et al 2007).

## Chapter 6 Soil Moisture Water Balance Study

### 6.1 Introduction

Rainfall and antecedent SM are two key factors influencing the generation of green roof runoff (Crow et al. 2011). SM affects the partitioning of precipitation into infiltration and runoff, thereby regulating surface and subsurface water flow (Dorigo et al. 2011; Joshi et al. 2011). SM in the root zone is also crucial for the growth and development of green roof vegetation, and plays a role in the apportioning of the surface energy budget (Joshi et al. 2011) which influences green roof ET. Similar to other natural systems, SM thus plays a central role in the hydrologic behavior of green roofs, indicating that direct studies of SM for assessing green roof water balance can be very valuable. Given the high instrumentation costs, labor and technical expertise required for current green roof hydrologic monitoring schemes, including those that were part of this study, the potential for SM to act as a proxy for green roof runoff and ET measurements presents an important avenue for research.

Using a “backwards hydrology” method, Kirchner (2009) showed that if a water catchment could be represented by a single storage element, where storage is assumed to be a function of water discharge alone, precipitation, ET, and discharge could be linked without the need to explicitly account for changes in water storage. After constructing a first-order nonlinear differential equation, the storage term was inferred from the resulting changes in water discharge, allowing for streamflow hydrographs to be predicted from precipitation and ET time series alone. A similar method was also adopted by Brocca et al. (2013) in order to estimate rainfall from SM observations using an “inverted soil-water balance equation.” Brocca et al. (2013) showed that the method was successfully able to reproduce daily rainfall data based on in situ SM observations at three different sites in Italy, Spain and France.

A water balance approach was used by Jarrett et al. (2006) to estimate green roof stormwater retention based on daily rainfall, ET, and the soil/substrate maximum water holding capacity in their Annual Green Roof Response (AGRR) model. This model requires estimating ET rates, which are dependent on location, climate, vegetation, water storage capacity, as well as SM levels. While conceptually the approach used by Jarrett et al. (2006) appears to effectively predict green roof runoff when enough information is available, no formal validation was carried out via a comparison of the predicted green roof runoff to observed runoff values. Sherrard and Jacobs (2012) present a vegetated roof water balance model (VR-WBM) that uses daily time steps, requires precipitation and dew as inputs and outputs green roof storage, runoff and ET. The model requires both vegetation parameters and soil/substrate characteristic parameters that need to be obtained from field observations. Good agreement between the model and data from a lysimeter experiment where shown following model calibration with several weeks of field data.

This Chapter reports a method for green roof runoff and ET estimation that was derived during the study and is termed the Soil Water Apportioning Method (SWAM). Similar to the Kirchner (2009) and Brocca et al. (2013) methods, a water balance model was constructed, analytically linking precipitation to SM, whereby runoff and ET were inferred from the resulting changes in SM over time. Thus, SWAM relies solely on the monitoring of local precipitation and green roof SM in order to predict green roof hydrological behavior and unlike the VR-WBM model does not require field calibration. In situ rainfall, runoff and SM observations from the W118 and W115 vegetated mat systems (see Chapter 3) were used to test the reliability of the proposed approach. Two different low-cost SM probes were compared for accuracy in estimating green roof runoff using SWAM.

### 6.2 Methodology

Rainfall data needed for this portion of the study was collected with a tipping bucket rain gauge while runoff was measured using a custom made weir device. For a detailed description of precipitation and runoff monitoring, see Chapters 3 and 4. Volumetric SM was collected with a CS615 water content reflectometer (Campbell Scientific, Logan, Utah, USA) on the W118 roof, and with a ECH2O EC-5 soil moisture probe (Decagon Devices, Pullman, Washington,

USA) on the W115 roof. The EC-5 probe was purchased from Onset Hobo® Dataloggers in order to be compatible with other instruments used in this research. Substrate temperature was recorded using a 12-Bit Temp Smart Sensor (S-TMB-M002). The study period for this work was from September 1, 2011 to August 1, 2012.

Recent advances in monitoring techniques, have allowed for less destructive and more accurate means of quantifying volumetric water content (Czarnomski et al. 2005). The most widely utilized sensors use either a time domain reflectometry (TDR) method or the capacitance technique. The TDR method measures soil or SM content through a relationship with the velocity of an electromagnetic wave that is passed along the waveguides, determined by measuring the time of travel (Walker et al. 2004). Capacitance sensors determine soil water content by measuring the frequency change induced by the changing permittivity of the soil permeated by the fringing fields of the capacitor sensor (Baumhardt et al. 2000). The accuracy and precision of these instruments vary and their calibration is dependent on soil type, electrical conductivity and temperature (Czarnomski et al. 2005).

The CS615 water content reflectometer consists of two 30 cm long stainless steel waveguides connected to a printed circuit board: it measures soil moisture content using the TDR method (Campbell Scientific Inc. 2012). The CS615 is specified to have an accuracy of  $\pm 3.0\%$  v/v when applied to typical mineral soils using the manufacturer's standard calibration and an operating environment from -10 to 70 °C (Campbell Scientific Inc. 2012). Soils with different dielectric properties show an error that appears as a constant offset (Campbell Scientific Inc. 2012). A single CS615 sensor was installed horizontally into the upper portion of substrate layer of the W118 green roof within the monitored drainage area.

The EC-5 soil moisture sensor calculates the apparent soil dielectric constant of a soil by measuring the charge time of a capacitor in the soil (Czarnomski et al. 2005). The time required to charge the capacitor is related to the output voltage of the instrument. An empirical equation is used to describe the relationship between the output voltage and SM. The EC-5 is specified to have an accuracy of  $\pm 2.0\%$  v/v when applied to typical mineral soils using the manufacturer's standard calibration and an operating environment from -40 to 60 °C (Decagon Devices Inc. 2012). However, according to Onset Hobo® Dataloggers, the sensor is able to accurately measure SM only from 0 to 50 °C. A single EC-5 probe was inserted at an angle, penetrating through the entire depth of the W115 green roof substrate.

Soil or substrate electrical conductivity and temperature can influence the accuracy of these SM measurement instruments (Baumhardt et al. 2000; Czarnomski et al. 2005; Campbell Scientific Inc. 2012). The factory calibration for CS615 will accurately predict SM if the electrical conductivity is  $< 3 \text{ dS}\cdot\text{m}^{-1}$  (Campbell Scientific Inc. 2012), while the factory calibration is valid for electrical conductivities  $< 8 \text{ dS}\cdot\text{m}^{-1}$  for the EC-5 probe (Decagon Devices Inc. 2012). However, the application of the sensors to conductive media, such as saline soils, certain clay and organic soils is hindered due to significant attenuation effects of the desired signal (Hook et al. 2004). Moreover, SM readings may be impacted by temperature variations due to effects on the dielectric permittivity of water, through soil-water interactions, as well as through direct effects on the sensor circuitry (Bogena et al. 2007). Given these instrument sensitivities, it is often necessary for individual users to calibrate the instruments for their specific measurement conditions if precise estimates of SM are required (Czarnomski et al. 2005).

In this study, SM readings were normalized to reflect a saturation value ranging from 0 to 1, corresponding to the minimum and maximum field SM conditions, respectively. Similar two point (dry-wet) TDR sensor field calibration methods have been suggested and applied in past studies with success (Robinson et al. 2005; Sakaki and Rajaram 2006). Due to the availability of several years of SM readings from each roof, the normalization calibration, i.e., obtaining the dry and wet volumetric soil moisture values for this study, was carried out using field data.

SWAM incorporates a normalized substrate water balance approach. The water balance for a layer of substrate with depth  $Z$  [L] can be described by the following expression:

$$nZ \frac{dS}{dt} = P(t) - Q(t) - ET(t) - L(t) \quad [6-1]$$

where  $S(t)$  [-] is the relative saturation of the substrate,  $t$  [T] is the time,  $n$  is the substrate effective porosity [unitless],  $P(t)$ ,  $Q(t)$ ,  $ET(t)$ , and  $L(t)$  [L/T] are the precipitation, runoff, ET, and losses, respectively.

Given the relative thinness of green roof substrates, particularly extensive green roofs, as well as their well-draining nature (Getter and Rowe 2006), the dominant process governing water flow was considered to be vertical infiltration through the growing media. Based on this, and an assumption that there was no water penetration through the roof's waterproof membrane, the losses term in equation [6-1] was taken to be negligible (e.g. losses due to canopy interception which is often neglected in many other green roof water balance approaches). Because green roofs promote rapid drainage through the growing media (Fassman and Simcock 2012), it was further assumed that the runoff from a green roof was simply the excess of precipitation depth over the substrate's storage capacity; meaning that the possibility of water ponding on the green roof was ignored. With these two assumptions, measurements of SM and precipitation can effectively capture all of the water going into and out of a green roof system over a specified period of time (aggregate period) with the following modified water balance equation:

$$nZ \frac{(S_2 - S_1)}{\Delta t} = P_{\Delta t} - Q_{\Delta t} - ET_{\Delta t} \quad [6-2]$$

where  $S_1$  denotes the relative saturation of the substrate at the start of the aggregate period,  $S_2$  denotes the relative saturation of the substrate at the end of the aggregate period,  $\Delta t$  is the time-step of the aggregate period, and the subscript  $\Delta t$  denotes the parameter value associated with the aggregate period.

If precipitation occurs during the aggregate period, green roof runoff is estimated from:

$$Q_{\Delta t} = P_{\Delta t} - nZ(1 - S_1) \quad [6-3]$$

where  $nZ(1-S_1)$  is the water storage capacity of the green roof at the start of the aggregate period. If the precipitation during the aggregate time period is less than  $nZ(1-S_1)$ , runoff is set to zero for the aggregate period.

If no precipitation occurs during the aggregate period, then no runoff is assumed and ET during the aggregate period is estimated from:

$$ET_{\Delta t} = nZ(S_2 - S_1) \quad [6-4]$$

If precipitation occurs during the aggregate period, but no runoff is generated, ET during the aggregate period is estimated from:

$$ET_{\Delta t} = P_{\Delta t} - nZ(S_2 - S_1) \quad [6-5]$$

If precipitation and runoff occur during the aggregate period, then ET during the aggregate period is estimated from:

$$ET_{\Delta t} = nZ(1 - S_2) \quad [6-6]$$

where it is assumed that the reduction in substrate field saturation below 100% at the end of the aggregate period is the result of ET during the aggregate period. Sometimes this assumption led to negative values of ET, primarily because green roof runoff can be generated before the green roof medium is fully saturated. When this occurred, ET was set to zero for the aggregate period.

Three different methods were used in assessing the performance of SWAM based on recommendations by Moriasi and Arnold (2007): Nash-Sutcliffe efficiency (NSE) index, percent bias (PBIAS), and the root mean square error (RMSE). The NSE is a normalized statistic that measures the relative magnitude of the residual variance in predicted values of runoff versus observed data variance (Nash and Sutcliffe 1970) using equation [6-7]:

$$NSE = 1 - \left[ \frac{\sum_{i=1}^n (Q_i^{obs} - Q_i^{pre})^2}{\sum_{i=1}^n (Q_i^{obs} - Q^{mean})^2} \right] \quad [6-7]$$

Where  $Q_i^{obs}$  is the  $i$ th value of the observed runoff data,  $Q_i^{pre}$  is the  $i$ th runoff value arrived at using SWAM,  $Q^{mean}$  is the mean of the observed runoff data, and  $n$  is the total number of observations. NSE ranges from  $-\infty$  to 1.0, with 1.0 being the optimal value. Values between 0 and 1 are generally viewed as acceptable model performance, while values below 0 indicate unacceptable performance (Moriasi and Arnold 2007). PBIAS measures the average tendency of simulated data to be larger or smaller than observed data and RMSE is a measure of the average squared deviation of simulated values from observed values. The maximization of the NSE and PBIAS statistics were selected as objective functions for arriving at the optimal time aggregate. All three statistics were used for general model performance assessments.

### 6.3 Results

A recent study by Fassman and Simcock (2012) indicated that the soil-water relationship for extensive green roofs varies greatly between laboratory and field measurements. For this reason, the maximum water holding capacity for each roof was arrived at statistically using SWAM with a 24-hour time aggregate ( $\Delta t = 24$  hours). The optimized effective porosities were found to be 0.3 and 0.5 for the W118 and W115 roofs, respectively, from which the maximum water holding capacities were calculated. Several time aggregates were considered before arriving at the optimal time of 24-hours. Results of the time aggregate optimization are shown in Table 6-1 and Figure 6-1.

Table 6-1: Time Aggregate Optimization for W118 and W115 Green Roofs.

Time Aggregate (hr)	W118 Green Roof				W115 Green Roof			
	RMSE (mm)	NSE	Negative PBIAS (%)	Positive PBIAS (%)	RMSE (mm)	NSE	Negative PBIAS (%)	Positive PBIAS (%)
1	1.77	0.27	-16	65	3.25	-1.58	-17	64
6	3.91	0.79	-11	45	5.21	0.49	-23	36
12	5.34	0.85	-13	35	8.4	0.46	-31	32
24	6.22	0.88	-16	23	7.76	0.72	-35	19
36	7.96	0.88	-18	19	13.33	0.43	-37	30

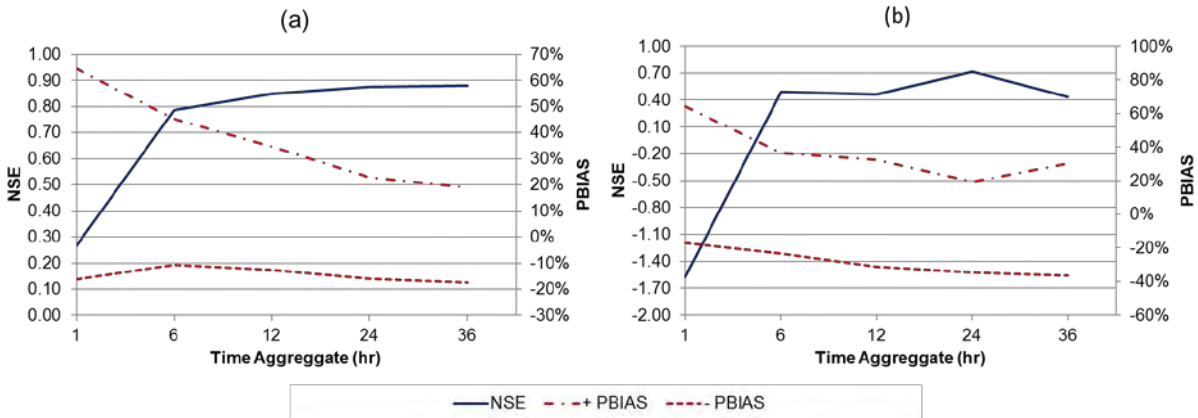


Figure 6-1: NSE and PBIAS for the (a) W118, and (b) W115 roofs at different time aggregates.

Figures 6-2 and 6-3 show the resulting hydrographs for the W118 and W115 roofs over the course of a year using SWAM at daily time aggregates, respectively. Figure 6-4 shows a restricted time period, i.e. from March to May 2012 only, to provide a closer view for the purpose of comparison. Figure 6-5 compares SWAM ET estimates versus ET measurements collected in 2009 using a chamber technique (Dome ET) (Marasco, 2014) on W118.

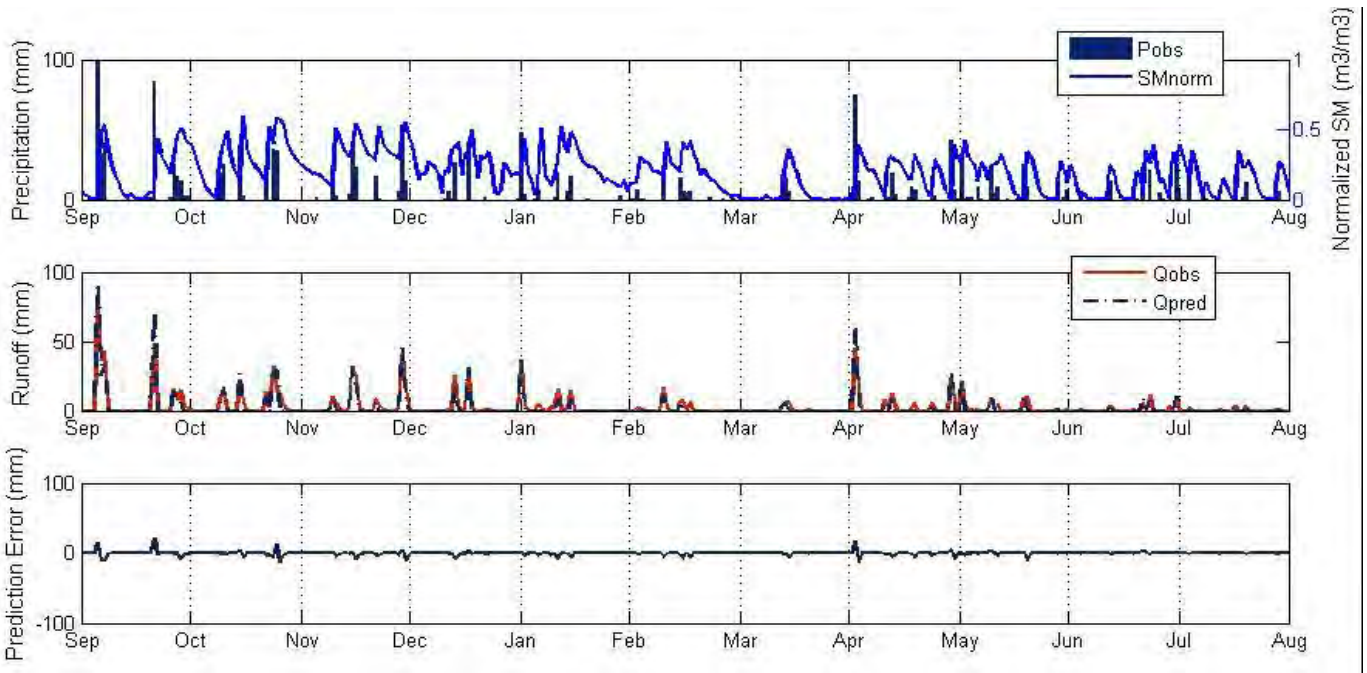


Figure 6-2 Precipitation, soil moisture, observed and simulated daily runoff and error for green roof W118.

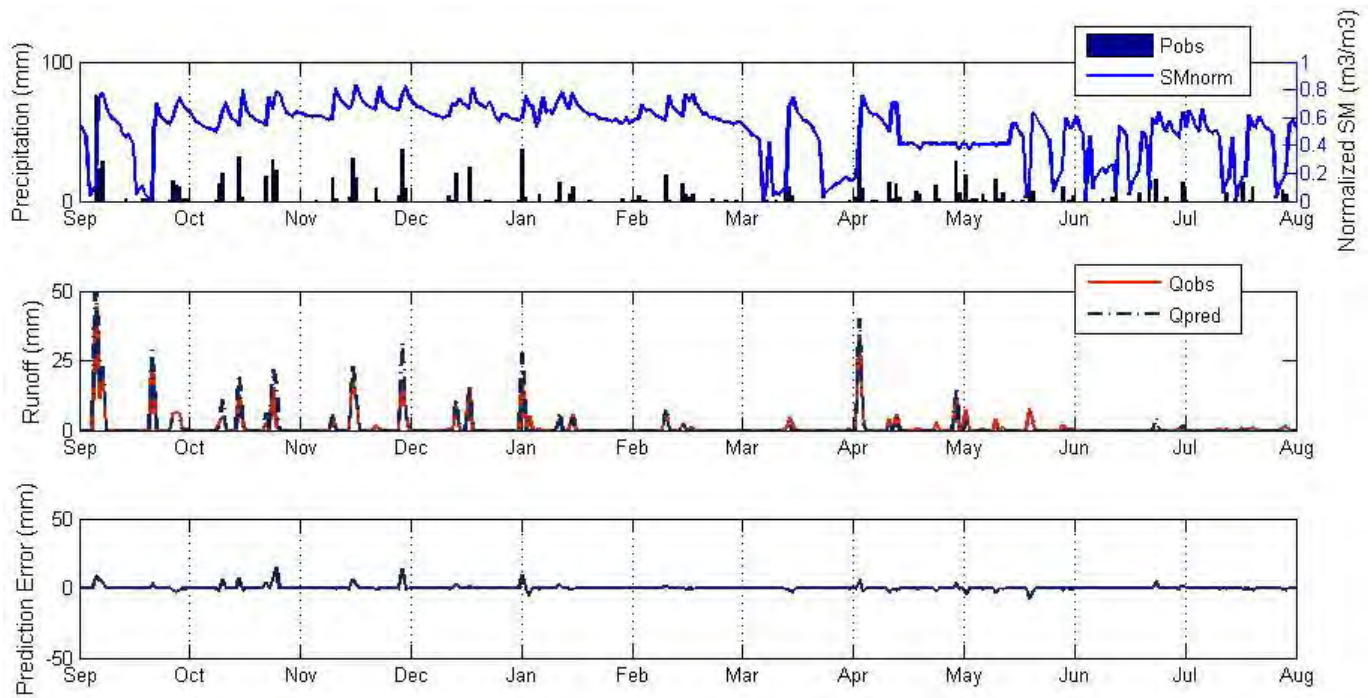


Figure 6-3: Precipitation, soil moisture, observed and simulated daily runoff and error for green roof W115.

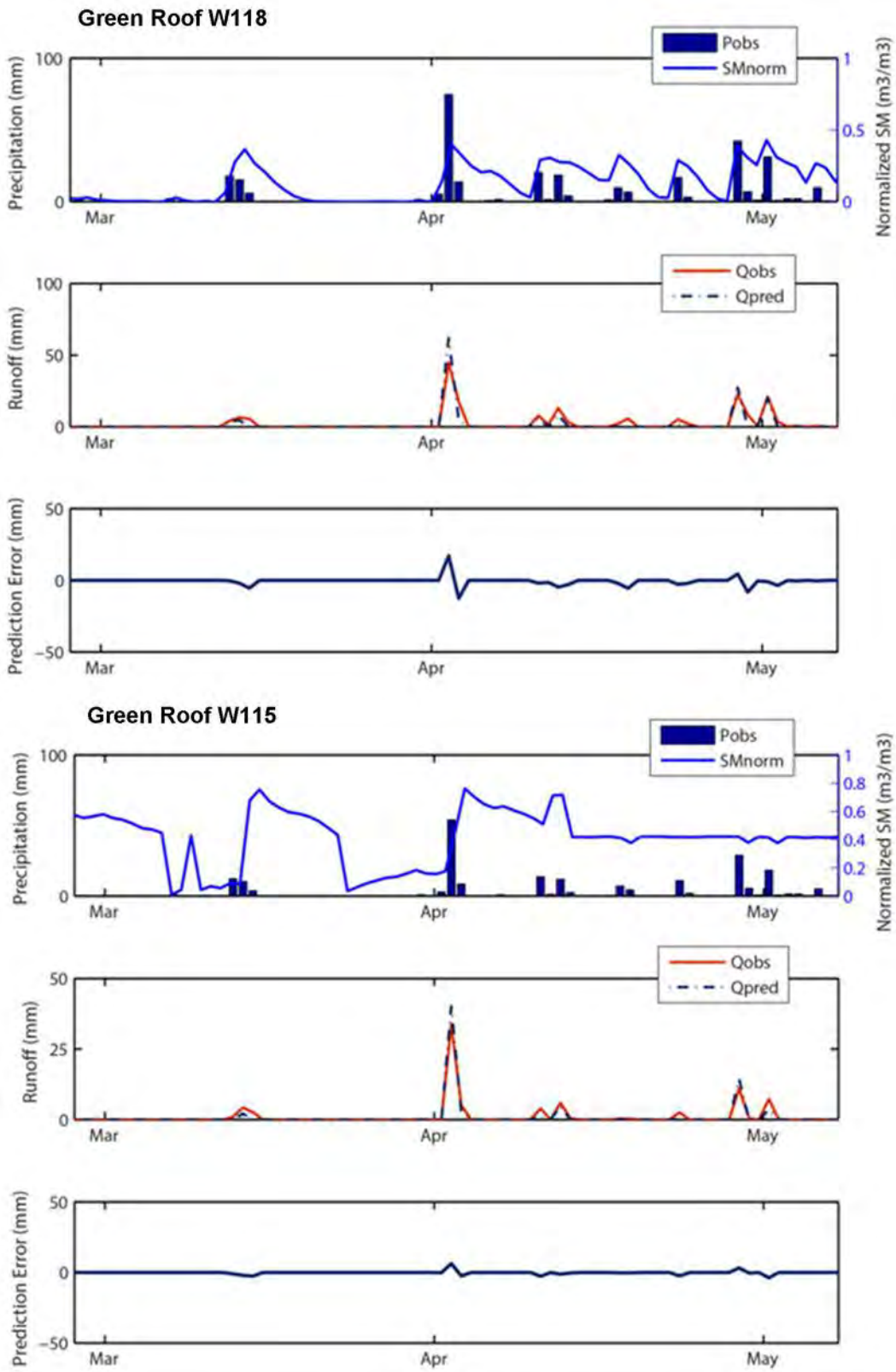


Figure 6-4: Comparison between green roof W118 and W115 from March to May 2012 only.

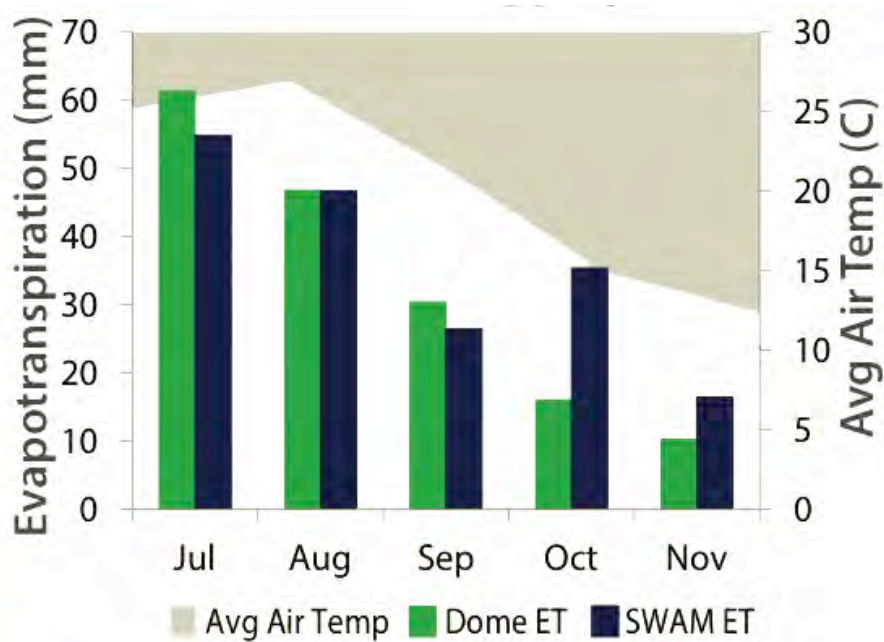


Figure 6-5: Comparison of measured versus modeled evapotranspiration (Dome ET to SWAM ET) on W118.

#### 6.4 Discussion of Results

Increasing the time aggregate in the model improves the NSE and reduces the positive PBIAS for both roof and SM probe types, yet has a minimal impact on the model’s negative PBIAS (see Figure 6-1); positive PBIAS values indicate model underestimation bias, and negative values indicate model overestimation bias. Thus, the runoff overestimation bias appears to be an issue regardless of changes in time aggregate. Time aggregates under 6 hours produced unacceptable results.

The analytical method proposed by SWAM is found to be capable of reproducing the observed daily runoff data with NSE values of 0.88 and 0.72 for the W118 and W115 green roofs, respectively. There are a number of factors that can be contributing to the performance differences, including the relative temperature sensitivities of each probe, seasonal differences between the performance of each roof (possibly affecting the substrate maximum water holding capacity), and instrument biases when collecting the observed data. However, it is believed that one of the greatest contributing factors is the relative location of the sensors within the respective drainage areas. Specifically, the W115 roof is a sloped roof that might support ponding at lower elevations (where the probe is currently situated) during larger rainfall events. As noted above, ponding is not considered in the water balance equations of the SWAM model. Another factor is a single measurement point for SM, which relies on spatially uniform green roof behavior whereas spatial heterogeneity could play a role in green roof runoff characteristics.

Figure 6-4 shows the performance of SWAM in predicting ET on monthly time aggregates. SWAM performs well in the months of July, August and September, however, declines in performance in the months of October and November. Average monthly air temperatures indicate that this drop in performance could be due to the sensitivity of the soil moisture probe to sharp changes in air temperature, as well as the sensor sensitivity to non-ambient temperatures (assumed to be temperatures above or below 25 °C). These preliminary results indicate that there is potential for this methodology to be used in estimating green roof ET, however, more extensive analysis is required in order to validate the approach. While there is some indirect indication of probe sensitivities to temperature changes, the effects are inconclusive and require further study.

## **6. 5 Conclusions**

The results presented in this chapter show that a soil water balance approach using monitored precipitation and SM, such as the proposed SWAM methodology, can provide a low-cost alternative to the custom made weir device or lysimeter systems frequently used to quantify runoff during green roof studies. Thus, this work has provided an important first step in developing a green roof runoff monitoring system that might be reliably deployed on a wider scale. The discrepancies in runoff estimates have been attributed to SM probe sensitivities to ambient factors such as temperature, which require further investigation, as well as possible effects of green roof spatial heterogeneity.

SWAM's ability to provide an indirect estimation of green roof ET is also considered important given the challenges involved with obtaining direct ET measurements on urban roofs. Nonetheless, more work and more data are required to validate the applicability of SWAM in estimating ET.

If deployed on new monitoring sites, this method would require knowledge of the water holding capacity of the soil as well as the range of soil moisture probe voltage readings, which could be determined through simple calibration tests.

## Chapter 7 References

- Aitkenhead-Peterson, J. A., Dvorak, B. D., Volder, A., and Stanley, N. C. (2010). Chemistry of growth medium and leachate from green roof systems in south-central Texas. *Urban Ecosystems*, 14(1), 17–33. doi:10.1007/s11252-010-0137-4
- Alsop, S., Ebbs, S., and Retzlaff, W. (2010). The exchangeability and leachability of metals from select green roof growth substrates. *Urban Ecosystems*, 13(1), 91–111. doi:10.1007/s11252-009-0106-y
- Baumhardt, R. L., Lascano, R. J., and Evett, S. R. (2000). Soil material, temperature, and salinity effects on calibration of multisensor capacitance probes. *Soil Sci. Soc. Am. J.* 64:1940-1946.
- Bengtsson, L., Grahn, L., and Olsson, J. (2005). Hydrological function of a thin extensive green roof in southern Sweden. *Nordic Hydrology*, 36(3), 259–268. Retrieved from <http://www.iwaponline.com/nh/036/0259/0360259.pdf>
- Berghage, R. D., Beattie, D., Jarrett, A. R., Thuring, C., Razaeei, F., and O'Connor, T. (2009). Green Roofs for Stormwater Runoff Control. EP A/600/R-09/026. Cincinnati, OH. Retrieved from <http://nepis.epa.gov/Exe/ZyNET.exe/P1003704.TXT>
- Berghage, R. D., and Gu, J. (2009). Effect of Drain Layers on Green Roof Stormwater Performance. In *Seventh Annual Greening Rooftops for Sustainable Communities Conference, Awards and Trade Show* (pp. 1–17). Atlanta, GA.
- Berghage, R. D., Miller, C., Bass, B., Moseley, D., and Weeks, K. (2010). Stormwater Runoff from a Large Commercial Roof in Chicago. In *CitiesAlive! Eighth Annual Green Roof and Wall Conference* (pp. 1–13). Vancouver, BC.
- Berndtsson, J. C. (2010). Green roof performance towards management of runoff water quantity and quality: A review. *Ecological Engineering*, 36(4), 351–360. doi:10.1016/j.ecoleng.2009.12.014
- Berndtsson, J. C., Bengtsson, L., and Jinno, K. (2009). Runoff water quality from intensive and extensive vegetated roofs. *Ecological Engineering*, 35(3), 369–380. doi:10.1016/j.ecoleng.2008.09.020
- Berndtsson, J. C., Emilsson, T., and Bengtsson, L. (2006). The influence of extensive vegetated roofs on runoff water quality. *The Science of the Total Environment*, 355(1-3), 48–63. doi:10.1016/j.scitotenv.2005.02.035
- Bliss, D. J., Neufeld, R. D., and Ries, R. J. (2009). Storm Water Runoff Mitigation Using a Green Roof. *Environmental Engineering Science*, 26(2), 407–418. doi:10.1089/ees.2007.0186
- Bogena, H. R., Huisman, J. A., Oberdörster, C., and Vereecken, H. (2007). Evaluation of a low-cost soil water content sensor for wireless network applications. *Journal of Hydrology*, 344(1-2), 32–42. doi:10.1016/j.jhydrol.2007.06.032
- Bricker, S., Longstaff, B., Dennison, W., Jones, A., Boicourt, K., Wicks, C., and Woerner, J. (2007). *Effects of Nutrient Enrichment in the Nation's Estuaries: A Decade of Change*. NOAA Coastal Ocean Program Decision Analysis Series No. 26 (p. 328). Silver Spring, MD.
- Brocca, L., and Moramarco, T. (2013). A new method for rainfall estimation through soil moisture observations. *Geophysical Research*, 40(October 2012), 1–6. doi:10.1002/GRL.50173
- Campbell Scientific Inc. (2012). CS650 and CS655 Water Content Reflectometers Instruction Manual (p. 56).
- Carpenter, D. D., and Kaluvakolanu, P. (2011). Effect of roof surface type on storm-water runoff from full-scale roofs in a temperate climate. *Journal of Irrigation and Drainage Engineering*, 137(3), 161–169. doi:10.1061/(ASCE)IR.1943-4774.0000185
- Carson, T. B., Marasco, D. E., Culligan, P. J., and McGillis, W. R. (2013). Hydrological performance of extensive green roofs in New York City: Observations and multi-year modeling of three full-scale systems. *Environmental Research Letters*, 8(2), 024036. doi:10.1088/1748-9326/8/2/024036
- Clark, S. E., Long, B. V., Siu, C. Y. S., Spicher, J., and Steele, K. A. (2008). Early-Life Roof Runoff Quality: Green vs. Traditional Roofs. In *Low Impact Development for Urban Ecosystem and Habitat Protection*. ASCE. (doi: [http://dx.doi.org/10.1061/41009\(333\)9](http://dx.doi.org/10.1061/41009(333)9))
- Coffman, L. (2000). *Low-Impact Development Design Strategies: An Integrated Design Approach* (p. 150). Prince George's County, MD.
- Connelly, M., Liu, K., and Schaub, J. (2006). BCIT Green Roof Research Program, Phase 1 Summary of Data Analysis (pp. 1–59). Vancouver, BC. Retrieved from <http://publications.gc.ca/site/eng/389231/publication.html>
- Crow, W. T., van den Berg, M. J., Huffman, G. J., and Pellarin, T. (2011). Correcting rainfall using satellite-based surface soil moisture retrievals: The Soil Moisture Analysis Rainfall Tool (SMART). *Water Resources Research*, 47(8), n/a–n/a. doi:10.1029/2011WR010576

- Culligan, P. J. (2011). Green roofs: A solution for urban stormwater management? *Geo-Strata - Geo Institute of ASCE*, 12(2), 30–32, 34.
- Czarnomski, N. M., Moore, G. W., Pypker, T. G., Licata, J., and Bond, B. J. (2005). Precision and accuracy of three alternative instruments for measuring soil water content in two forest soils of the Pacific Northwest, *Can. J. For. Res.* 35:1867–1876. doi:10.1139/X05-121
- De Cuyper, K., Dinne, K., and Van De Vel, L. (2004). Rainwater Discharge from Green Roofs. In CIB W062 30th International Symposium on Water Supply and Drainage for Buildings (p. 12). Rotterdam, Netherlands. Retrieved from <http://www.irb.fraunhofer.de/CIBlibrary/search-quick-result-list.jsp?AandidSuche=CIB+DC10549>
- Decagon Devices Inc. (2012). EC-5 Soil Moisture Sensor User's Manual (p. 24).
- DiGiovanni, K., Gaffin, S. R., and Montalto, F. (2010). Green Roof Hydrology: Results from a Small-Scale Lysimeter Setup (Bronx, NY). In *Low Impact Development 2010: Redefining Water in the City* (pp. 1328–1341). San Francisco, CA: ASCE. Retrieved from <http://link.aip.org/link/?ASCECP/367/114/1>
- Dorigo, W. A., Wagner, W., Hohensinn, R., Hahn, S., Paulik, C., Xaver, A., Gruber, A., Drusch, M., S. Mecklenburg, S., van Oevelen, P., Robock, A., and Jackson, T. (2011). The International Soil Moisture Network: A data hosting facility for global in situ soil moisture measurements. *Hydrology and Earth System Sciences*, 15(5), 1675–1698. doi:10.5194/hess-15-1675-2011
- Dvorak, B., and Volder, A. (2010). Green roof vegetation for North American ecoregions: A literature review. *Landscape and Urban Planning*, 96(4), 197–213. Retrieved from <http://www.scopus.com/inward/record.url?eid=2-s2.0-77953324216andpartnerID=40andmd5=e4fa44b9f91f819d2b2f32c102745332>
- EPA. (2004). Report to Congress: Impacts and Control of CSOs and SSOs. Washington, DC. Retrieved from [http://cfpub.epa.gov/npdes/cso/cpolicy\\_report2004.cfm](http://cfpub.epa.gov/npdes/cso/cpolicy_report2004.cfm).
- EPA (2009). National Primary Drinking Water Regulations. Water: Drinking Water Contaminants U.S. Environmental Protection Agency, Report No. EPA 816-F-09-0004, pp. 6, <http://water.epa.gov/drink/contaminants/upload/mcl-2.pdf>.
- Erlichman, P., and Peck, S. W. (2013). Annual green roof industry survey for 2012 (p. 11).
- Fassman, E. and Simcock, R. (2012) Moisture measurements as performance criteria for extensive living roof substrates. *Journal of Environmental Engineering*, 138(8), 841-851. doi:10.1061/(ASCE)EE.1943-7870.0000532.
- Fassman-Beck, E., Voyde, E., Simcock, R., and Hong, Y. S. (2013). 4 Living roofs in 3 locations: Does configuration affect runoff mitigation? *Journal of Hydrology*, 490, 11–20. doi:10.1016/j.jhydrol.2013.03.004
- Field, R., and Sullivan, D. (2001). Overview of EPA's wet-weather flow research program. *Urban Water*, 3, 165–169.
- GeoSyntec Consultants Inc. (2012). High performance green infrastructure for CSO Reduction and Advanced Rainwater Harvesting. Retrieved from [https://www.optirtc.com/CSO\\_ARWH.aspx](https://www.optirtc.com/CSO_ARWH.aspx)
- Getter, K. L., and Rowe, D. B. (2006). The role of extensive green roofs in sustainable development. *HortScience*, 41(5), 1276–1285.
- Getter, K. L., Rowe, D. B., and Andresen, J. A. (2007). Quantifying the effect of slope on extensive green roof stormwater retention. *Ecological Engineering*, 31, 225–31. doi:10.1016/j.ecoleng.2007.06.004
- GreenRoofs.com. (2014). The International Greenroof and Greenwall Projects Database! <http://www.greenroofs.com/projects/plist.php>
- Gregoire, B. G., and Clausen, J. C. (2011). Effect of a modular extensive green roof on stormwater runoff and water quality. *Ecological Engineering*, 37, 963–9. doi:10.1016/j.ecoleng.2011.02.004
- Hathaway, A. M., Hunt, W. F., and Jennings, G. D. (2008). A field study of green roof hydrologic and water quality performance. *American Society of Agricultural and Biological Engineers*, 51(1), 37–44.
- Hook, W. R., Ferre, T. P. A., and Livingston, N. J. (2004). The effects of salinity on the accuracy and uncertainty of water content measurement. *Soil Science Society of America*, 68 (1), 47–56, doi:10.2136/sssaj2004.4700.
- Howarth, R. W., Marino, R., Swaney, D. P., and Boyer, E. W. (2011). Chapter 10: Wastewater and Watershed Influences on Primary Productivity and Oxygen Dynamics in the Lower Hudson River Estuary. *The Hudson River Estuary*, Edited by J. S. Levinton and J. R. Waldman, Cambridge University Press, ISBN: 9780521207980.
- Hutchinson, D., Abrams, P., Retzlaff, R., and Liptan, T. (2003). Stormwater monitoring two ecoroofs in Portland, Oregon, USA. In *Greening Rooftops for Sustainable Communities* (pp. 1–18). Chicago, IL. Conference sponsored by Green Roofs for Healthy Cities, Toronto, and the City of Chicago, May 29-30, 2003.
- Jarrett, A. R., Hunt, W. F., and Berghage, R. D. (2006). Annual and Individual-Storm Green Roof Stormwater Response

- Models. In 2006 ASAE Annual Meeting (p. 062310). St. Joseph, MI: American Society of Agricultural and Biological Engineers. doi:10.13031/2013.20793
- Joshi, C., Mohanty, B. P., Jacobs, J. M., and Ines, A. V. M. (2011). Spatiotemporal analyses of soil moisture from point to footprint scale in two different hydroclimatic regions. *Water Resources Research*, 47, W01508, doi:10.1029/2009WR009002.
- Kirchner, J. W. (2009). Catchments as simple dynamical systems: Catchment characterization, rainfall-runoff modeling, and doing hydrology backward. *Water Resources Research*, 45, W02429, doi:10.1029/2008WR006912.
- Köhler, M., and Keeley, M. (2004). Chapter: The Green Roof Tradition in Germany: The Example of Berlin. Green Roofs: Ecological Design and Construction. By Eath Pledge Foundation, Schiffer Publishing ISBN-10: 0764321897, ISBN-13: 978-0764321894.
- Kurtz, T. (2008). Flow Monitoring of Three Ecoroofs in Portland, Oregon. In 2008 Low Impact Development Conference. Seattle, WA: ASCE.
- Liu, K., and Minor, J. (2005). Performance evaluation of an extensive green roof. In *Greening Rooftops for Sustainable Communities* (pp. 1–11). Washington, DC.
- Marasco, D. E., *Alternative Metrics of Green Roof Hydrological Performance: Evapotranspiration and Peak Flow Reduction*, PhD Thesis, Columbia University, 2014.
- Mayor's Office of Long-Term Planning and Sustainability. (2008). Sustainable Stormwater Management Plan. Management. New York. Retrieved from [www.nyc.gov/PlaNYC2030](http://www.nyc.gov/PlaNYC2030)
- Mentens, J., Raes, D., and Hermy, M. (2003). Effect of Orientation on the Water Balance of Greenroofs. In *Greening Rooftops for Sustainable Communities* (pp. 1–9). Chicago, IL. Conference sponsored by Green Roofs for Healthy Cities, Toronto, and the City of Chicago, May 29-30, 2003.
- Miller, C. (2012). The Need for Establishing Performance Metrics. In *Mid-Atlantic Green Roof Science and Technology Symposium*. College Park, MD.
- Montalto, F., Behr, C., Alfredo, K., Wolf, M., Arye, M., and Walsh, M. (2007). Rapid assessment of the cost-effectiveness of low impact development for CSO control. *Landscape and Urban Planning*, 82(3), 117–131. doi:10.1016/j.landurbplan.2007.02.004
- Monterusso, M. A., Rowe, D. B., and Rugh, C. L. (2005). Establishment and persistence of Sedum spp. and Native Taxa for green roof applications. *HortScience*, 40(2), 391–396.
- Moran, A. C., Hunt, W. F., and Smith, J. T. (2005). Green Roof Hydrologic and Water Quality Performance from Two Field Sites in North Carolina. In *Managing Watersheds for Human and Natural Impacts* (pp. 1–12). Reston, VA: American Society of Civil Engineers. doi:10.1061/40763(178)99
- Morgan, S., Celik, S., and Retzlaff, W. (2013). Green roof storm-water runoff quantity and quality. *Journal of Environmental Engineering*, 139(4), 471–478. doi:10.1061/(ASCE)EE.1943-7870.0000589
- Moriassi, D., and Arnold, J. (2007). Model evaluation guidelines for systematic quantification of accuracy in watershed simulations. *Transactions of the ASABE*, 50(3), 885–900.
- Nardini, A., Andri, S., and Crasso, M. (2011). Influence of substrate depth and vegetation type on temperature and water runoff mitigation by extensive green roofs: shrubs versus herbaceous plants. *Urban Ecosystems*, 15(3), 697–708. doi:10.1007/s11252-011-0220-5
- Nash, J. E., and Sutcliffe, J. V. (1970). River flow forecasting through conceptual models part I—A discussion of principles. *Journal of Hydrology*, 10(3), 282-290.
- National Atmospheric Deposition Program, 2012. (2012). National Atmospheric Deposition Program 2011 Annual Summary. Illinois at Urbana-Champaign, IL.
- NRCS (1986). *Urban Hydrology for Small Watersheds*, TR-55 (p. 164). Washington, D.C.
- NYC DEP. (2010). *NYC Green Infrastructure Plan: A sustainable strategy for clean waterways* (pp. 1–154). New York, NY.
- NYS DEC. (2008). *The Lower Hudson River Basin Waterbody Inventory and Priority Waterbodies List*. Bureau of Watershed Assessment and Management, Division of Water, [http://www.dec.ny.gov/docs/water\\_pdf/pwllhudintr.pdf](http://www.dec.ny.gov/docs/water_pdf/pwllhudintr.pdf)
- Oberndorfer, E., Lundholm, J., Bass, B., Coffman, R. R., Doshi, H., Dunnett, N., Gaffin, S., Köhler, M, Liu, K. and Rowe, B. (2007). Green roofs as urban ecosystems: Ecological structures, runctions, and services. *BioScience*, 57(10), 823–833. doi:10.1641/B571005
- Palla, A., Sansalone, J. J., Gnecco, I., and Lanza, L. G. (2011). Storm water infiltration in a monitored green roof for

hydrologic restoration. *Water Science and Technology*, 64(3), 766. doi:10.2166/wst.2011.171

Peel, M. C., Finlayson, B. L., and McMahon, T. A. (2007). Updated world map of the Köppen-Geiger climate classification. *Hydrology and Earth System Sciences*, 11(5), 1633–1644. doi:10.5194/hess-11-1633-2007

Robinson, D. A., Jones, S. B., Blonquist, J. M., and Friedman, S. P. (2005). A physically derived water content/permittivity calibration model for coarse-textured, layered soils. *Soil Science Society of America Journal*, 69(5), 1372. doi:10.2136/sssaj2004.0366

Sakaki, T., and Rajaram, H. (2006). Performance of different types of time domain reflectometry probes for water content measurement in partially saturated rocks. *Water Resources Research*, 42(7), n/a–n/a. doi:10.1029/2005WR004643

Schroll, E., Lambrinos, J., Righetti, T., and Sandrock, D. (2011). The role of vegetation in regulating stormwater runoff from green roofs in a winter rainfall climate. *Ecological Engineering*, 37(4), 595–600. doi:10.1016/j.ecoleng.2010.12.020

She, N. and Pang, J. (2010). "Physically Based Green Roof Model." *J. Hydrol. Eng.* 15, Special Issue: Low Impact Development, Sustainability Science, and Hydrological Cycle, 458–464.

Sherrard, J. A., and Jacobs, J. M. (2012). Vegetated roof water-balance model: Experimental and model results. *Journal of Hydrologic Engineering*, 17(8), 858–868. doi:10.1061/(ASCE)HE.1943-5584.0000531

Spolek, G. (2008). Performance monitoring of three ecoroofs in Portland, Oregon. *Urban Ecosystems*, 11, 349–359. doi:10.1007/s11252-008-0061-z

Starry, O. (2013). The Comparative Effects of Three Sedum Species on Green Roof Stormwater Retention. University of Maryland, Dissertation, URI: <http://hdl.handle.net/1903/14622>.

Stovin, V. (2010). The potential of green roofs to manage Urban Stormwater. *Water and Environment Journal*, 24, 192–199. doi:10.1111/j.1747-6593.2009.00174.x

Stovin, V., Vesuviano, G., and Kasmin, H. (2012). The hydrological performance of a green roof test bed under UK climatic conditions. *Journal of Hydrology*, 414–415, 148–161. doi:10.1016/j.jhydrol.2011.10.022

Strecker, E., B. Urbonas, M. Quigley, J. Howell, and T. Hesse (2002). "Urban Stormwater BMP Performance Monitoring: A Guidance Manual for Meeting the National Stormwater BMP Database Requirements" Office of Water, US EPA. Report No. EPA-821-B-02-001, April, 2002.

Teemusk, A., and Mander, Ü. (2007). Rainwater runoff quantity and quality performance from a greenroof: The effects of short-term events. *Ecological Engineering*, 30, 271–277. doi:10.1016/j.ecoleng.2007.01.009

Toronto and Region Conservation Authority. (2006). Evaluation of an Extensive Greenroof (p. 167). Toronto, ON.

Trejo, E. (2013). Insecticide application at W118. Personal Communication.

VanWoert, N. D. (2005). Watering regime and green roof substrate design affect sedum plant growth. *HortScience*, 40(3), 659–664.

VanWoert, N. D., Rowe, D. B., Andresen, J. a, Rugh, C. L., Fernandez, R. T., and Xiao, L. (2005). Green roof stormwater retention: Effects of roof surface, slope, and media depth. *Journal of Environmental Quality*, 34(3), 1036–44. doi:10.2134/jeq2004.0364

Vijayaraghavan, K., Joshi, U. M., and Balasubramanian, R. (2012). A field study to evaluate runoff quality from green roofs. *Water Research*, 46(4), 1337–1345. doi:10.1016/j.watres.2011.12.050

Villarreal, E. L. (2007). Runoff detention effect of a sedum green-roof. *Nordic Hydrology*, 38(1), 99. doi:10.2166/nh.2007.031

Voyde, E., Fassman, E., and Simcock, R. (2010). Hydrology of an extensive living roof under sub-tropical climate conditions in Auckland, New Zealand. *Journal of Hydrology*, 394, 384–395. doi:10.1016/j.jhydrol.2010.09.013

Walker, J. P., Willgoose, G. R., and Kalma, J. D. (2004). In situ measurement of soil moisture: A comparison of techniques. *Journal of Hydrology*, 293(1-4), 85–99. doi:10.1016/j.jhydrol.2004.01.008

Williams, E. S. (2003). Hydrologic and Economic Impacts of Alternative Residential Land Development Methods. University of Florida.

Williams, E. S., and Wise, W. R. (2006). Hydrologic impacts of alternative approaches to storm water management and land development. *Journal of the American Water Resources Association*, 42(2), 443–456.

## Appendix A Site Equipment Tables

Table 7-1: Monitoring Equipment at the W115 Office Building at Columbia University.

<b>SITE NAME - W115</b>		
Scientific Equipment	Description	Range of Tolerance
HOBO U30 Wi-Fi Data Logger W/ Analog Input - U30-WIF	Data Logger – Wi-Fi	-20°C to 40°C
2-bit Temperature/Relative Humidity (RH) Smart Sensor (2 m cable) - S-THB-M002	Air Temp/RH Sensor	-40°C to 75°C
Wind Speed and Direction Smart Sensor (3 m cable) - S-WCA-M003	Wind and Gust Speed/Wind Direction Sensor	-40°C to 75°C
Solar Radiation Sensor (Silicon Pyranometer) Smart Sensor - S-LIB-M003	Solar Radiation Sensor	-40° to 75°C
Barometric Pressure Smart Sensor - S-BPA-CM10	Barometric Pressure Sensor	-40° to 70°C
EC-5 Soil Moisture Smart Sensor - S-SMC-M005	Soil Moisture Sensor	0 to 50°C
12-Bit Temp Smart Sensor (2 m cable) - S-TMB-M002	Soil Temp Sensor	-40° to 100°C
.2 mm Rainfall Smart Sensor (2 m cable) - S-RGB-M002	Tipping Bucket Rain Gauge	0° to 50°C
Custom Drainage Pipe Weir with Senix ToughSonic Ultrasonic Distance Sensor - TSPC-30S1	Runoff sensor	0° to 70°C

Table 7-2: Monitoring Equipment at the W118 Residence Hall at Columbia University.

<b>SITE NAME - W118</b>		
Scientific Equipment	Description	Range of Tolerance
HOBO U30 Wi-Fi Data Logger W/ Analog Input - U30-WIF	Data Logger – Wi-Fi	-20°C to 40°C
2-bit Temperature/Relative Humidity (RH) Smart Sensor (2m cable) - S-THB-M002	Air Temp/RH Sensor	-40°C to 75°C
Soil Moisture Smart Sensors - CS-615 L50	Soil Moisture Sensor	0 to 70°C
EC-5 Soil Moisture Smart Sensor - S-SMC-M005	Soil Moisture Sensor	0 to 50°C
12-Bit Temp Smart Sensor (2 m cable) - S-TMB-M002	Soil Temp Sensor	-40° to 100°C
.2 mm Rainfall Smart Sensor (2 m cable) - S-RGB-M002	Tipping Bucket Rain Gauge	0° to 50°C
EC-5 Soil Moisture Smart Sensor - S-SMC-M005	Soil Moisture Sensor	0 to 50°C
Custom Drainage Pipe Weir with Senix ToughSonic Ultrasonic Distance Sensor - TSPC-30S1	Runoff sensor	0° to 70°C

Table 7-3: Monitoring Equipment at the US Postal Service Morgan Distribution Facility.

<b>SITE NAME - USPS</b>		
Scientific Equipment	Description	Range of Tolerance
HOBO U30 GSM Data Logger W/ Analog Input - U30-GSM	Data Logger - GSM Cellular	-20°C to 40°C
2-bit Temperature/Relative Humidity (RH) Smart Sensor (2 m cable) - S-THB-M002	Air Temp/RH Sensor	-40°C to 75°C
Wind Speed and Direction Smart Sensor (3 m cable) - S-WCA-M003	Wind and Gust Speed/Wind Direction Sensor	-40°C to +75°C
Solar Radiation Sensor (Silicon Pyranometer) Smart Sensor - S-LIB-M003	Solar Radiation Sensor	-40° to 75°C
EC-5 Soil Moisture Smart Sensor - S-SMC-M005	Soil Moisture Sensor	0 to 50°C
12-Bit Temp Smart Sensor (2 m cable) - S-TMB-M002	Soil Temp Sensor	-40° to 100°C
.2 mm Rainfall Smart Sensor (2 m cable) - S-RGB-M002	Tipping Bucket Rain Gauge	0° to 50°C
Custom Drainage Pipe Weir with Senix ToughSonic Ultrasonic Distance Sensor - TSPC-30S1	Runoff sensor	0° to 70°C

Table 7-4: Monitoring Equipment at the Con Edison Facility in Long Island City (HOBO Vendor).

<b>SITE NAME – ConEd</b>		
Scientific Equipment	Description	Range of Tolerance
HOBO U30 GSM Data Logger W/ Analog Input - U30-GSM	Data Logger - GSM Cellular	-20°C to 40°C
2-bit Temperature/Relative Humidity (RH) Smart Sensor (2 m cable) - S-THB-M002	Air Temp/RH Sensor	-40°C to 75°C
Photosynthetic Light (PAR) Smart Sensor - S-LIB-M003	PAR Sensor	-40° to 75°C
Barometric Pressure Smart Sensor - S-BPA-CM10	Barometric Pressure Sensor	-40° to 70°C
EC-5 Soil Moisture Smart Sensor - S-SMC-M005	Soil Moisture Sensor	0 to 50°C
12-Bit Temp Smart Sensor (2 m cable) - S-TMB-M002	Soil Temp Sensor	-40° to 100°C
.2 mm Rainfall Smart Sensor (2 m cable) - S-RGB-M002	Tipping Bucket Rain Gauge	0° to 50°C
2 Custom Drainage Pipe Weirs with Senix ToughSonic Ultrasonic Distance Sensors - TSPC-30S1	Runoff sensor	0° to 70°C

Table 7-5: Weather Monitoring Equipment at the Con Edison Facility (Campbell Scientific Vendor).

<b>SITE NAME – ConEd</b>		
Scientific Equipment	Description	Range of Tolerance
Campbell Scientific (CS) CR3000-ST-SW-RC-NC	Data Logger	-25°C to 50°C
Temperature/Relative Humidity (RH) Sensor - CS215-L50	Air Temp/RH Sensor	-40°C to 70°C
RM Young Wind Monitor - 05103-L65	Wind and Gust Speed/Wind Direction Sensor	-50°C to +50°C
Net Radiometer - CNR 4L	Allwave Radiation Sensors	-40° to 80°C
Soil Moisture Smart Sensors - CS-615 L50	Soil Moisture Sensors	0 to 70°C
Temperature Probes - 107-L50	Soil Temp Sensor	-35° to 50°C
Nova Lynx Rain Gage 0.01 inch tip	Tipping Bucket Rain Gauge	-20° to 70°C
Apogee IR Temperature Radiometers	IR Surface Temperature Sensors	-30° to 65°C

Table 7-6: Weather Monitoring Equipment at the Fieldston School in Riverdale, Bronx.

<b>SITE NAME - Fldstn</b>		
Scientific Equipment	Description	Range of Tolerance
Campbell Scientific (CS) CR3000-ST-SW-RC-NC	Data Logger	-25°C to 50°C
Temperature/Relative Humidity (RH) Sensor - CS215-L50	Air Temp/RH Sensor	-40°C to 70°C
RM Young Wind Monitor - 05103-L65	Wind and Gust Speed/Wind Direction Sensor	-50°C to +50°C
Kipp and Zonen Solar Radiation Sensors - CMP3	Solar Radiation Sensors	-40° to 80°C
Soil Moisture Smart Sensors - CS-615 L50	Soil Moisture Sensors	0 to 70°C
Temperature Probes - 107-L50	Soil Temp Sensor	-35° to 50°C
Met One AC Rain Gage 0.01 inch tip	Tipping Bucket Rain Gauge	-20° to 50°C
Apogee IR Temperature Radiometers	IR Surface Temperature Sensors	-30° to 65°C

Table 7-7: Monitoring Equipment at the Bronx Design and Construction Academy

<b>SITE NAME – BDCA</b>		
Scientific Equipment	Description	Range of Tolerance
HOBO U30 GSM Data Logger W/ Analog Input - U30-Wi-Fi	Data Logger - GSM Cellular	-20°C to 40°C
2-bit Temperature/Relative Humidity (RH) Smart Sensor (2 m cable) - S-THB-M002	Air Temp/RH Sensor	-40°C to 75°C
Soil Moisture Smart Sensor - EC-5 S-SMC-M005	Soil Moisture Sensor	0 to 50°C
.2 mm Rainfall Smart Sensor (2 m cable) - S-RGB-M002	Tipping Bucket Rain Gauge	0° to 50°C
Custom Drainage Pipe Weir with Senix ToughSonic Ultrasonic Distance Sensors - TSPC-30S1	Runoff sensor	0° to 70°C

Table 7-8: Weather Monitoring Equipment at Regis High School

<b>SITE NAME – Regis</b>		
Scientific Equipment	Description	Range of Tolerance
Campbell Scientific (CS) CR3000-ST-SW-RC-NC	Data Logger	-25°C to 50°C
Temperature/Relative Humidity (RH) Sensor - CS215-L50	Air Temp/RH Sensor	-40°C to 70°C
RM Young Wind Monitor - 05103-L65	Wind and Gust Speed/Wind Direction Sensor	-50°C to +50°C
Net Radiometer - CNR 4L	Allwave Radiation Sensors	-40° to 80°C
Soil Moisture Smart Sensors - CS-615 L50	Soil Moisture Sensors	0 to 70°C
Temperature Probes - 107-L50	Soil Temp Sensor	-35° to 50°C
Nova Lynx Rain Gage 0.01 inch tip	Tipping Bucket Rain Gauge	-20° to 70°C
Apogee IR Temperature Radiometers	IR Surface Temperature Sensors	-30° to 65°C
3 Custom Drainage Pipe Weirs with Senix ToughSonic Ultrasonic Distance Sensors - TSPC-30S1	Runoff sensor	0° to 70°C

## **Appendix B    Water Quality Results**

Table 7-9: Summary of Results from Water Quality Monitoring (March 10, 2011 – August 2, 2012). The average of the pH was calculated by first transforming the measurements using this equation:  $[H^+] = 10^{-pH}$ . Once averaged, the  $[H^+]$  value was converted back via this equation:  $pH = -\log[H^+]$ .

Sample ID	Sample Date	pH	Conductivity (uS/cm)	Turbidity (NTU)	Apparent Color (PtCo)	NO <sub>3</sub> <sup>-</sup>	NH <sub>4</sub> <sup>+</sup>	P	Ca	K	Na	Mg	B
34-W115.C	3/10/2011	5.95	148.40	0.00	na	1.72	na	na	na	na	na	na	na
35-W118.C	3/10/2011	6.23	218.90	1.16	na	3.34	na	na	na	na	na	na	na
36-Fdston.C	3/10/2011	7.03	21.00	0.02	na	0.78	na	na	na	na	na	na	na
37-W115.GR	3/10/2011	7.82	138.90	2.89	na	na	na	na	na	na	na	na	na
38-W118.GR	3/10/2011	8.06	96.67	0.58	na	0.77	na	na	na	na	na	na	na
39-Fdston.GR	3/10/2011	7.99	144.60	0.89	na	1.64	na	na	na	na	na	na	na
40-Rain	3/10/2011	5.50	66.82	0.04	na	1.41	na	na	na	na	na	na	na
41-W118.C	3/21/2011	6.77	40.37	0.67	na	1.14	na	na	na	na	na	na	na
42-W118.GR	3/21/2011	7.63	72.93	0.51	na	0.00	na	na	na	na	na	na	na
43-W115.C	3/23/2011	6.23	13.67	1.76	na	1.19	na	na	na	na	na	na	na
44-W118.C	3/23/2011	7.42	25.75	1.84	na	1.69	na	na	na	na	na	na	na
45-W115.GR	3/23/2011	7.42	77.00	4.57	na	0.58	na	na	na	na	na	na	na
46-W118.GR	3/23/2011	7.97	95.77	0.60	na	0.00	na	na	na	na	na	na	na
47-Rain	3/23/2011	4.59	53.69	1.03	na	2.01	na	na	na	na	na	na	na
48-W115.C	4/5/2011	6.41	21.00	1.21	na	2.70	na	na	na	na	na	na	na
49-W118.C	4/5/2011	6.13	188.80	2.79	na	6.12	na	na	na	na	na	na	na
50-W115.GR	4/5/2011	7.55	143.10	0.35	na	0.59	na	na	na	na	na	na	na
51-W118.GR	4/5/2011	7.40	89.05	0.72	na	0.91	na	na	na	na	na	na	na
52-W118.C	4/12/2011	7.25	na	1.40	39.45	3.82	na	na	na	na	na	na	na
53-Rain	4/12/2011	4.99	26.32	1.07	23.44	1.11	na	na	na	na	na	na	na
54-W118.GR	4/13/2011	7.18	86.23	2.96	127.04	0.55	na	na	na	na	na	na	na
55-USPS.GR	4/13/2011	7.64	212.00	10.47	482.66	0.94	na	na	na	na	na	na	na
56-W115.C	4/28/2011	7.21	33.38	1.13	29.66	0.42	0.60	0.00	2.51	0.28	0.54	0.28	0.00
57-W118.C	4/28/2011	7.04	36.28	1.60	81.83	0.08	0.32	0.00	2.69	0.40	1.37	0.51	0.47
58-W115.GR	4/28/2011	7.92	116.02	0.59	115.55	0.00	0.11	0.73	12.31	0.33	3.38	2.31	0.00
59-W118.GR	4/28/2011	7.19	73.40	0.73	150.21	0.00	0.10	0.00	7.07	0.13	2.45	2.08	2.62
60-USPS.C	6/17/2011	8.17	138.76	1.37	55.27	na	na	na	na	na	na	na	na
61-W118.GR	6/17/2011	7.37	123.05	0.98	268.69	0.00	0.12	0.00	10.16	0.92	16.60	5.69	3.26

62-USPS.GR	6/17/2011	7.67	154.10	9.24	325.76	0.11	0.28	0.00	14.67	1.51	2.26	3.55	0.00
63-Rain	6/17/2011	4.72	18.45	1.33	13.27	0.38	0.45	0.00	0.19	0.00	0.30	0.00	0.00
64-W115.C	6/23/2011	5.71	55.23	1.93	86.73	1.05	1.94	0.00	2.17	0.15	1.17	0.43	0.00
65-USPS.C	6/23/2011	7.78	199.01	4.43	69.21	0.90	5.45	0.34	18.90	9.93	14.36	4.78	0.00
66-ConEd.C	6/23/2011	6.22	52.38	0.95	39.83	0.68	1.48	0.00	2.13	0.20	3.27	0.86	0.00
67-USPS.GR	6/23/2011	7.49	208.90	3.01	148.51	0.00	2.44	0.73	20.26	1.55	2.52	4.47	0.00
68-ConEd.GR	6/23/2011	6.80	164.25	2.21	186.37	0.05	1.19	0.80	7.48	3.77	4.58	3.95	0.00
69-Rain	6/23/2011	4.37	57.65	1.42	31.54	1.32	1.52	0.33	2.00	0.17	2.25	0.38	0.00
70-W115.C	8/9/2011	4.94	12.38	na	4.98	na	na	na	na	na	na	na	na
71-W118.C	8/9/2011	6.47	5.90	na	8.75	na	na	na	na	na	na	na	na
72-W115.GR	8/9/2011	9.28	163.00	na	187.69	na	na	na	na	na	na	na	na
73-W118.GR	8/9/2011	7.38	42.74	na	126.47	na	na	na	na	na	na	na	na
74-Rain	8/9/2011	4.73	13.39	na	11.57	na	na	na	na	na	na	na	na
75-USPS.GR	8/15/2011	7.29	215.90	0.96	235.35	0.04	0.07	0.36	29.50	2.80	3.31	4.63	0.00
76-Fdston.GR	8/15/2011	7.45	101.80	0.67	152.09	0.00	0.18	0.00	13.02	2.88	3.00	1.53	0.00
77-Rain	8/15/2011	lost	5.00	0.60	0.46	0.21	0.45	0.00	0.21	0.00	0.26	0.00	0.00
78-USPS.C	8/25/2011	7.73	66.89	2.23	13.65	0.16	0.74	0.00	7.06	0.27	0.51	1.71	0.00
79-USPS.GR	8/25/2011	7.08	112.80	3.36	146.06	0.00	0.46	0.36	13.03	0.57	1.14	2.43	0.00
80-Rain	8/25/2011	4.80	17.60	0.43	0.00	0.38	0.48	0.00	0.56	0.00	1.15	0.18	0.00
81-W115.C	9/6/2011	6.31	41.40	0.45	0.00	0.00	0.10	0.00	0.42	0.13	0.00	0.15	0.00
82-W118.C	9/6/2011	6.53	5.31	0.36	12.52	0.09	0.00	0.45	0.12	0.05	0.39	0.00	0.00
83-W115.GR	9/6/2011	7.79	231.40	0.80	106.70	0.00	0.06	0.00	8.68	0.97	2.28	2.34	0.00
84-W118.GR	9/6/2011	7.44	106.10	1.51	166.97	0.00	0.54	0.62	6.43	2.04	14.44	3.85	0.64
85-W115.C	9/23/2011	6.56	11.65	0.59	na	0.24	0.20	0.00	0.59	0.13	1.80	0.33	0.00
86-W118.C	9/23/2011	6.37	2.77	0.71	na	0.00	0.03	0.00	0.11	0.00	0.09	0.00	0.00
87-W118.GR	9/23/2011	7.35	23.86	2.66	na	0.00	0.11	0.25	3.65	0.84	2.59	1.74	0.30
88-Rain	10/13/2011	5.48	17.72	0.24	0.00	0.22	0.21	0.00	0.39	0.00	1.69	0.13	0.00
89-USPS.C	10/19/2011	7.63	69.96	1.78	10.26	0.12	0.60	0.39	5.67	0.37	0.87	1.89	0.00
90-ConEd.C	10/19/2011	6.44	17.80	0.24	0.00	0.16	0.22	0.00	0.70	0.00	1.26	0.21	0.00
91-USPS.GR	10/19/2011	7.33	150.00	0.96	85.79	0.00	0.22	0.00	19.80	0.31	1.30	3.52	0.00
92-ConEd.GR	10/19/2011	6.98	68.34	0.70	112.54	0.00	0.03	0.00	5.62	0.78	1.43	2.42	0.00
93-Rain	10/19/2011	5.00	15.93	0.13	0.00	0.13	0.07	0.35	0.15	0.00	1.22	0.28	0.00
94-Rain	10/27/2011	4.71	24.15	0.33	0.00	0.47	0.34	0.00	0.96	0.00	0.05	0.12	0.00

95-ConEd.C	11/16/2011	6.38	17.57	0.59	9.69	0.39	0.30	0.00	0.59	0.00	0.23	0.07	0.00
96-ConEd.GR	11/16/2011	6.99	87.82	1.21	111.59	0.03	0.68	0.68	6.30	0.85	2.69	2.61	0.00
97-Rain	11/16/2011	4.99	27.78	0.47	0.00	0.32	0.11	0.00	0.62	0.11	0.27	0.10	0.00
98-USPS.C	11/17/2011	7.91	147.20	2.89	81.08	0.00	2.59	0.00	14.08	0.20	1.95	4.21	0.00
99-USPS.GR	11/17/2011	7.90	192.00	1.72	237.23	0.02	0.02	0.14	21.47	0.82	6.32	4.15	0.00
100-USPS.GR	11/17/2011	8.04	183.08	3.38	217.54	na	na	na	na	na	na	na	na
101-USPS.C	11/23/2011	7.67	65.63	na	54.14	na	na	na	na	na	na	na	na
102-USPS.GR	11/23/2011	8.09	192.31	na	105.06	na	0.18	0.51	28.53	0.62	0.21	na	0.00
103-Rain	11/23/2011	5.17	17.92	na	0.00	0.17	0.08	0.00	0.91	0.06	0.00	0.06	0.00
104-W118.C	12/7/2011	6.83	32.29	na	11.95	0.07	0.66	0.00	1.01	0.08	0.87	0.28	0.10
105-USPS.C	12/7/2011	7.17	86.56	na	50.94	0.13	0.84	0.00	8.96	0.16	1.25	2.53	0.00
106-Fdston.C	12/7/2011	7.26	10.30	na	0.00	0.12	0.00	1.13	0.41	0.11	0.00	0.11	0.00
107-W118.GR	12/7/2011	7.59	121.30	na	80.70	0.00	0.07	0.98	13.31	1.34	0.21	3.97	0.52
108-USPS.GR	12/7/2011	8.11	198.09	na	69.17	0.00	0.32	0.00	23.03	0.70	2.48	3.75	0.00
109-Fdston.GR	12/7/2011	7.48	170.90	na	179.03	0.02	0.01	1.41	20.51	5.51	0.61	2.22	0.00
110-Rain	12/7/2011	4.65	46.50	na	0.00	0.69	0.60	0.46	0.38	0.16	3.09	0.74	0.00
111-Rain	12/21/2011	5.05	21.21	na	3.29	0.59	0.30	0.00	1.03	0.13	0.94	0.23	0.00
112-Fdston.C	1/12/2012	6.51	65.03	na	2.16	0.84	0.93	0.00	3.50	0.23	2.06	1.36	0.00
113-Fdston.GR	1/12/2012	7.65	148.00	na	154.54	0.05	0.00	0.66	16.24	8.53	3.15	1.84	0.00
114-Rain	2/29/2012	4.76	20.96	0.86	22.88	0.42	6.00	0.00	0.75	0.23	0.35	0.00	0.00
115-USPS.C	2/29/2012	7.43	106.40	7.78	108.77	0.53	0.80	0.64	11.00	0.22	2.28	2.60	0.00
116-USPS.GR	2/29/2012	7.18	143.50	9.91	207.85	0.11	4.00	0.00	17.63	0.74	2.69	2.96	0.00
117-W118.C	2/29/2012	7.30	18.98	0.80	0.00	0.47	7.00	0.72	1.44	0.14	0.59	0.20	0.00
118-W118.GR	2/29/2012	7.40	93.51	0.67	20.43	0.01	9.00	0.99	10.23	0.23	4.22	2.32	0.72
119-ConEd.C	2/29/2012	6.49	12.52	1.63	2.04	0.29	0.14	0.95	0.51	0.00	0.29	0.00	0.00
120-ConEd.GR	2/29/2012	6.77	60.92	1.03	82.59	0.22	0.45	0.00	3.38	1.27	2.76	1.54	0.00
121-Fdston.C	3/17/2012	8.28	24.30	1.09	24.57	0.82	0.38	0.60	1.12	1.06	7.32	0.77	0.00
122-Fdston.GR	3/17/2012	8.86	111.30	2.80	108.39	0.03	0.03	1.15	13.53	9.26	4.87	2.50	0.00
123-Rain	4/23/2012	5.17	8.89	0.19	0.00	0.01	5.00	0.00	0.43	0.00	0.59	0.00	0.00
124-USPS.GR	5/1/2012	7.74	111.46	1.06	166.84	0.17	0.35	1.19	19.65	0.78	3.03	2.57	0.00
125-W118.GR	5/1/2012	6.91	109.60	1.06	185.62	0.03	0.33	1.27	14.24	1.43	3.29	3.47	2.76
126-Rain	5/9/2012	4.50	56.93	0.64	0.00	0.88	3.00	0.83	1.49	0.00	1.53	0.19	0.00

127-W118.GR	5/9/2012	6.67	106.90	0.67	90.87	0.03	0.06	0.00	13.83	0.23	6.68	3.60	4.94
128-W118.C	5/15/2012	6.77	8.84	0.33	8.18	0.10	11.00	0.00	0.41	0.64	1.25	0.00	0.00
129-W118.GR	5/15/2012	6.79	74.51	1.03	95.96	0.11	0.24	0.34	6.21	0.72	3.17	2.05	1.32
130-USPS.GR	6/2/2012	7.60	120.35	2.23	78.97	0.39	0.60	0.53	13.59	1.08	1.99	2.13	0.04
131-W118.C	6/4/2012	7.35	13.10	0.75	0.00	0.02	0.14	0.26	0.70	0.39	0.90	0.00	0.16
132-USPS.C	6/4/2012	7.51	129.30	3.63	0.00	0.01	1.29	0.00	14.26	2.38	na	10.62	0.00
133-ConEd.C	6/4/2012	7.39	19.60	0.57	0.00	0.38	0.37	1.10	1.05	2.64	0.35	0.20	0.00
134-W118.GR	6/4/2012	7.22	61.03	3.93	98.79	0.16	0.18	0.00	6.22	11.63	1.51	1.88	1.35
135-Rain	6/4/2012	na	9.23	0.56	0.00	0.12	0.00	1.45	0.74	0.79	1.59	0.77	0.00
136-Rain	6/13/2012	na	59.62	0.67	0.00	0.58	0.36	0.00	1.05	0.00	0.35	0.00	0.00
137-USPS.GR	6/22/2012	7.51	176.88	9.69	73.73	3.23	4.93	1.24	15.44	5.82	3.39	2.38	0.00
138-Rain	7/20/2012	na	64.93	0.58	0.00	na	na	na	na	na	na	na	na
139-ConEd.C	7/20/2012	7.08	76.71	0.28	10.07	na	na	na	na	na	na	na	na
140-ConEd.GR	7/20/2012	6.65	142.00	1.85	243.26	na	na	na	na	na	na	na	na
141-W118.C	7/20/2012	6.78	20.92	0.81	12.59	na	na	na	na	na	na	na	na
142-W118.GR	7/20/2012	7.11	159.90	5.38	368.71	na	na	na	na	na	na	na	na
143-W118.C	8/1/2012	6.77	59.44	1.70	82.02	na	na	na	na	na	na	na	na
144-W118.GR	8/1/2012	7.26	150.90	0.76	237.42	na	na	na	na	na	na	na	na
145-Rain	8/2/2012	5.91	53.30	0.54	0.00	na	na	na	na	na	na	na	na

Avg ± SD	pH	Conductivity (uS/cm)	Turbidity (NTU)	Apparent Color (PtCo)	NO <sub>3</sub> <sup>-</sup>	NH <sub>4</sub> <sup>+</sup>	P	Ca	K	Na	Mg	B
GR	7.28 ± 0.51	127.67 ± 48.89	2.47 ± 2.74	162.53 ± 90.24	0.27 ± 0.59	0.86 ± 1.86	0.47 ± 0.47	13.59 ± 6.8	2.22 ± 2.86	3.58 ± 3.47	2.92 ± 1.03	0.58 ± 1.19
C	6.27 ± 0.69	57.11 ± 57.63	1.47 ± 1.48	28.45 ± 32.42	0.87 ± 1.31	1.47 ± 2.55	0.25 ± 0.38	3.93 ± 5.23	0.78 ± 1.98	1.80 ± 3.01	1.31 ± 2.30	0.03 ± 0.1
Rain	4.82 ± 0.39	32.00 ± 20.71	0.62 ± 0.39	5.32 ± 9.79	0.60 ± 0.53	1.19 ± 1.85	0.21 ± 0.41	0.74 ± 0.50	0.10 ± 0.2	0.98 ± 0.88	0.20 ± 0.24	0.0 ± 0.0

## Appendix C Water Quality Analysis

The tables on the left on the following pages compare water quality within sample types (sample types = Rain, GR, and C). The statistics for pH were calculated by transforming the measurements using this equation:  $[H^+] = 10^{-pH}$ . Once averaged, the  $[H^+]$  value was converted back via this equation:  $pH = -\log[H^+]$ . Dark grey highlighted boxes indicate comparisons among the different GRs, medium grey diagonal boxes compare GR and C within one site and white boxes indicate comparisons among C roofs. Bolded and underlined p-values indicate significance. The smaller tables on the right compare water quality between sample types. Other parameters that were measured but not listed below had no significant difference between Rain, GR and C.

Table 7-10: Summary of Statistical Analysis Results from Water Quality Monitoring (March 10, 2011 – August 2, 2012). One-way ANOVA tests were run. The tables show the post-hoc Tukey HSD test to the seventh decimal place at the 0.05 level of significance.

**pH**

Site	Rain	W115	W118	USPS	Fdston	ConEd
Rain	-	<u>&lt;0.001</u>	<u>&lt;0.001</u>	<u>&lt;0.001</u>	<u>&lt;0.001</u>	<u>&lt;0.001</u>
W115	<u>0.001</u>	0.227	1.000	1.000	1.000	1.000
W118	<u>&lt;0.001</u>	0.988	<u>0.001</u>	1.000	1.000	1.000
USPS	<u>&lt;0.001</u>	0.988	1.000	0.584	1.000	1.000
Fdston	<u>0.006</u>	0.997	1.000	1.000	0.153	1.0000
ConEd	<u>&lt;0.001</u>	0.996	1.000	1.000	1.000	0.151
Rain-C's: ANOVA F <sub>5,59</sub> = 11.12, p-value = <0.001						
W115GR's-C's: ANOVA F <sub>1,12</sub> = 1.621, p-value = 0.227						
W118GR's-C's: ANOVA F <sub>1,36</sub> = 12.41, p-value= 0.001						
USPSGR's-C's: ANOVA F <sub>1,21</sub> = 0.309, p-value= 0.584						
FdstonGR's-C's: ANOVA F <sub>1,7</sub> = 2.577, p-value= 0.153						
ConEdGR's-C's: ANOVA F <sub>1,9</sub> = 2.46, p-value= 0.151						
Rain-GR's: ANOVA F <sub>5,66</sub> = 14.47, p-value = <0.001						

**pH**

Sample	p-value
Rain-All GR	<u>&lt;0.001</u>
Rain-All C	<u>&lt;0.001</u>
All GR-All C	0.878

Rain-All GR-All C:

ANOVA F<sub>2,113</sub> = 65.87

p-value <0.001

### Conductivity

Site	Rain	W115	W118	USPS	Fdston	ConEd
Rain	-	<b>&lt;0.001</b>	<b>&lt;0.001</b>	<b>&lt;0.001</b>	<b>&lt;0.001</b>	<b>&lt;0.001</b>
W115	0.984	<b>0.002</b>	0.076	0.711	0.998	0.418
W118	0.869	1.000	<b>0.003</b>	<b>&lt;0.001</b>	0.340	1.000
USPS	<b>&lt;0.001</b>	<b>0.013</b>	<b>0.004</b>	<b>0.003</b>	0.436	<b>0.009</b>
Fdston	1.000	0.997	0.985	<b>0.021</b>	<b>&lt;0.001</b>	0.740
ConEd	1.000	0.998	0.987	<b>0.008</b>	1.000	<b>0.010</b>
Rain-C's: ANOVA F <sub>5,61</sub> = 5.404, p-value = <0.001						
W115GR's-C's: ANOVA F <sub>1,12</sub> = 15.57, p-value = 0.002						
W118GR's-C's: ANOVA F <sub>1,35</sub> = 9.905, p-value = 0.003						
USPSGR's-C's: ANOVA F <sub>1,21</sub> = 10.96, p-value = 0.003						
FdstonGR's-C's: ANOVA F <sub>1,7</sub> = 34.81, p-value = <0.001						
ConEdGR's-C's: ANOVA F <sub>1,9</sub> = 10.74, p-value = 0.010						
Rain-GR's: ANOVA F <sub>5,69</sub> = 32.47, p-value = <0.001						

### Turbidity

Site	Rain	W115	W118	USPS	Fdston	ConEd
Rain	-	0.811	0.770	<b>&lt;0.001</b>	0.983	0.967
W115	0.920	0.294	0.999	0.092	1.000	0.999
W118	0.609	1.000	0.404	<b>&lt;0.001</b>	1.000	1.000
USPS	<b>1.000</b>	<b>&lt;0.001</b>	<b>&lt;0.001</b>	0.462	0.133	<b>0.032</b>
Fdston	1.000	0.989	0.963	<b>0.003</b>	0.419	1.000
ConEd	1.000	0.991	0.938	<b>&lt;0.001</b>	1.000	0.074
Rain-C's: ANOVA F <sub>5,50</sub> = 10.59, p-value = <0.001						
W115GR's-C's: ANOVA F <sub>1,10</sub> = 1.227, p-value = 0.294						
W118GR's-C's: ANOVA F <sub>1,30</sub> = 0.718, p-value = 0.404						
USPSGR's-C's: ANOVA F <sub>1,17</sub> = 0.567, p-value = 0.462						
FdstonGR's-C's: ANOVA F <sub>1,3</sub> = 0.874, p-value = 0.419						
ConEdGR's-C's: ANOVA F <sub>1,9</sub> = 4.092, p-value = 0.074						
Rain-GR's: ANOVA F <sub>5,57</sub> = 6.699, p-value = <0.001						

### Conductivity

Sample	p-value
Rain-All GR	<b>&lt;0.001</b>
Rain-All C	0.104
All GR-All C	<b>&lt;0.001</b>

Rain-All GR-All C:

ANOVA F<sub>2,115</sub> = 43.78

p-value = <0.001

### Turbidity

Sample	p-value
Rain-All GR	<b>0.004</b>
Rain-All C	0.293
All GR-All C	0.099

Rain-All GR-All C:

ANOVA F<sub>2,96</sub> = 5.82

p-value = 0.004

### Apparent Color

Site	Rain	W115	W118	USPS	Fdston	ConEd
Rain	-	0.058	<b>&lt;0.001</b>	<b>&lt;0.001</b>	<b>0.009</b>	<b>0.004</b>
W115	0.399	<b>0.021</b>	1.000	0.911	1.000	1.000
W118	0.267	0.998	<b>&lt;0.001</b>	0.719	1.000	1.000
USPS	<b>&lt;0.001</b>	0.768	0.207	<b>0.003</b>	0.955	0.927
Fdston	1.000	0.842	0.911	0.129	<b>&lt;0.001</b>	1.000
ConEd	0.998	0.777	0.840	<b>0.034</b>	1.000	<b>&lt;0.001</b>
Rain-C's: ANOVA $F_{5,49} = 4.934$ , p-value = <0.001 W115GR's-C's: ANOVA $F_{1,5} = 11.14$ , p-value = 0.021 W118GR's-C's: ANOVA $F_{1,24} = 18.35$ , p-value = <0.001 USPSGR's-C's: ANOVA $F_{1,21} = 11.54$ , p-value = 0.003 FdstonGR's-C's: ANOVA $F_{1,5} = 54.43$ , p-value = <0.001 ConEdGR's-C's: ANOVA $F_{1,9} = 24.82$ , p-value = <0.001 Rain-GR's: ANOVA $F_{5,57} = 12.87$ , p-value = <0.001						

### Apparent Color

Sample	p-value
Rain-All GR	<b>&lt;0.001</b>
Rain-All C	0.390
All GR-All C	<b>&lt;0.001</b>

Rain-All GR-All C:

ANOVA  $F_{2,93} = 60.52$

p-value = <0.001

### Nitrate

Site	Rain	W115	W118	USPS	Fdston	ConEd
Rain	-	0.927	0.240	0.954	0.954	0.574
W115	0.934	0.165	0.999	0.999	1.000	0.995
W118	0.405	0.997	<b>0.023</b>	0.857	0.988	1.000
USPS	0.980	0.748	0.284	0.684	1.000	0.910
Fdston	1.000	0.990	0.861	0.993	0.486	0.981
ConEd	0.998	0.894	0.537	1.000	0.999	<b>0.024</b>
Rain-C's: ANOVA $F_{5,49} = 1.378$ , p-value = 0.249 W115GR's-C's: ANOVA $F_{1,9} = 2.283$ , p-value = 0.165 W118GR's-C's: ANOVA $F_{1,27} = 5.858$ , p-value = 0.023 USPSGR's-C's: ANOVA $F_{1,17} = 0.172$ , p-value = 0.684 FdstonGR's-C's: ANOVA $F_{1,7} = 0.541$ , p-value = 0.486 ConEdGR's-C's: ANOVA $F_{1,7} = 8.229$ , p-value = 0.024 Rain-GR's: ANOVA $F_{5,54} = 1.253$ , p-value = 0.298						

### Nitrate

Sample	p-value
Rain-All GR	0.377
Rain-All C	0.571
All GR-All C	<b>0.013</b>

Rain-All GR-All C:

ANOVA  $F_{2,93} = 4.189$

p-value = 0.018

### Ammonium

Site	Rain	W115	W118	USPS	Fdston	ConEd
Rain	-	0.971	1.000	1.000	0.894	0.993
W115	0.999	0.382	0.984	0.976	1.000	1.000
W118	0.678	0.725	0.356	1.000	0.943	0.998
USPS	0.994	0.978	0.967	0.471	0.915	0.995
Fdston	0.995	1.000	0.700	0.960	0.160	0.999
ConEd	0.992	1.000	0.570	0.936	1.000	0.818
Rain-C's: ANOVA $F_{5,36} = 0.856$ , p-value = 0.520						
W115GR's-C's: ANOVA $F_{1,4} = 0.964$ , p-value = 0.382						
W118GR's-C's: ANOVA $F_{1,15} = 0.906$ , p-value = 0.356						
USPSGR's-C's: ANOVA $F_{1,17} = 0.543$ , p-value = 0.471						
FdstonGR's-C's: ANOVA $F_{1,5} = 2.719$ , p-value = 0.160						
ConEdGR's-C's: ANOVA $F_{1,7} = 0.057$ , p-value = 0.818						
Rain-GR's: ANOVA $F_{5,42} = 0.373$ , p-value = 0.864						

### Calcium

Site	Rain	W115	W118	USPS	Fdston	ConEd
Rain	-	<b>0.006</b>	<b>&lt;0.001</b>	<b>&lt;0.001</b>	<b>&lt;0.001</b>	0.127
W115	0.990	<b>0.003</b>	0.996	<b>0.013</b>	0.485	0.598
W118	1.000	0.999	<b>&lt;0.001</b>	<b>&lt;0.001</b>	<b>0.024</b>	0.547
USPS	<b>&lt;0.001</b>	<b>&lt;0.001</b>	<b>&lt;0.001</b>	<b>0.003</b>	0.384	<b>&lt;0.001</b>
Fdston	0.977	1.000	0.994	<b>&lt;0.001</b>	<b>0.001</b>	<b>0.002</b>
ConEd	1.000	1.000	1.000	<b>&lt;0.001</b>	0.997	<b>&lt;0.001</b>
Rain-C's: ANOVA $F_{5,36} = 31$ , p-value = <0.001						
W115GR's-C's: ANOVA $F_{1,4} = 43.8$ , p-value = 0.003						
W118GR's-C's: ANOVA $F_{1,15} = 31.69$ , p-value = <0.001						
USPSGR's-C's: ANOVA $F_{1,17} = 11.57$ , p-value = 0.003						
FdstonGR's-C's: ANOVA $F_{1,5} = 42.41$ , p-value = 0.001						
ConEdGR's-C's: ANOVA $F_{1,7} = 32.06$ , p-value = <0.001						
Rain-GR's: ANOVA $F_{5,42} = 45.46$ , p-value = <0.001						

### Ammonium

Sample	p-value
Rain-All GR	0.868
Rain-All C	0.911
All GR-All C	0.526

Rain-All GR-All C:

ANOVA  $F_{2,71} = 0.594$

p-value = 0.555

### Calcium

Sample	p-value
Rain-All GR	<b>&lt;0.001</b>
Rain-All C	0.166
All GR-All C	<b>&lt;0.001</b>

Rain-All GR-All C:

ANOVA  $F_{2,71} = 37.7$

p-value = <0.001

### Potassium

Site	Rain	W115	W118	USPS	Fdston	ConEd
Rain	-	0.999	0.214	0.498	<b>&lt;0.001</b>	0.721
W115	1.000	0.080	0.957	0.995	<b>0.016</b>	0.991
W118	1.000	1.000	0.215	0.991	<b>0.004</b>	1.000
USPS	0.117	0.463	0.333	0.682	<b>&lt;0.001</b>	1.000
Fdston	0.999	1.000	1.000	0.739	<b>0.018</b>	<b>0.014</b>
ConEd	0.991	0.999	0.999	0.658	1.000	0.240
Rain-C's: ANOVA F <sub>5,36</sub> = 1.503, p-value = 0.213						
W115GR's-C's: ANOVA F <sub>1,4</sub> = 5.463, p-value = 0.080						
W118GR's-C's: ANOVA F <sub>1,15</sub> = 1.674, p-value = 0.215						
USPSGR's-C's: ANOVA F <sub>1,17</sub> = 0.174, p-value = 0.682						
FdstonGR's-C's: ANOVA F <sub>1,5</sub> = 11.99, p-value = 0.018						
ConEdGR's-C's: ANOVA F <sub>1,7</sub> = 1.647, p-value = 0.240						
Rain-GR's: ANOVA F <sub>5,42</sub> = 6.924, p-value = <0.001						

### Magnesium

Site	Rain	W115	W118	USPS	Fdston	ConEd
Rain	-	<b>0.013</b>	<b>&lt;0.001</b>	<b>&lt;0.001</b>	<b>0.003</b>	<b>&lt;0.001</b>
W115	1.000	<b>&lt;0.001</b>	0.841	0.595	0.998	0.998
W118	1.000	1.000	<b>&lt;0.001</b>	0.976	0.266	0.943
USPS	<b>&lt;0.001</b>	<b>&lt;0.001</b>	<b>&lt;0.001</b>	0.470	0.084	0.687
Fdston	0.984	0.997	0.984	<b>0.009</b>	<b>0.023</b>	0.890
ConEd	1.000	1.000	1.000	<b>&lt;0.001</b>	0.996	<b>0.002</b>
Rain-C's: ANOVA F <sub>5,36</sub> = 10.06, p-value = <0.001						
W115GR's-C's: ANOVA F <sub>1,4</sub> = 555.1, p-value = <0.001						
W118GR's-C's: ANOVA F <sub>1,15</sub> = 35.88, p-value = <0.001						
USPSGR's-C's: ANOVA F <sub>1,16</sub> = 0.548, p-value = 0.470						
FdstonGR's-C's: ANOVA F <sub>1,5</sub> = 10.44, p-value = 0.023						
ConEdGR's-C's: ANOVA F <sub>1,7</sub> = 25.19, p-value = 0.002						
Rain-GR's: ANOVA F <sub>5,41</sub> = 25.91, p-value = <0.001						

### Potassium

Sample	p-value
Rain-All GR	<b>0.008</b>
Rain-All C	0.611
All GR-All C	<b>0.044</b>

Rain-All GR-All C:

ANOVA F<sub>2,71</sub> = 5.725

p-value = 0.005

### Magnesium

Sample	p-value
Rain-All GR	<b>&lt;0.001</b>
Rain-All C	0.065
All GR-All C	<b>&lt;0.001</b>

Rain-All GR-All C:

ANOVA F<sub>2,70</sub> = 18.15

p-value = <0.001

### Phosphorus

Site	Rain	W115	W118	USPS	Fdston	ConEd
Rain	-	0.998	0.807	0.837	0.213	0.990
W115	0.916	0.178	1.000	1.000	0.874	1.000
W118	1.000	0.956	0.261	1.000	0.769	1.000
USPS	1.000	0.964	1.000	0.237	0.699	1.000
Fdston	0.664	0.380	0.722	0.703	0.640	0.760
ConEd	0.917	0.611	0.941	0.930	0.991	0.911
Rain-C's: ANOVA F <sub>5,36</sub> = 1.015, p-value = 0.423						
W115GR's-C's: ANOVA F <sub>1,4</sub> = 2.667, p-value = 0.178						
W118GR's-C's: ANOVA F <sub>1,15</sub> = 1.362, p-value = 0.261						
USPSGR's-C's: ANOVA F <sub>1,17</sub> = 1.5, p-value = 0.237						
FdstonGR's-C's: ANOVA F <sub>1,5</sub> = 0.247, p-value = 0.640						
ConEdGR's-C's: ANOVA F <sub>1,7</sub> = 0.013, p-value = 0.911						
Rain-GR's: ANOVA F <sub>5,42</sub> = 1.173, p-value = 0.339						

### Boron

Site	Rain	W115	W118	USPS	Fdston	ConEd
Rain	-	1.000	<0.001	1.000	1.000	1.000
W115	1.000	NaN	0.017	1.000	1.000	1.000
W118	0.027	0.198	0.009	<0.001	<0.001	<0.001
USPS	1.000	1.000	0.087	0.461	1.000	1.000
Fdston	1.000	1.000	0.289	1.000	NaN	1.000
ConEd	1.000	1.000	0.144	1.000	1.000	NaN
Rain-C's: ANOVA F <sub>5,36</sub> = 2.551, p-value = 0.045						
W118GR's-C's: ANOVA F <sub>1,15</sub> = 9.091, p-value = 0.009						
USPSGR's-C's: ANOVA F <sub>1,17</sub> = 0.569, p-value = 0.461						
Rain-GR's: ANOVA F <sub>5,42</sub> = 11.1, p-value = <0.001						

### Phosphorus

Sample	p-value
Rain-All GR	0.134
Rain-All C	0.955
All GR-All C	0.145

Rain-All GR-All C:

ANOVA F<sub>2,71</sub> = 2.671

p-value = 0.076

### Boron

Sample	p-value
Rain-All GR	0.050
Rain-All C	0.993
All GR-All C	0.027

Rain-All GR-All C:

ANOVA F<sub>2,71</sub> = 4.607

p-value = 0.013

### Sodium

Site	Rain	W115	W118	USPS	Fdston	ConEd
<b>Rain</b>	-	0.949	<b>0.003</b>	0.682	0.819	0.831
<b>W115</b>	1.000	<b>0.045</b>	0.815	1.000	1.000	1.000
<b>W118</b>	1.000	1.000	<b>0.042</b>	0.157	0.619	0.604
<b>USPS</b>	0.230	0.506	0.305	<b>0.553</b>	1.000	1.000
<b>Fdston</b>	0.693	0.806	0.697	1.000	0.921	1.000
<b>ConEd</b>	1.000	1.000	1.000	0.523	0.836	0.079
Rain-C's: ANOVA $F_{5,35} = 1.571$ , p-value = 0.194						
W115GR's-C's: ANOVA $F_{1,4} = 8.349$ , p-value = 0.045						
W118GR's-C's: ANOVA $F_{1,15} = 4.96$ , p-value = 0.042						
USPSGR's-C's: ANOVA $F_{1,16} = 0.367$ , p-value = 0.553						
FdstonGR's-C's: ANOVA $F_{1,5} = 0.011$ , p-value = 0.921						
ConEdGR's-C's: ANOVA $F_{1,7} = 4.228$ , p-value = 0.079						
Rain-GR's: ANOVA $F_{5,42} = 3.246$ , p-value = 0.014						

### Sodium

Sample	p-value
Rain-All GR	<b>0.014</b>
Rain-All C	0.658
All GR-All C	0.066

Rain-All GR-All C:

ANOVA  $F_{2,70} = 4.998$

p-value = 0.009